Texas Water Development Board

Report 358

Groundwater Availability Modeling: Northern Segment of the Edwards Aquifer, Texas

by
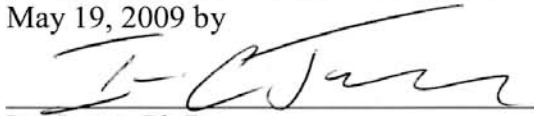Ian C. Jones, Ph.D., P.G.

December 2003

Geoscientist Seal

The contents of this report (including figures and tables) document the work of the Following Licensed Texas Geoscientist:
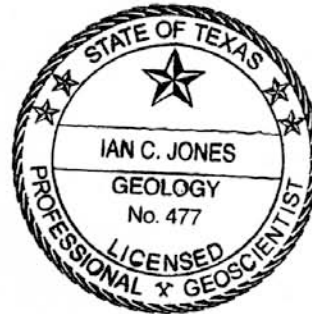
Ian Jones, P.G. No. 477

> Dr. Ian Jones was responsible for all original work documented in this publication.

The seal appearing on this document was authorized on May 19, 2009 by

Ian Jones, Ph.D.

Report 358 - Groundwater Availability Model: Northern Segment of the Edwards Aquifer, Texas, 2003

Texas Water Development Board

Authorization for use or reproduction of any original material contained in this publication, i.e., not obtained from other sources, is freely granted. The Board would appreciate acknowledgment. The use of brand names in this publication does not indicate an endorsement by the Texas Water Development Board or the State of Texas.

This page intentionally blank.

Table of Contents

List of Tables

This page intentionally blank.

1.0   Executive Summary

The northern segment of the Edwards aquifer covers an area that includes some of the fastest growing counties in Texas. As a result of rapid population growth, demand for water in this region is also rising. A groundwater availability model simulating flow through this segment of the Edwards aquifer was constructed as a groundwater resource management tool. The purpose of this tool is to aid groundwater conservation districts, regional water planning groups, and others in evaluating groundwater resource management strategies to meet projected groundwater demands. This model was constructed by calibrating to steady-state conditions for 1980 and historical transient conditions for the period 1980-2000. The calibrated model can be used to predict future water-level changes that may result from projected pumping rates and/or climatic conditions.

The model results indicate that (1) no historical regional-scale cones-of-depression exist in the northern Edwards aquifer, (2) 60-80 percent of natural discharge is baseflow to perennial streams that cross the aquifer outcrop, (3) pumping is less than 20 percent of total discharge, (4) the flow system is more active in the unconfined part of the aquifer than in downdip portions, and (5) gradual long-term water-level decline is occurring in the Pflugerville-Georgetown area. Historical pumping trends indicate steadily increasing municipal, rural domestic, and industrial pumping, rising from 20,000 to 30,000 acre-feet/year over the past 20 years. Regional-scale drawdown associated with increasing pumping has not been observed, so far, largely because pumping is a relatively small portion of the total water budget of this segment of the Edwards aquifer. However, pumping results in local drawdown.

2.0   Introduction

The northern segment of the Edwards aquifer is an important source of groundwater for municipalities, industries, and landowners in central Texas. Rapid population growth in this part of Texas has increased interest in the northern segment of the Edwards aquifer and heightened concerns about groundwater availability in the aquifer.

This is the first published model to simulate groundwater flow in the northern segment of the Edwards aquifer. The San Antonio and Barton Springs segments have received higher priority because groundwater flow models were needed to address pressing issues related to conflicts over groundwater demand for municipal, agricultural, recreational, and ecological uses (fig. 2-1). The San Antonio segment has been given highest priority because historically it has been the sole source of water for many municipalities, including San Antonio, a city with a population exceeding 1 million. The San Antonio segment is also an important source of irrigation water in that region. Increasing pumping associated with municipal and irrigation demands, together with the effects of drought, lowers spring discharge in Barton, San Marcos, and Comal springs. Declines in spring discharge affect recreation, flora, and fauna associated with the springs. These issues have made understanding groundwater flow through the respective segments of the Edwards aquifer of vital importance.
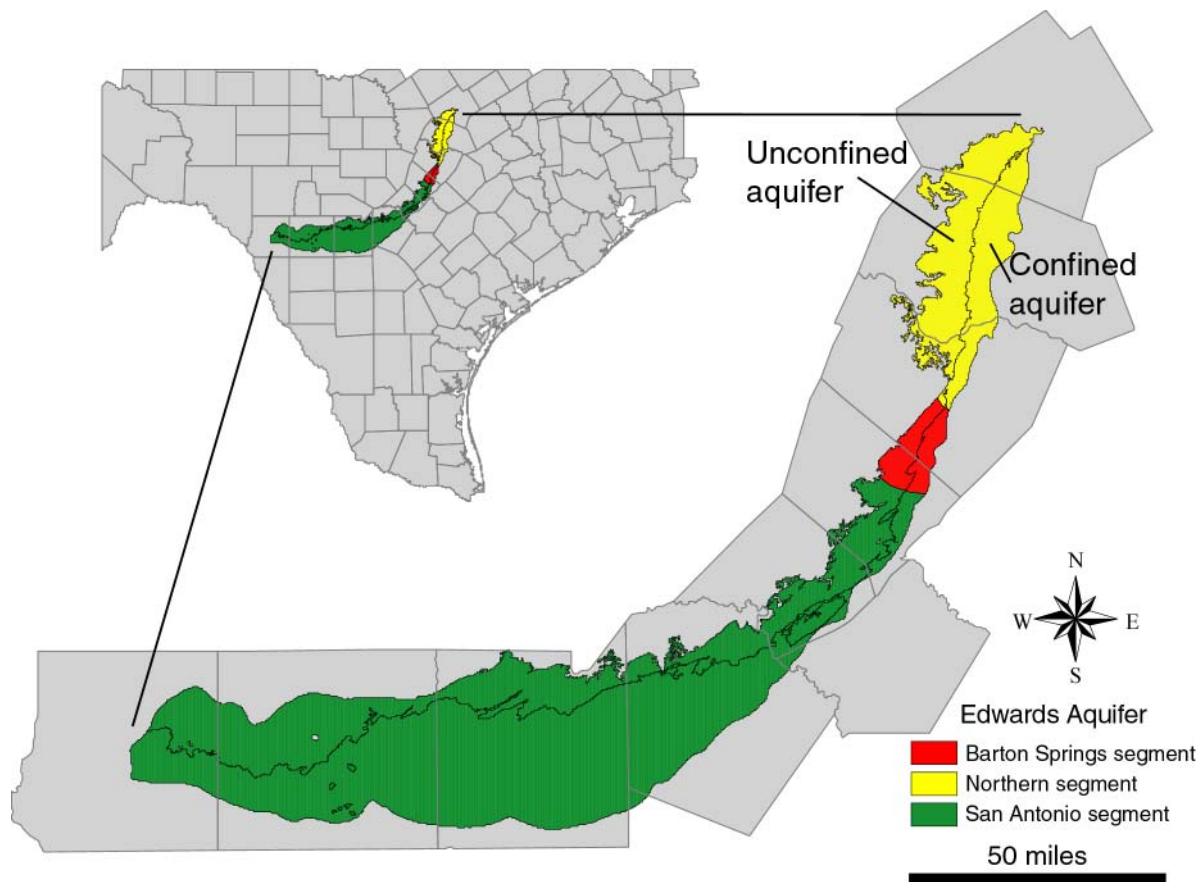
Figure 2-1.   Segments of the Edwards (Balcones Fault Zone) aquifer.

The northern segment has received lower priority largely because the largest city in the region, Austin, does not rely on the northern segment of the Edwards aquifer for groundwater to meet its water demands. However, other smaller municipalities, such as Georgetown, Pflugerville, and Round Rock, use groundwater from the Edwards aquifer. Rapid population growth in these and adjacent municipalities is likely to be accompanied by rapid growth in demand for groundwater from the Edwards aquifer. This growth necessitates our gaining a better understanding of the hydrology of this segment of the Edwards aquifer and the potential effects of future population growth. This understanding can be achieved through groundwater availability modeling (GAM)—development of a state-of-the-art, publicly available, numerical groundwater flow model that will provide reliable information on groundwater availability in this aquifer.

The general approach used in developing this model involved (1) developing a conceptual model, (2) organizing and distributing aquifer information for input into the model, (3) calibrating a steady-state model for 1980, (4) calibrating a historical transient model for the years 1980 through 2000, and (5) making predictive simulations. This report describes (1) the study area, previous work, and hydrogeologic setting used to develop the conceptual model; (2) the code, grid, and model parameters assigned during model construction; (3) calibration and sensitivity analysis of steady-state and transient models; (4) predictions of water-level changes; (5) limitations of the current model; and (6) suggestions for future improvements.
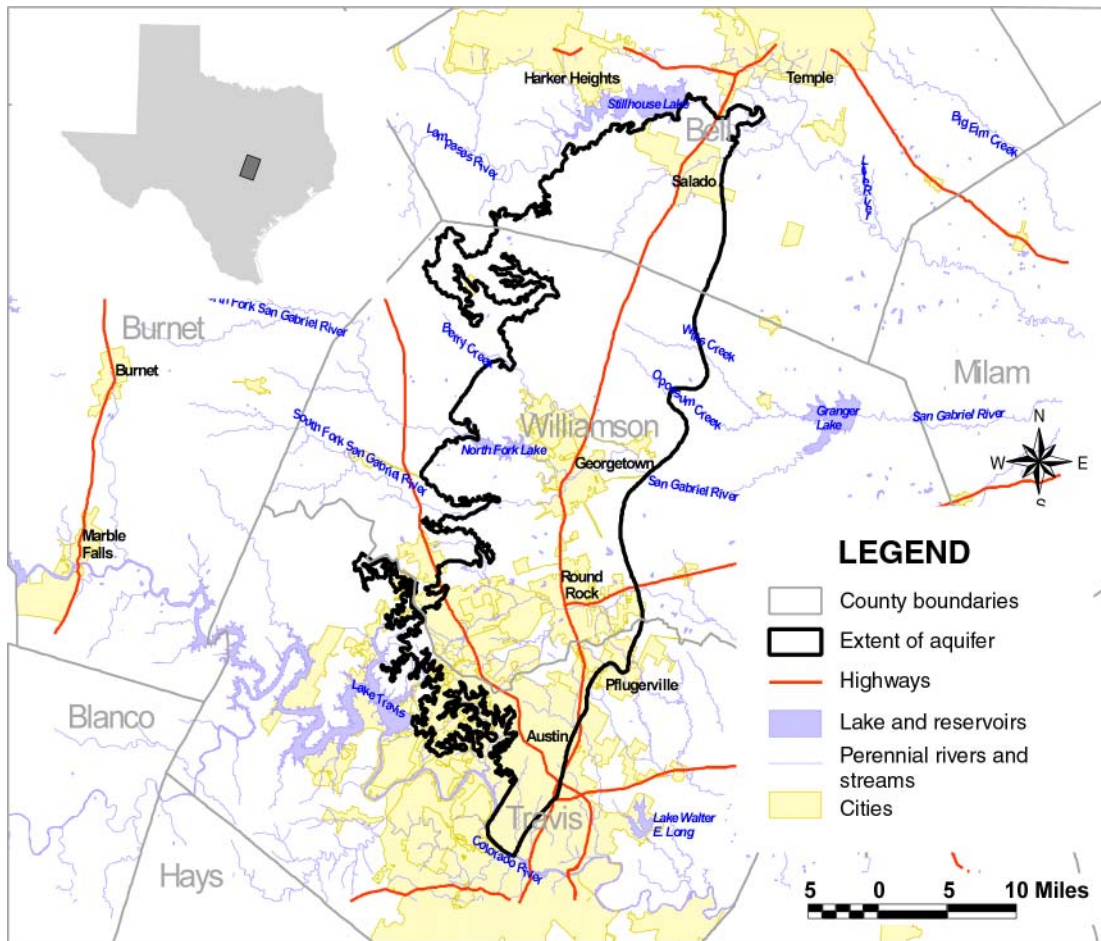
Figure 3-1.   Location of the study area.

3.0   Study Area

The northern segment of the Edwards aquifer is located in central Texas (fig. 3-1). It is the northernmost of the three segments that make up the Edwards (Balcones Fault Zone) aquifer (fig. 2-1). The study area underlies parts of Bell, Travis, and Williamson counties and extends over parts of two regional water planning areas, the Lower Colorado (K) and Brazos (G) Regional Water Planning Areas (fig. 3-2). The northern part of the study area also lies within the Clearwater Underground Water Conservation District (fig. 3-3). The northern segment of the Edwards aquifer extends from the Colorado River in Travis County to the Lampasas River in southern Bell County. This segment of the Edwards aquifer is bounded by the Colorado River to the south, the western margin of the Edwards and associated limestones outcrop to the west and north, and to the east by the easternmost extent of fresh groundwater, referred to as the bad water line.

3
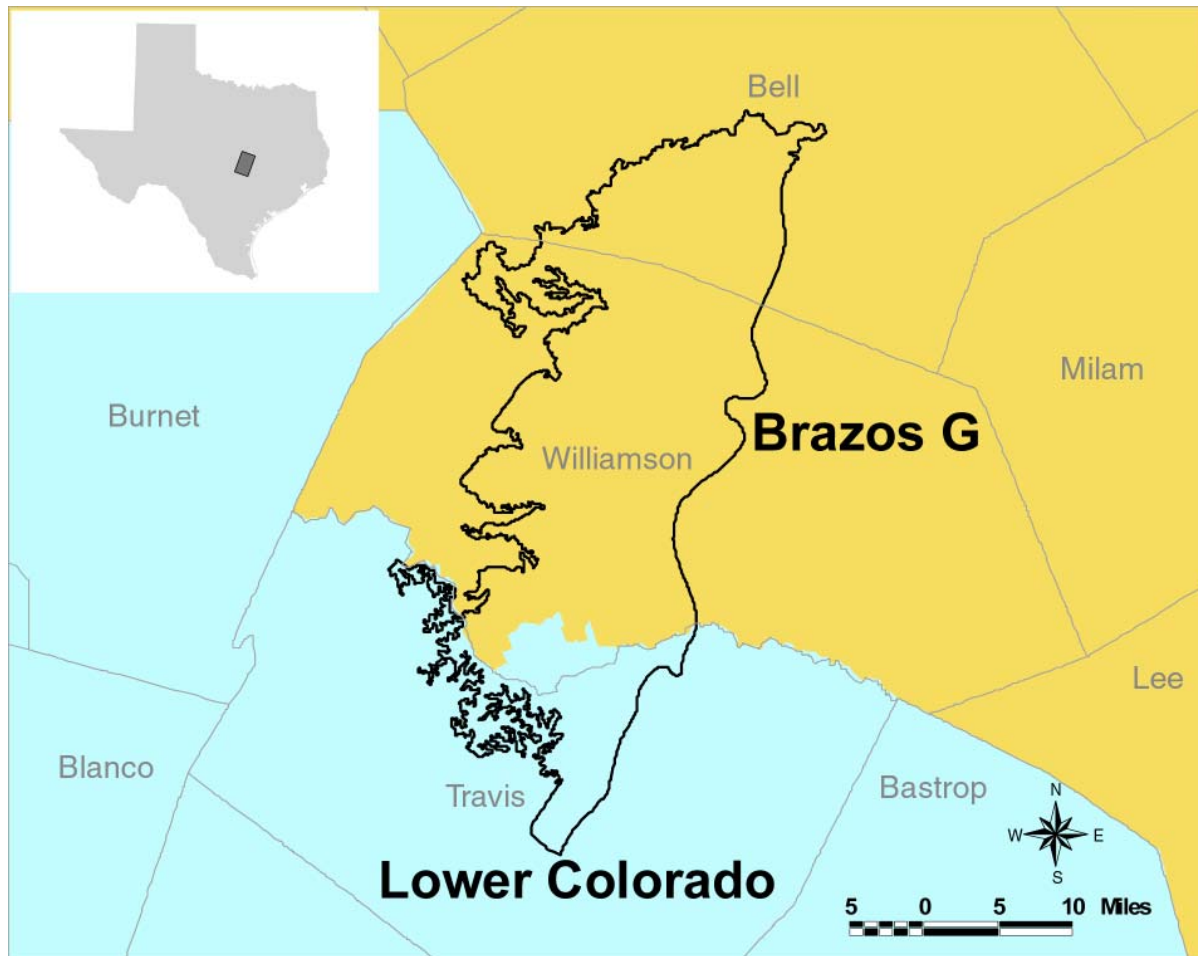
Figure 3-2.   Location of regional water planning group boundaries in the study area.

3.1   *Physiography and Climate*

The topography of central Texas is relatively flat, with an elevation range of 500 to 1,000 feet above sea level (fig. 3-4). There are three physiographic provinces in the study area, the Edwards Plateau, Rolling Prairie, and Blackland Prairie (fig. 3-5). The occurrence of these three physiographic provinces is related to the underlying geology that will be discussed in more detail later in this section.

In the study area, the Edwards Plateau is composed of the Hill Country, Jollyville Plateau, and Lampasas Cutplains. The Jollyville Plateau has been separated from the Hill Country by erosion that resulted in the formation of the Colorado River valley. The Hill Country and Jollyville Plateau are characterized by highly dissected canyonland, while the Lampasas Cutplains is characterized by gently rolling terrain. The Rolling Prairie developed in the Balcones Fault Zone and coincides with the outcrop of limestone rocks that overlie the aquifer. The Blackland Prairie occurs where the limestones are overlain by younger alluvial units that occur along the margin of the Gulf Coastal Plain (Senger and others, 1990). The most prominent topographic feature is the Balcones Escarpment, a product of normal faulting in this region. This escarpment forms the

4
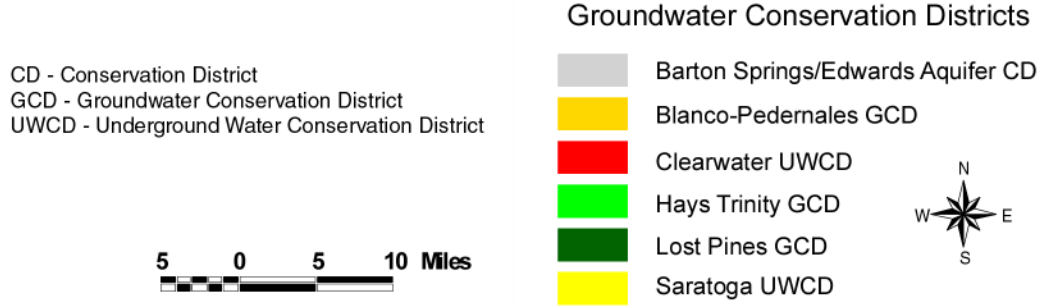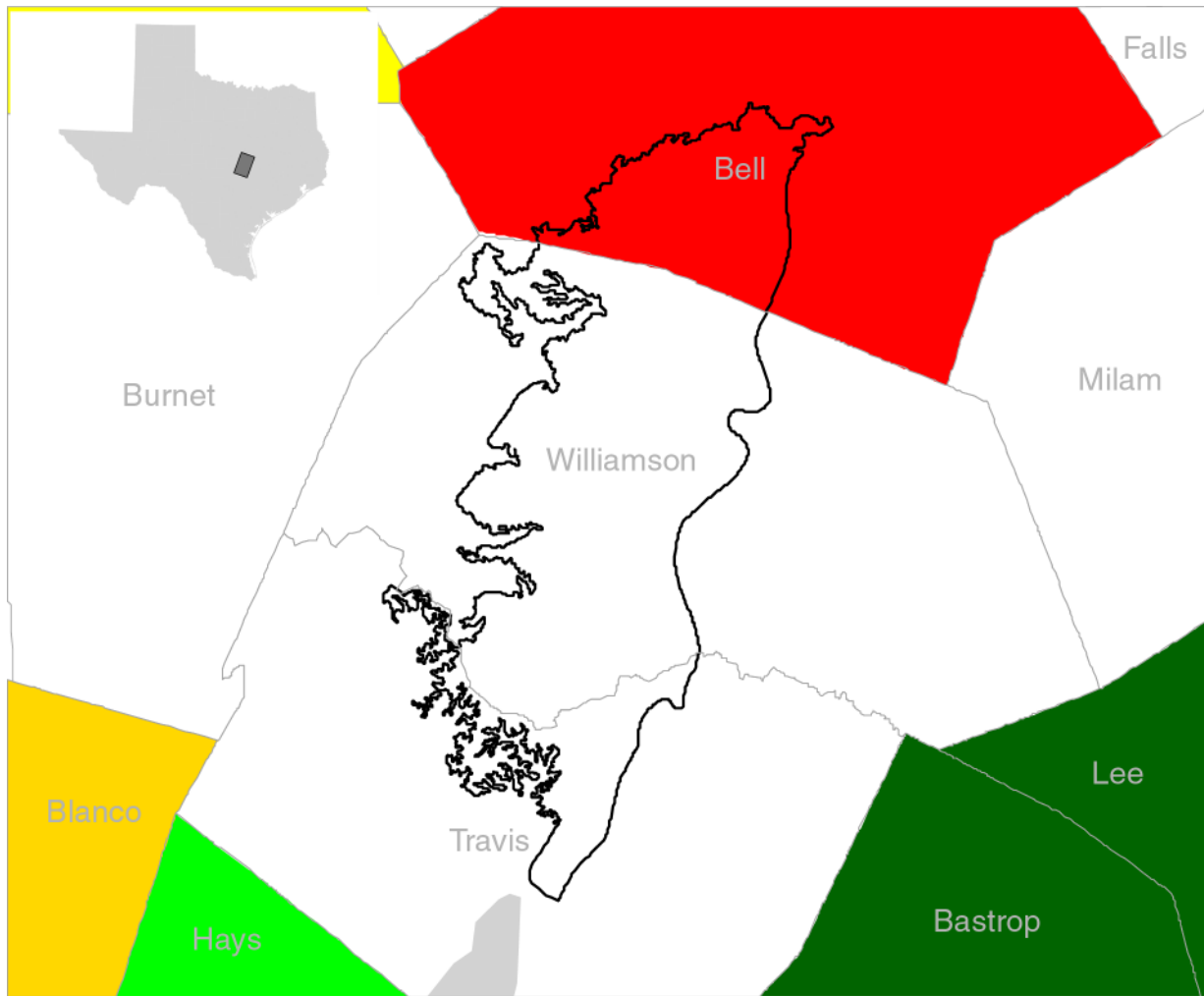
Figure 3-3.   Location of groundwater conservation districts in the study area.
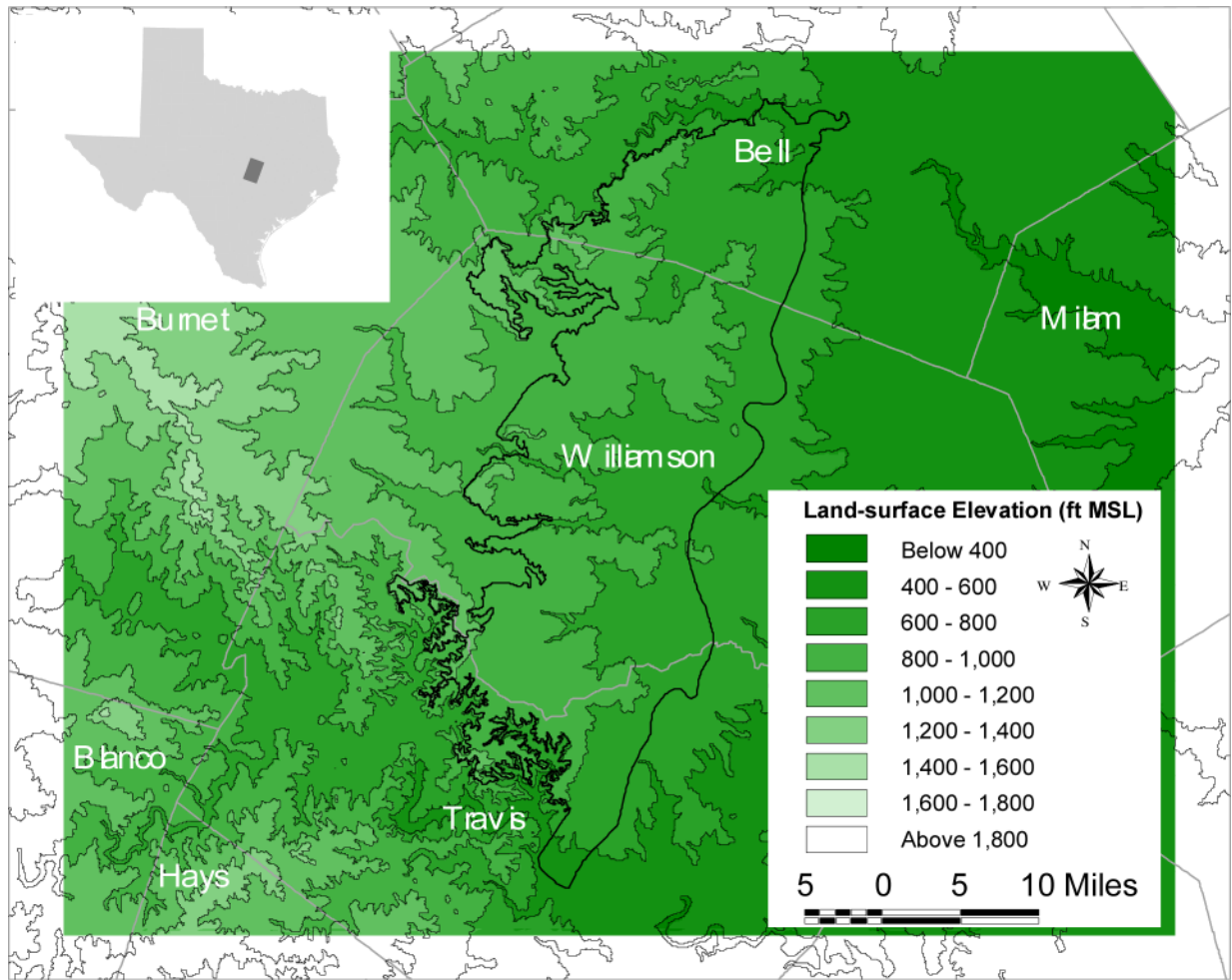
Figure 3-4.   Land-surface elevation in the study area.

boundary between the Jollyville Plateau and Hill Country parts of the Edwards Plateau and the Rolling Prairie (Trippet and Garner, 1976). This boundary becomes more subdued to the north in the Lampasas Cutplains.

Central Texas has a sub-humid climate. At weather stations located within the study area, median annual precipitation ranges from 20 to 30 inches (fig. 3-6). Approximately 60 percent of annual precipitation falls in April through June and September through October (fig. 3-7). Some of this precipitation takes the form of severe thunderstorms. These thunderstorms frequently produce major flash floods that have the potential to generate recharge to the underlying aquifer (Senger and others, 1990). Monthly precipitation is typically lowest during July and August. Precipitation data display a wide range of annual precipitation in the study area. Data for the period 1930 through 1997 indicate annual precipitation ranging from 10 to 55 inches (fig. 3-8). Lowest annual precipitation occurred during 1954 through 1956 at some stations. This coincides with the drought of the 1950s, which affected the entire state.
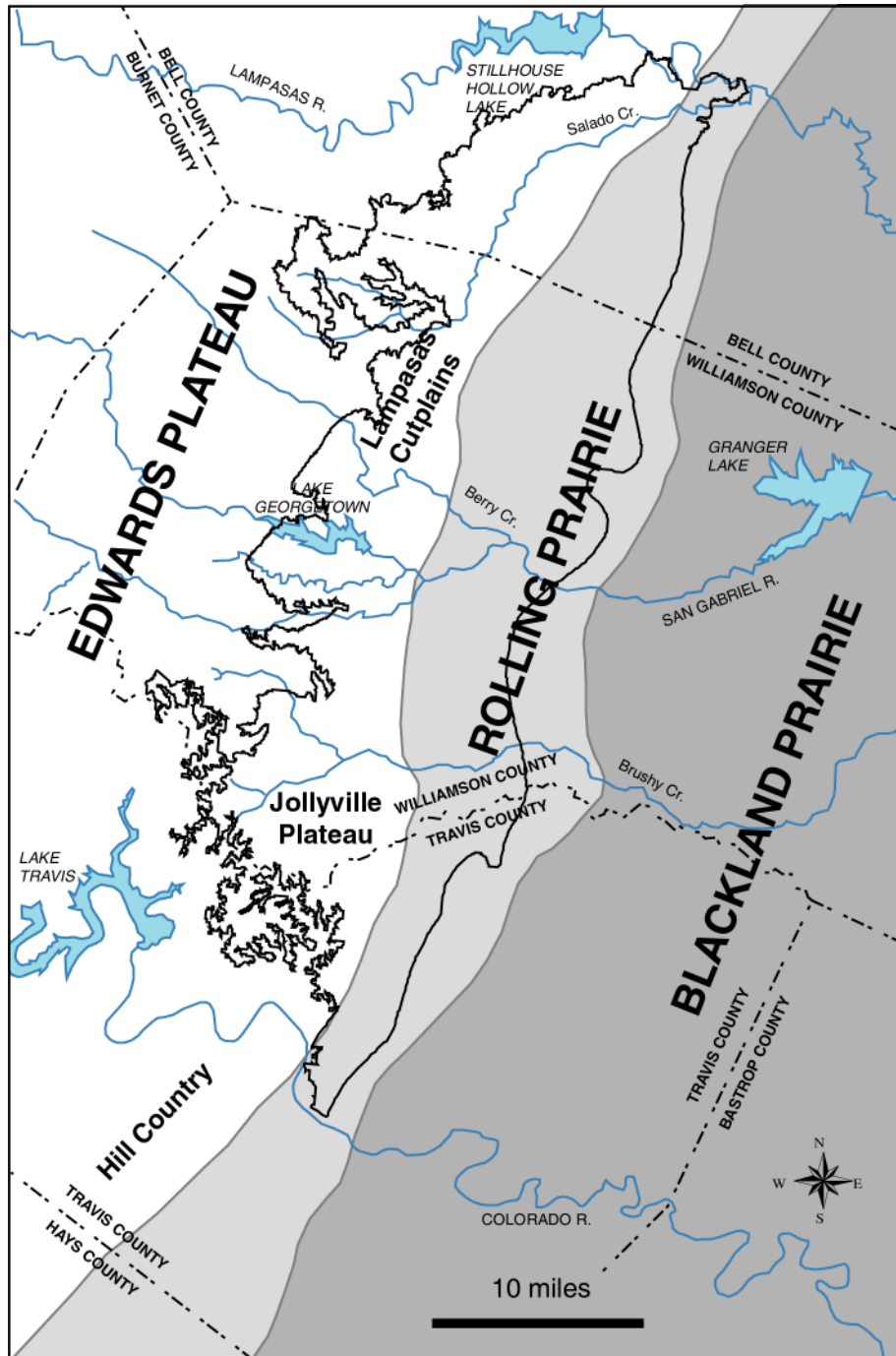
Figure 3-5.   Physiographic provinces in the study area (modified from Senger and others, 1990).
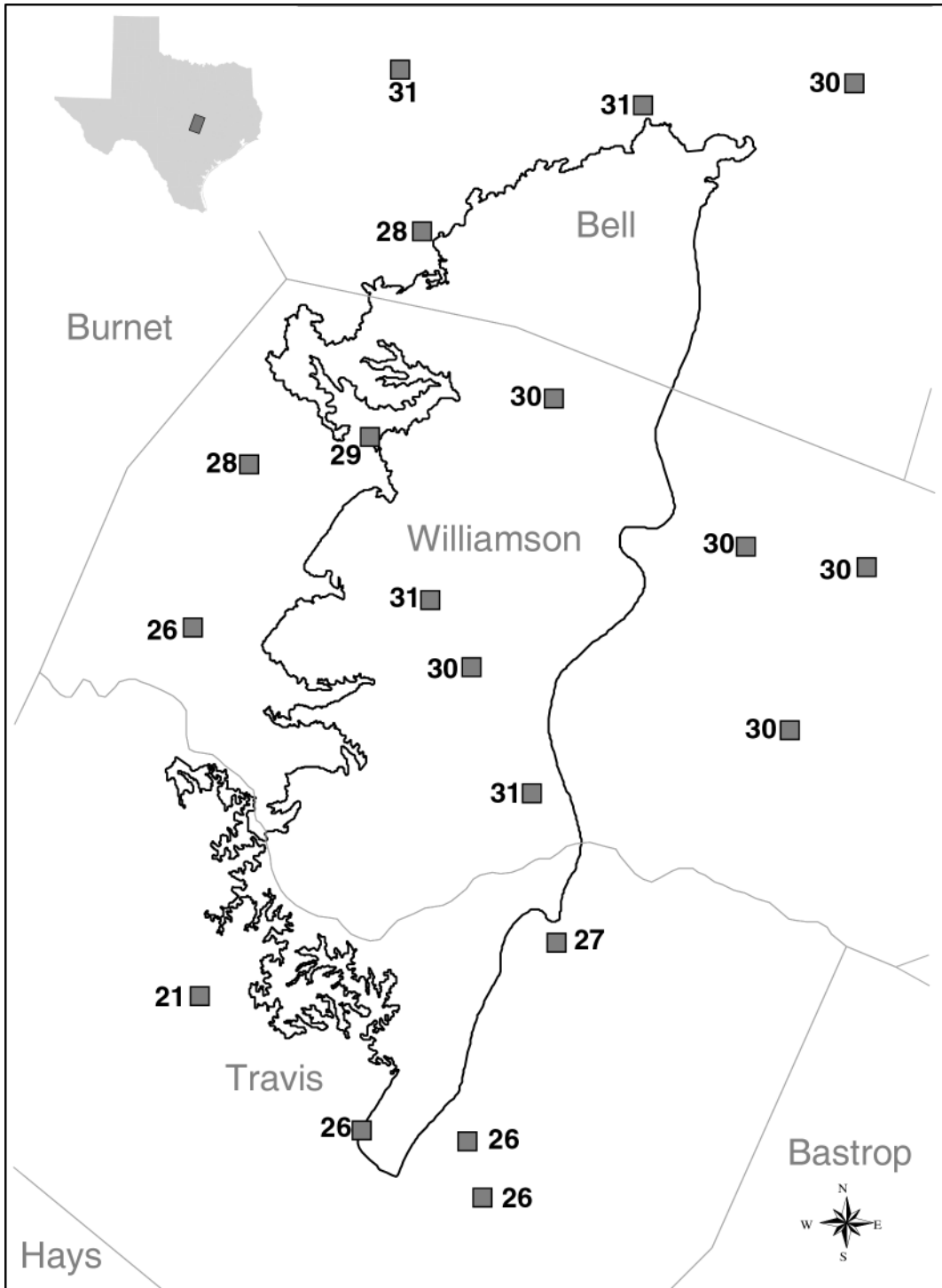
Figure 3-6.   Mean annual precipitation (inches) in the study area, from National Climate Data Center.
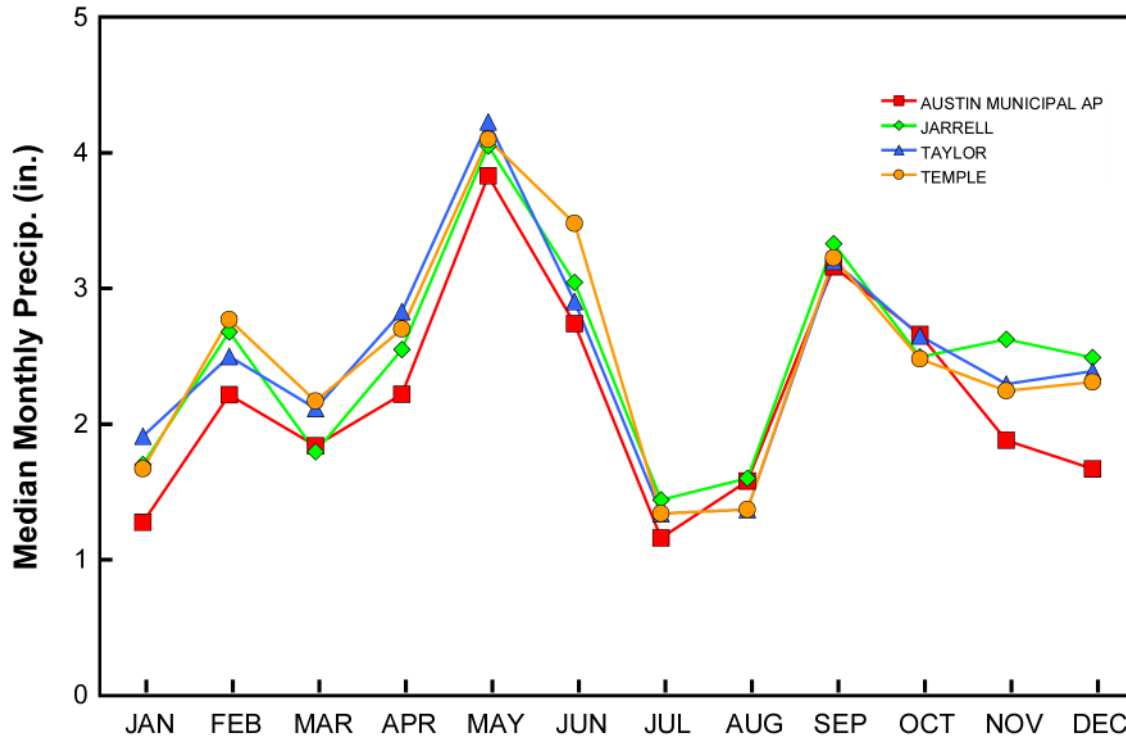
Figure 3-7.   Mean monthly precipitation at selected stations in the study area, from National Climate Data Center.

Average monthly lake-surface evaporation in this region ranges between 2 and 8 inches (fig. 3-9). Lake-surface evaporation is typically highest during summer months (June through August) and lowest during winter months (December through February), when precipitation exceeds evaporation. The average annual temperature in this region is 68 °F, with mean maximum and minimum temperatures of 95 °F and 41 °F, respectively (Brune and Duffin, 1983).

3.2   Geology

Stratigraphic units underlying the study area range in age from the Paleozoic Ellenburger Group to Recent alluvium (Brune and Duffin, 1983). Only Cretaceous and younger rocks are exposed at the surface (fig. 3-10). Most of these stratigraphic units crop out along the Balcones Fault Zone, a zone of normal faulting that trends northeast-southwest through the study area (Trippet and Garner, 1976). Total displacement of the Balcones Fault Zone is up to 1,200 feet. Stratigraphic units in the study area are composed mainly of limestone and shale or clay. The oldest rock units, the Ordovician Ellenburger Group and the Pennsylvanian Bend and Strawn groups, occur at great depth and are not known to yield usable water in the study area (Brune and Duffin, 1983). The most important aquifer units in the study area occur in the Cretaceous Trinity, Fredericksburg, and Washita Groups (fig. 3-11). These Cretaceous units are approximately 2,000 feet thick and dip gently toward the southeast (Trippet and Garner, 1976).

9
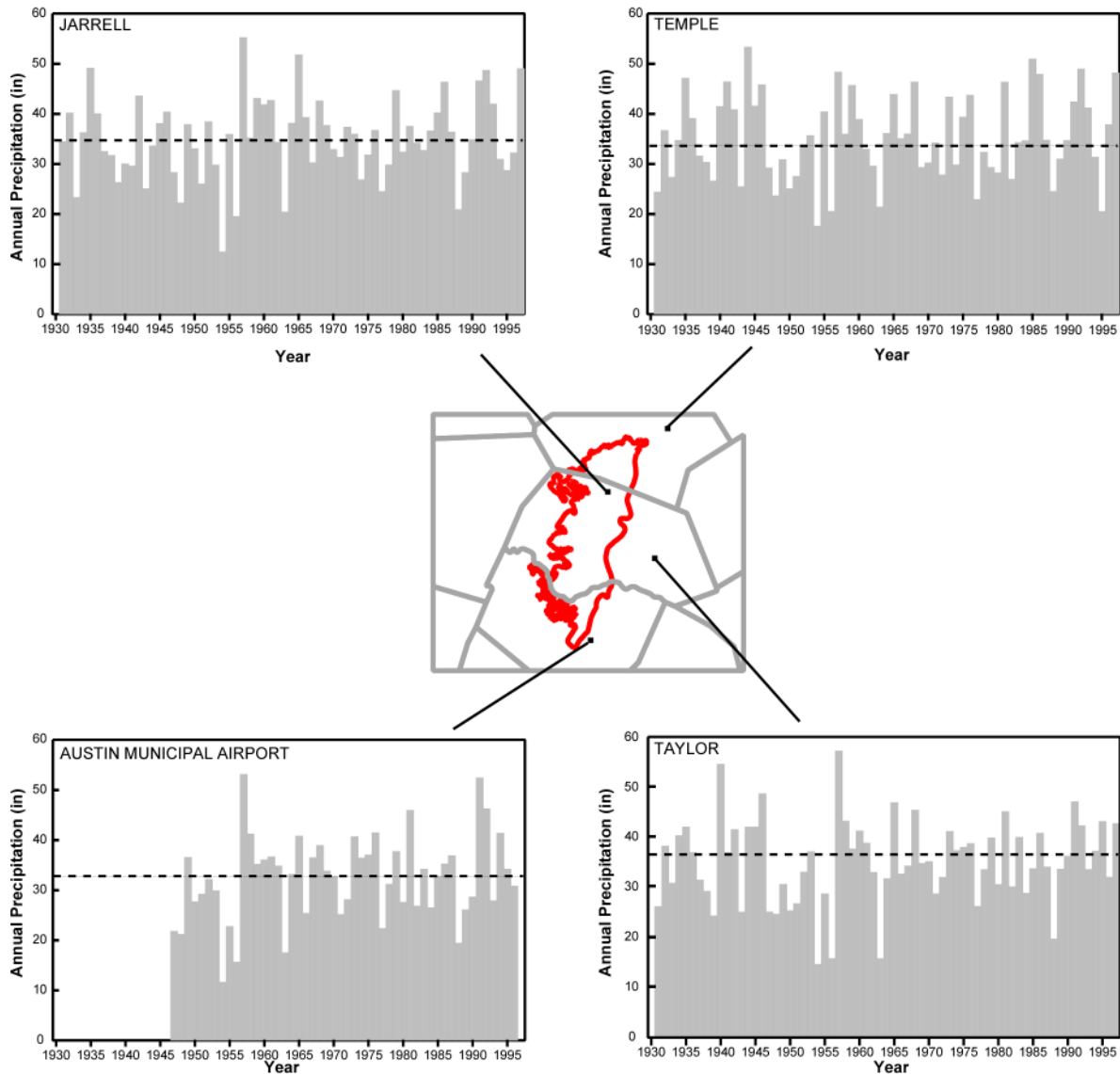
Figure 3-8.   Historical annual precipitation at selected stations in the study area, from National Climate Data Center. The dashed lines represents the mean average precipitation for each station.

The Trinity Group is divided into the Travis Peak, Glen Rose, and Paluxy Formations (Brune and Duffin, 1983). The Travis Peak Formation consists primarily of limestone, sand, and shale. The Glen Rose Formation is predominantly composed of alternating layers of limestone and dolomite at the top and massive layers of limestone and dolomite at the base. The Paluxy Formation is composed of fine quartz sand cemented by calcium carbonate. In the study area, this formation is relatively thin, up to 10 feet thick.

The Fredericksburg Group is divided into the Walnut Formation, Comanche Peak Limestone, and Edwards Limestone (Brune and Duffin, 1983). The Walnut and Comanche Peak Formations

10
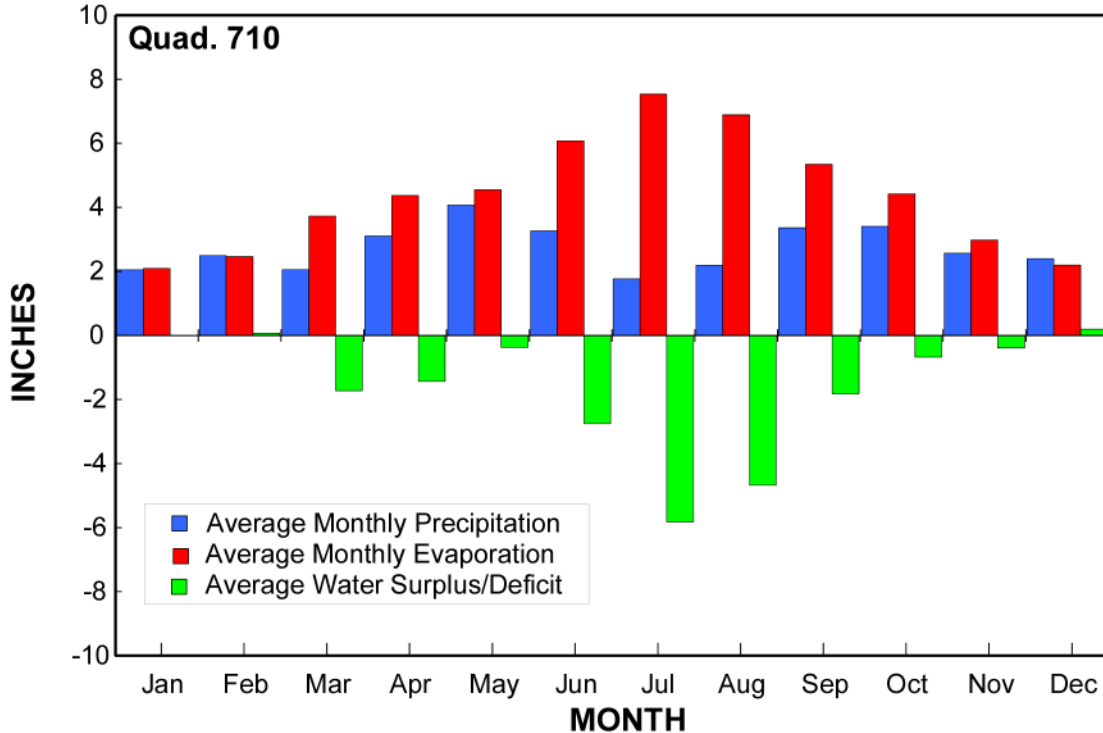
Figure 3-9.   Mean monthly precipitation and pan evaporation from TWDB database.

are composed of fine-grained limestone and shale. The Walnut and Comanche Peak Formations occur primarily in the subsurface in the northern part of the study area. The Edwards Limestone is composed of massive vuggy limestone with fine-grained marl at the top of the formation. This marl is very thin in the study area and tends to become thicker toward the north.

The Washita Group is divided into the Georgetown Formation, Del Rio Clay, and Buda Limestone (Brune and Duffin, 1983). The Georgetown Formation thins southward and is composed of fine-grained limestone that in places is hydraulically connected to the Edwards Limestone. The Del Rio Clay and Buda Limestone are composed of shale and fine-grained limestone, respectively (Brune and Duffin, 1983).

The stratigraphic nomenclature of units that compose the Edwards aquifer differs north and south of the Colorado River. South of the river, the "Edwards" is treated as a group composed of two formations, the Kainer and Person Formations (Rose, 1972). The Kainer Formation is equivalent to the Walnut Formation, Comanche Peak Limestone, and lower parts of the Edwards Limestone. Equivalents of the Person Formation are largely absent north of the Colorado River. North of the Colorado River, the uppermost parts of the Edwards Limestone are equivalent to the basal members of the Person Formation.
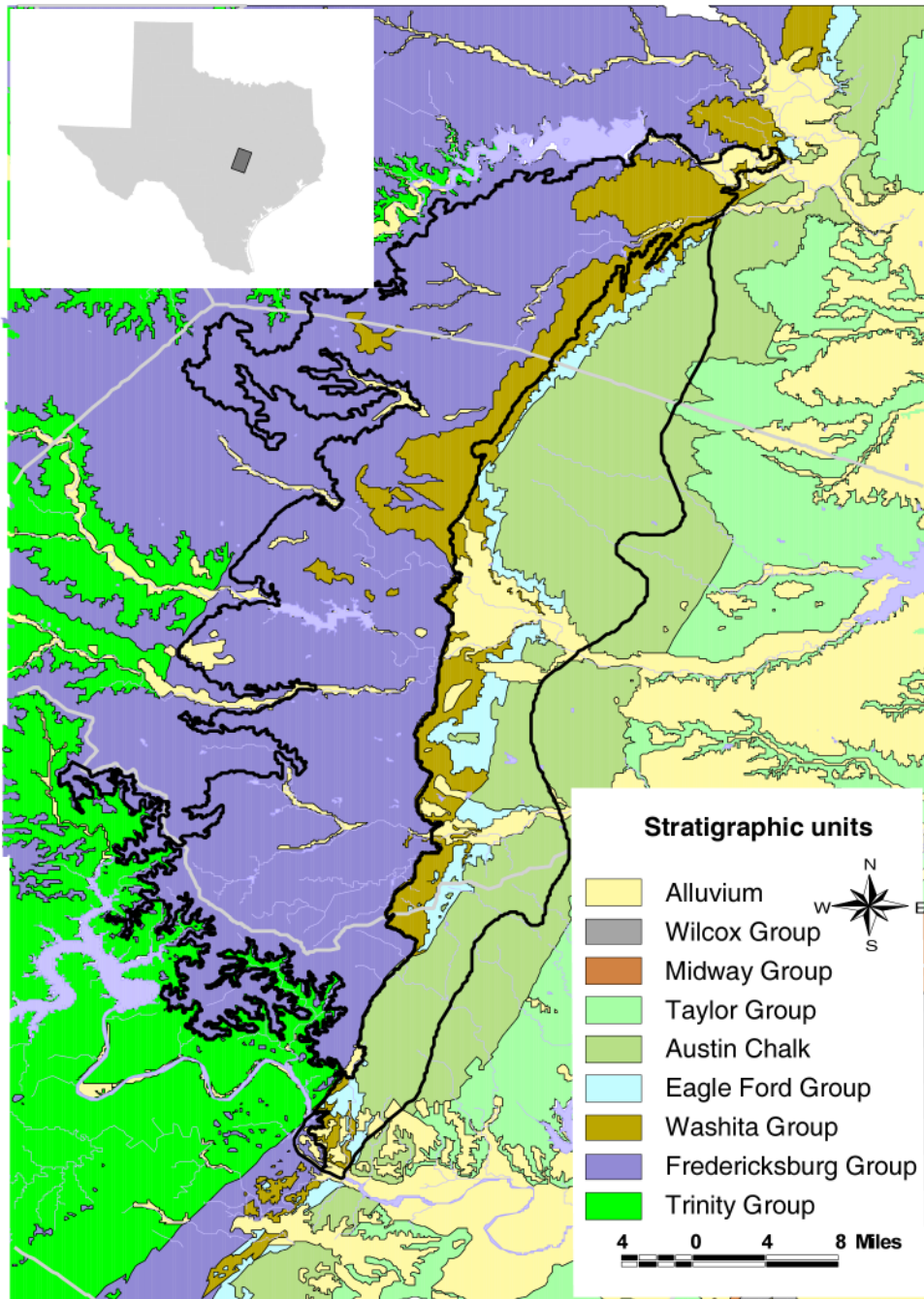
Figure 3-10.   Surface geology in the study area.

Series	Group	Stratigraphic Unit		Hydrologic Unit	Maximum Thickness (feet)
Gulf	Navarro			Navarro and Taylor Group	850
	Taylor				
	Austin			Austin Chalk	450
Comanche	Eagle Ford				50
	Washita	Buda Limestone			50
		Del Rio Clay			60
		Georgetown Formation		Edwards aquifer	100
	Fredericksburg	Edwards Limestone			200
		Comanche Peak Limestone			50
		Walnut Formation			150
	Trinity	Paluxy Formation		Upper Trinity	10
		Glen Rose	Upper Member		450
			Lower Member	Middle Trinity	450
		Travis Peak	Hensell Sand Member		100
			Cow Cr. Limestone Member		100
			Hammett Shale Member		50
			Sligo Member	Lower Trinity	150
			Hosston Member		850

Figure 3-11.   Stratigraphic and hydrostratigraphic units in the study area.

4.0   Previous Work

Many geologic and hydrogeologic reports include the northern segment of the Edwards aquifer. Studies of the stratigraphy and structure of the area include Tucker (1962), Proctor and others (1974), Collins (1987), and Kreitler and others (1987). Woodruff and others (1985) and Yelderman and others (1987) are compendia that provide information on different aspects of the hydrogeology of the northern segment, such as water supply development, transmissivity distribution, and pump-test analysis. More detailed hydrogeologic studies include Klemt and others (1975), Brune and Duffin (1983), Senger and Kreitler (1984), Baker and others (1986), Kreitler and others (1987), Flores (1990), Duffin and Musick (1991), and Ridgeway and Petrini (1999). Senger and others (1990) discussed both the groundwater geochemistry and hydrology of the northern segment. The review of groundwater flow models conducted in Texas by Mace (2001b) indicates that there are no published models for the northern segment of Edwards aquifer.

Several regional and sub-regional models have simulated groundwater flow in the San Antonio and Barton Springs segments of the Edwards aquifer (Campana, 1975; Knowles and Klemt, 1978; Mahin, 1978; Klemt and others, 1979; Mahin and Campana, 1983; Slade and others, 1985; Maclay and Land, 1988; Kuniansky, 1993; Kuniansky and Holligan, 1994; Barrett, 1996; Uliana

and Sharp, 1996; Scanlon and others, 2001). However, none of these models extended north of the Colorado River.

5.0 Hydrogeology

The hydrogeologic setting of the northern segment of the Edwards aquifer is described by hydrostratigraphy, structure, water levels, recharge, discharge, surface-water features, and hydraulic properties. Each of these factors is described in more detail below.

5.1. Hydrostratigraphy

The northern segment of the Edwards aquifer generally consists of the Comanche Peak Limestone, Edwards Limestone, and Georgetown Formation (fig. 5-1). These stratigraphic units constitute the upper Fredericksburg and lower Washita Groups and are collectively referred to as the Edwards and associated limestones (Brune and Duffin, 1983). The aquifer overlies older Cretaceous rock of the Walnut and Glen Rose formations and is overlain by younger units that consist of the Del Rio Clay, Buda Limestone, Austin Chalk, Taylor Marl, and Navarro Group. The Walnut Formation and Del Rio Clay are recognized as confining units (Brune and Duffin, 1983; Baker and others, 1986). The base of the aquifer is defined as the base of rocks having greater water-yielding capabilities (Baker and others, 1986). In most areas, this excludes the Walnut Formation, although in other areas the Walnut Formation is composed of potentially permeable shell beds and may thus be included in the Edwards aquifer. Karstification in the form of honeycombing, sinkholes, and caves allows rapid infiltration and percolation of water through the aquifer.
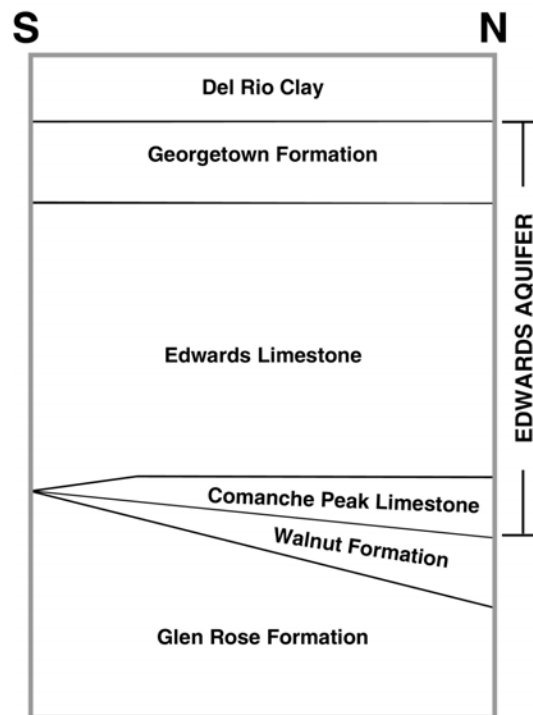
Figure 5-1.   Schematic stratigraphic column of the study area.

The Comanche Peak Limestone is composed of nodular and fossiliferous marly limestone. This unit is characterized by considerable jointing (Brune and Duffin, 1983). The Edwards Limestone is composed of 200 to 350 feet of highly fractured and thickly bedded to massive limestone or dolomite, with minor shale, clay, and siliceous limestone. The Edwards Limestone consists of the Kainer, Person, Kiamichi, and Duck Creek formations. The Person and Kainer formations are composed of brittle, massive limestone that is sometimes dolomitic (Flores, 1990). The Edwards Limestone is vuggy in places because of the occurrence of solution-collapse zones (Brune and Duffin, 1983). These zones, parallel to bedding planes, are the result of dissolution of gypsum beds that formerly occurred in this stratigraphic unit. They are cavernous and iron stained and contain brecciated limestone, chert, crystalline calcite, and residual clay. They occur mainly 60 to 80 feet above the base of the Edwards Limestone, within the Person and Kainer formations, and are often referred to as the Kirschberg solution zone (Brune and Duffin, 1983; Flores, 1990). These solution-collapse zones, as much as 20 feet thick, are the main water-bearing horizons in the aquifer, with well yields greater than 300 gallons per minute (Brune and Duffin, 1983; Flores, 1990). The Kiamichi and Duck Creek formations constitute the Regional Dense Member near the top of the Edwards Limestone, especially in the northern part of the study area. The Regional Dense Member separates the Edwards aquifer into upper and lower units that may be circumvented by fault displacement (Flores, 1990). The Georgetown Formation is a massive nodular limestone that is often hydrologically connected to the underlying Edwards Limestone (Brune and Duffin, 1983).

In addition to solution-collapse zones, groundwater in the Edwards aquifer flows through a network of steeply dipping faults and joints (Brune and Duffin, 1983). Field measurements indicate that effective porosity is greatest in the Comanche Peak Limestone and decreases in the overlying Edwards Limestone and Georgetown Formation (Dahl, 1990; Flores, 1990). This trend has been attributed to limestone in the Comanche and Edwards being more brittle than that in the Georgetown Formation. Additionally, the lower units of the Edwards aquifer display greater effects of karstification (Dahl, 1990; Flores, 1990). Fracture porosity of the Edwards aquifer ranges from 0.4 to 2.5 percent away from major faults, to 1.5 to 4.25 percent adjacent to faults (Dahl, 1990). These porosity values are lower than porosities (4 to 42 percent) measured in the San Antonio segment of the Edwards aquifer (Hovorka and others, 1996).

5.2   *Structure*

The structural features that most influence groundwater flow in the study area are regional dip and the occurrence of the Balcones Fault Zone. Cretaceous rock overlies Paleozoic rock, forming an angular unconformity (Brune and Duffin, 1983), indicating that the Cretaceous rock was deposited on an erosional surface over steeply westward-dipping Paleozoic rock. The Cretaceous rock dips toward the southeast at 10 to 300 feet per mile, generally increasing with depth (Figure 4-2; Brune and Duffin, 1983). This dip angle excludes the effects of faulting.

The unconfined portion of the northern segment of the Edwards aquifer consists of the outcrop of the Edwards and associated limestones, which is wider in the north than in Travis County, near the Colorado River (fig. 3-10). This narrowing of the outcrop in the south occurs as a result of the combined effects of intense faulting and large topographic variations (fig. 5-2 and 5-3)

15
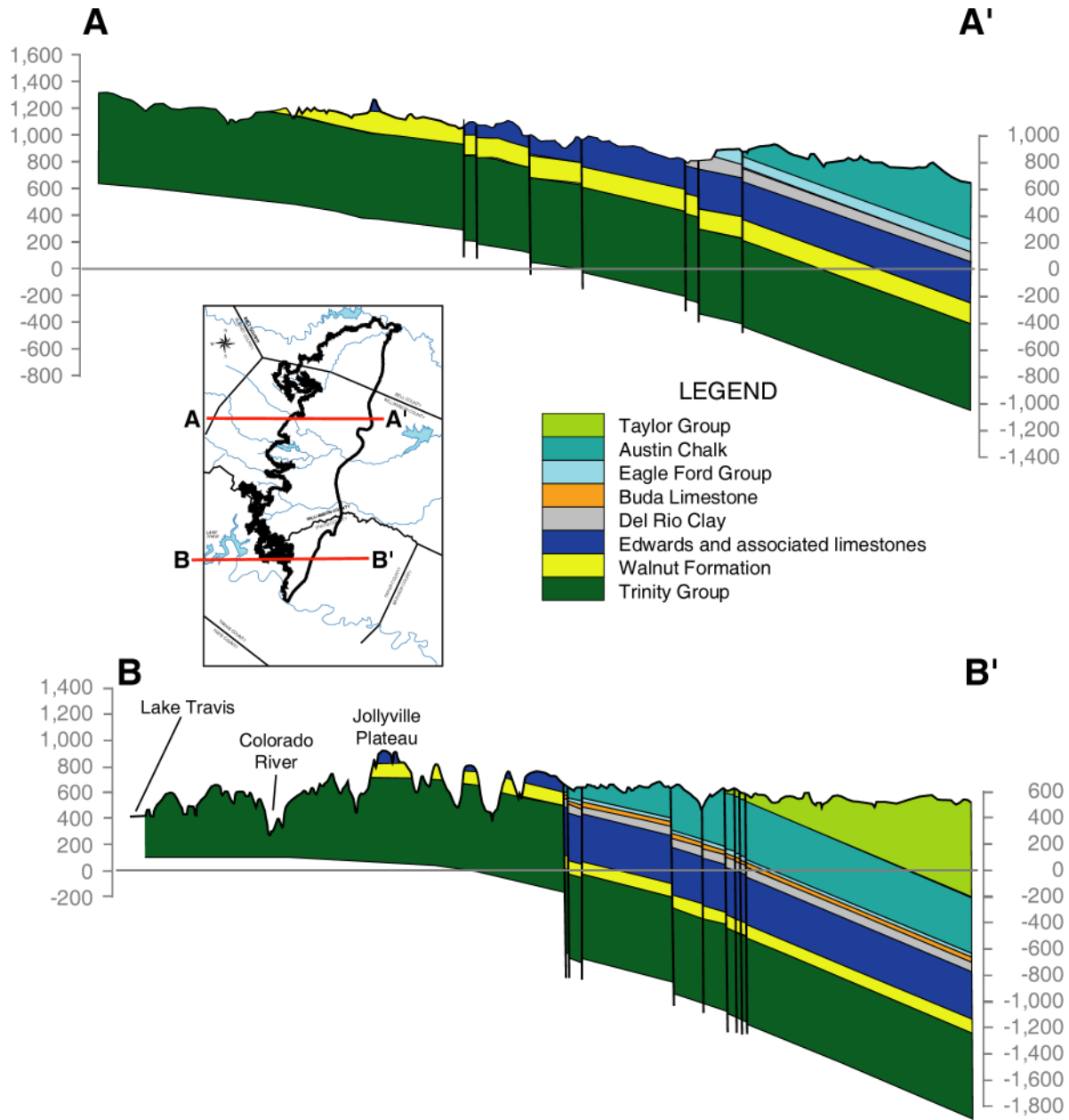
Figure 5-2. Geologic cross sections of the northern segment of the Edwards aquifer.

(Baker and others, 1986). Fracturing of the limestone also enhances the porosity of the limestone and plays a role in the development of karst features. Normal faulting, common in the southern portion of the study area, generally decreases toward the north (Baker and others, 1986). It is associated with the Balcones Fault Zone, a zone of faults about 6 to 8 miles wide that extends from Del Rio in south-central Texas to Dallas. This zone of normal faulting is characterized by major faults that strike north-south to northeast-southwest and dip 40 to 80° to the east, with a
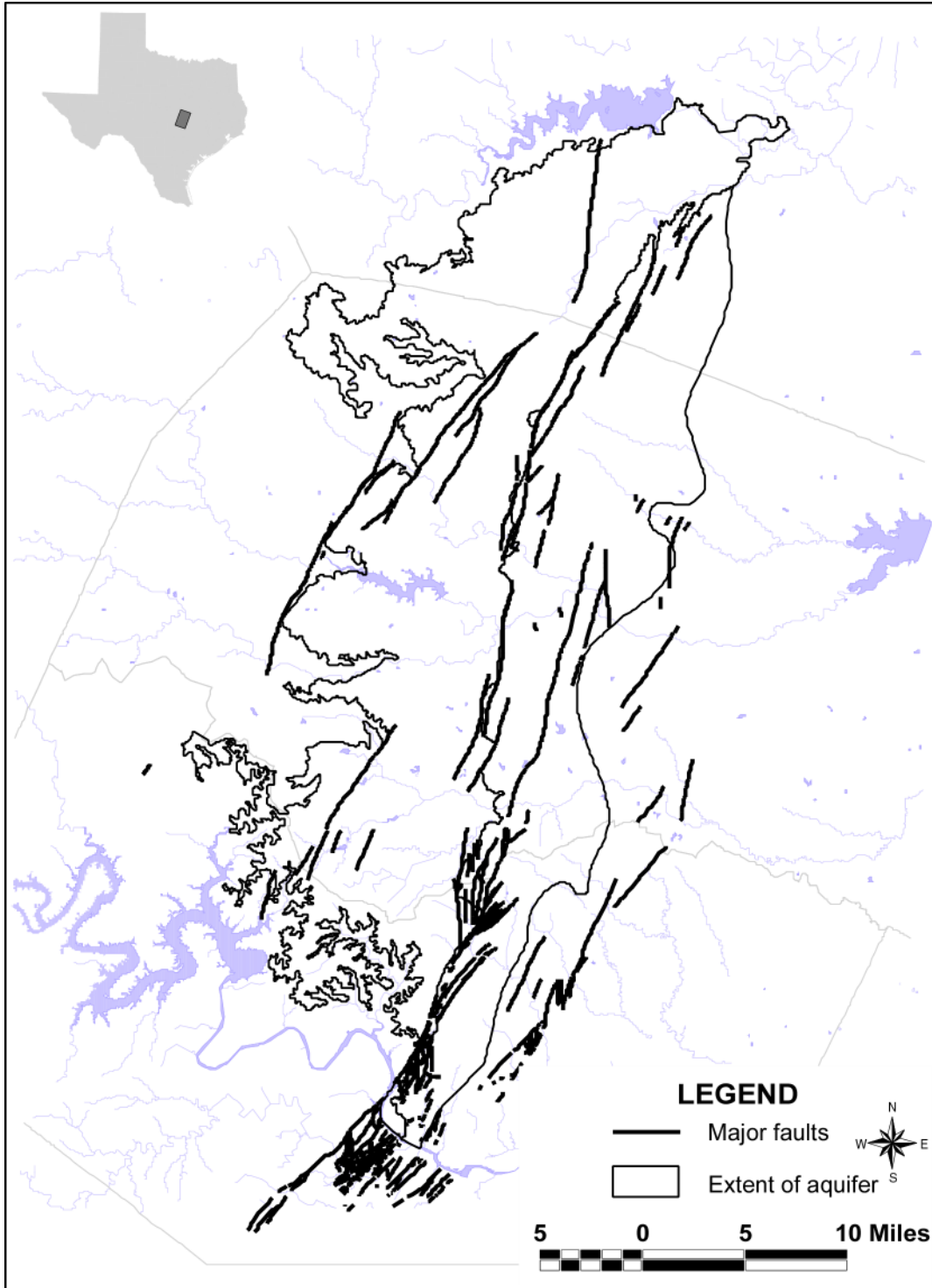
Figure 5-3.   Major faults in the study area (adapted from Bureau of Economic Geology, 1981).

net displacement of 600 to 1,000 feet (Brune and Duffin, 1983; Collins, 1987). Cross faults, sub-perpendicular to major faults, are also common (Collins, 1987). In the Balcones Fault Zone, minor faults and joints occur mainly adjacent to the major faults and flexures. These minor faults, characterized by displacement of less than 6 feet, tend to form fracture zones up to 1 mile wide. Fracture densities in these zones lie in the range of 6 to 120 joints per 100 feet. Many of these minor faults are filled partly by calcite. However, the joints that occur in this area do not have mineral fillings, and abutting relationships suggest that these minor faults formed before the joints (Collins, 1987). Fracture apertures vary with stratigraphic units in the Edwards aquifer. Fracture apertures are generally less than 0.04 inches in Comanche Peak and Georgetown Formations and are up to several inches wide in the Edwards Limestone (Collins, 1987). These faults influence groundwater flow in two ways: faults provide preferential flow paths, and fault displacement in some cases produces barriers to groundwater flow (Brune and Duffin, 1983). Preferential groundwater flow along faults and joints in this aquifer often results in formation of solution cavities such as caves (Brune and Duffin, 1983).

Evaluation of fracture and lineament orientations in the northern part of the study area at different scales by Dahl (1990) shows different orientations of fractures varying in size from mapped major faults to field-observed fractures. The orientations of these fractures play a role in determining anisotropy in the aquifer. Dahl (1990) divided fractures into four groups: major mapped faults, high-altitude Landsat lineaments, field fractures, and topographic map lineaments. Major faults generally trend northeast-southwest. High-altitude Landsat lineaments are sparsely distributed and, together with the field fractures, are preferentially oriented northwest-southeast and northeast-southwest. The topographic map lineaments are generally randomly oriented, with only a slight northeast-southwest trend (Dahl, 1990). Adjacent to major faults, fractures are oriented generally northeast-southwest, approximately parallel to major faults of the Balcones Fault Zone. Away from major faults, fractures are oriented generally northwest-southeast. This trend of northwest-southeast- and northeast-southwest-oriented fractures is also observed in the more intensely faulted parts of the aquifer farther south (Kreitler and others, 1987).

The Edwards aquifer dips to the east at an average slope of 60 to 75 feet per mile (fig. 5-4 and 5-5). The slope varies generally because of faulting that produces a stair-step configuration downdip (Baker and others, 1986). The thickness of the northern segment of the Edwards aquifer increases generally toward the east, varying from less than 100 feet along the southern and western margins of the aquifer to more than 500 feet in the east (fig. 5-6).

5.3   *Water Levels and Regional Groundwater Flow*

In the northern segment of the Edwards aquifer, the potentiometric surface slopes generally toward the east and south adjacent to the Colorado River (fig. 5-7). Hydraulic gradients in the aquifer decrease east of the main faults of the Balcones Fault Zone (Senger and others, 1990). Intense fracturing in the Balcones Fault Zone suggests that the aquifer is anisotropic because of preferential flow through the generally northeast-southwest-oriented fractures (Baker and others, 1986; Duffin and Musick, 1991). Groundwater flow along fractures is responsible for the southward flow in the southern part of the study area, where fracturing is most intense. Senger and others (1990) suggested that some of the major faults, especially in the south, also act as

18
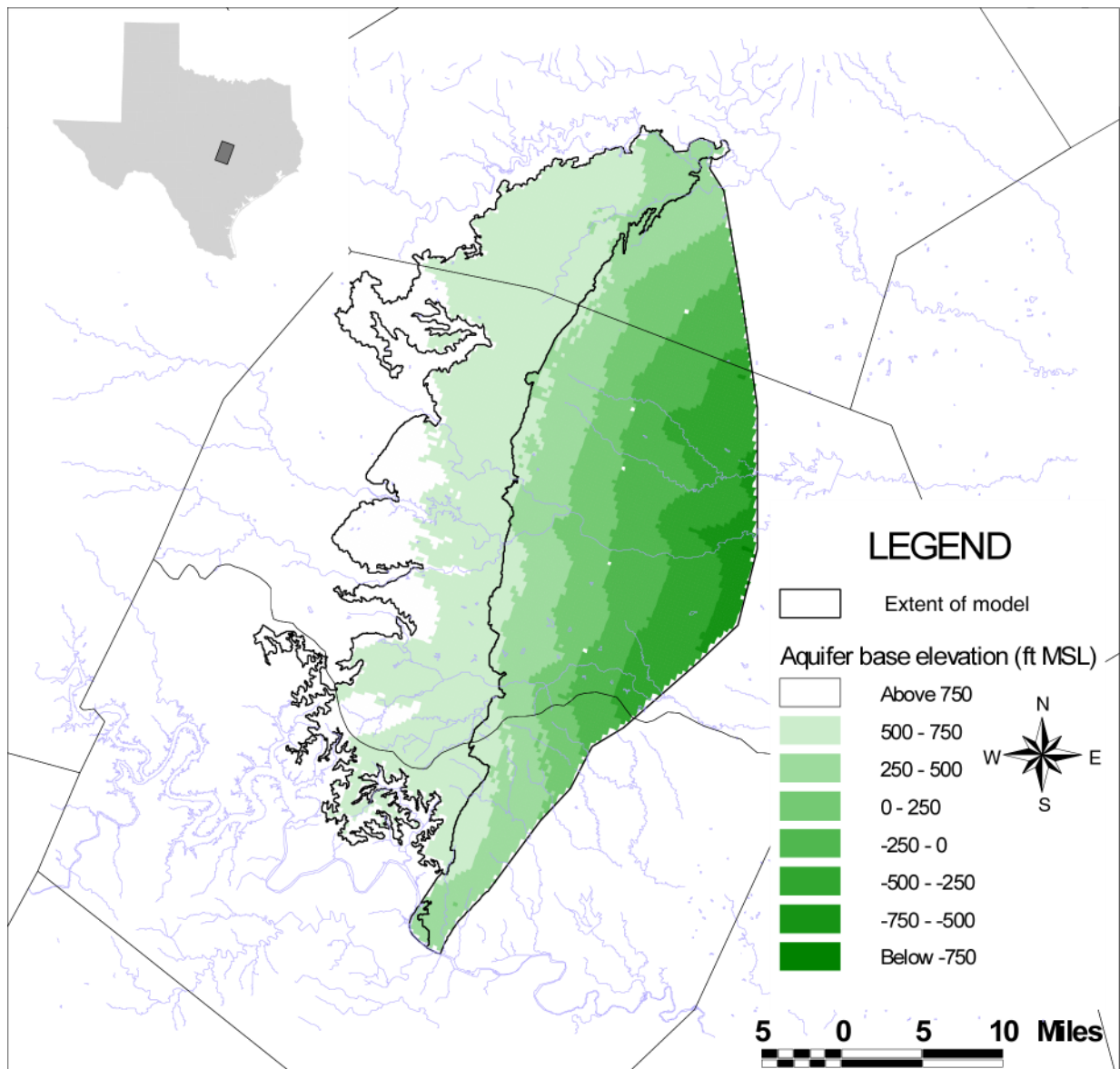
Figure 5-4. Elevation of the base of the Edwards aquifer (based on data from Collins and others, 2002).

hydraulic barriers, restricting west-to-east groundwater flow. In the central and northern parts of the aquifer, where faulting is less intense, the influence of fractures on regional groundwater flow is less apparent (Senger and others, 1990).

In the unconfined part of the aquifer, the water table occurs generally less than 100 feet below land surface and may approach land surface along incised streams (Senger and others, 1990). In the confined part of the aquifer, water levels approach or may in some cases exceed land surface, resulting in flowing wells. Water-level fluctuations observed in this aquifer are responses to changes in recharge and discharge rates associated with rapid recharge during wet periods (Baker and others, 1986). Adjacent to the Colorado River, water-level fluctuations are relatively small

19
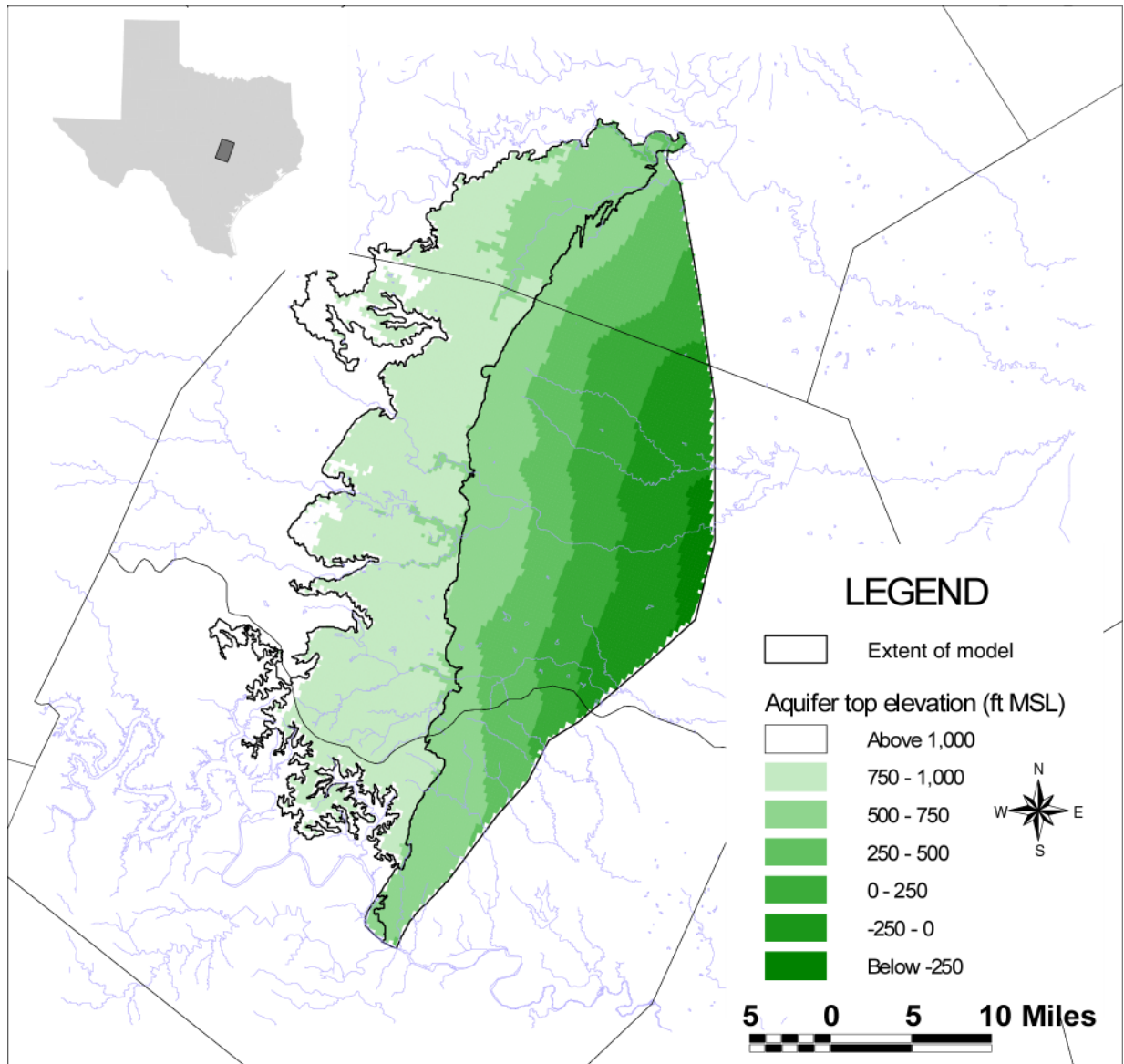
Figure 5-5.   Elevation of the top of the Edwards aquifer (based on data from Collins and others, 2002).

because of the stabilizing effect of adjacent Lake Austin and Town Lake. Water-level declines have been observed during severe drought periods, such as the mid-1950s, 1983-84, and 1996 (Ridgeway and Petrini, 1999). A few available hydrographs indicate effects of pumping resulting in gradual long-term water-level decline. These hydrographs are from wells located mostly in the Pflugerville-Georgetown area. However, most hydrographs indicate a general balance between recharge and discharge in the aquifer (Baker and others, 1986; Dahl, 1990; Duffin and Musick, 1991; Ridgeway and Petrini, 1999).

Hydrographs in the unconfined part of the aquifer show generally synchronous water-level variations at many locations and a close correlation between precipitation and water-level
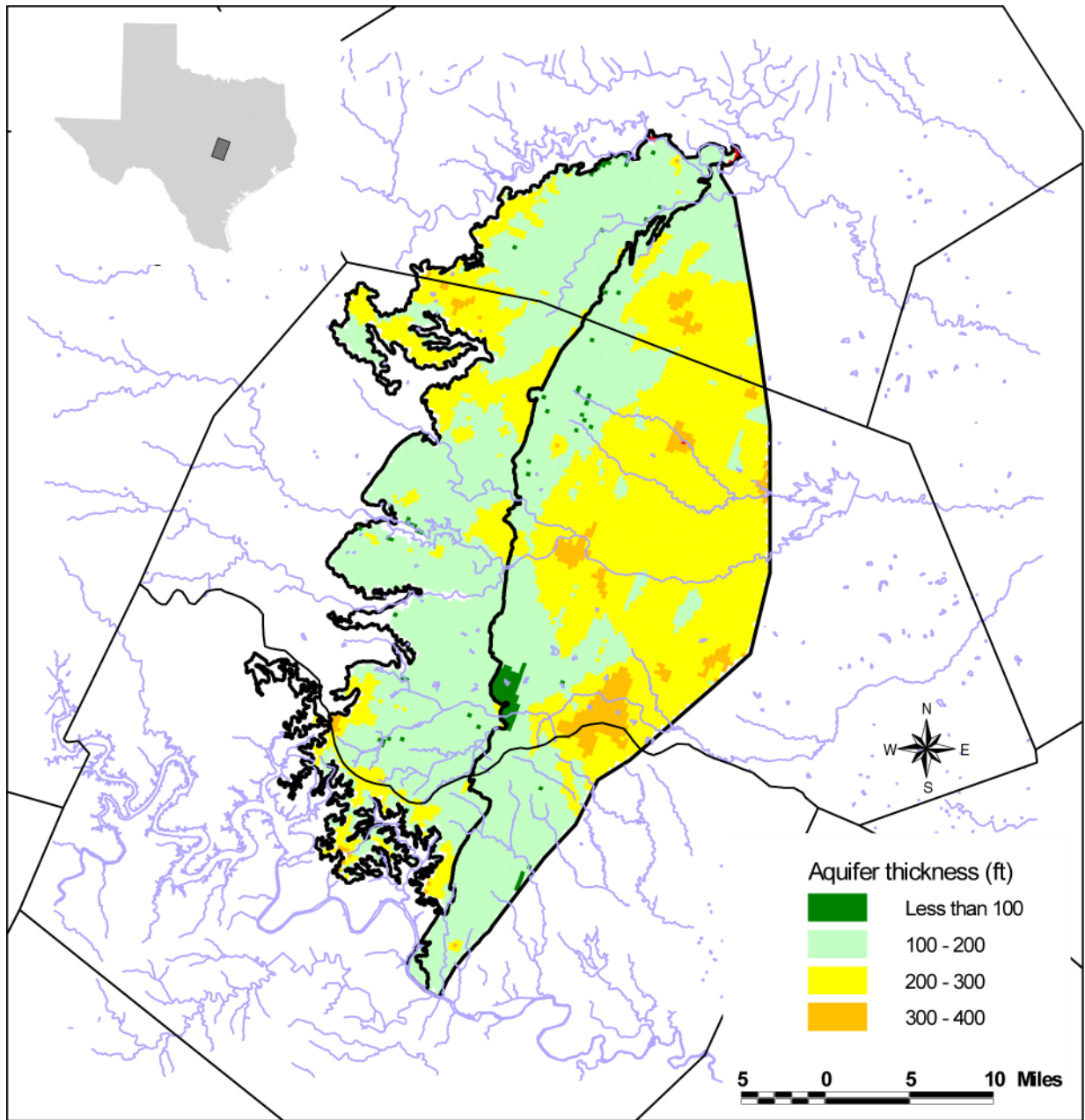
Figure 5-6.   Thickness of the Edwards aquifer (based on data from Collins and others, 2002).

variation (Senger and others, 1990). Rapid water-level rises coincide with major rainfall events, especially during late spring and fall (fig. 5-8). The rate of water-level decline depends on the amount of recharge occurring during the recession period and the amount of nearby pumping (Senger and others, 1990). Continued rainfall tends to retard water-level declines, whereas pumping results in accelerated water-level declines. Hydrographs for wells in the confined part of the aquifer indicate a lag between major recharge events and water-level responses (Senger and others, 1990). In some parts of the aquifer, reversal of hydraulic gradients, partly related to increased pumping, has been observed during drought periods. This reversal suggests a potential

21
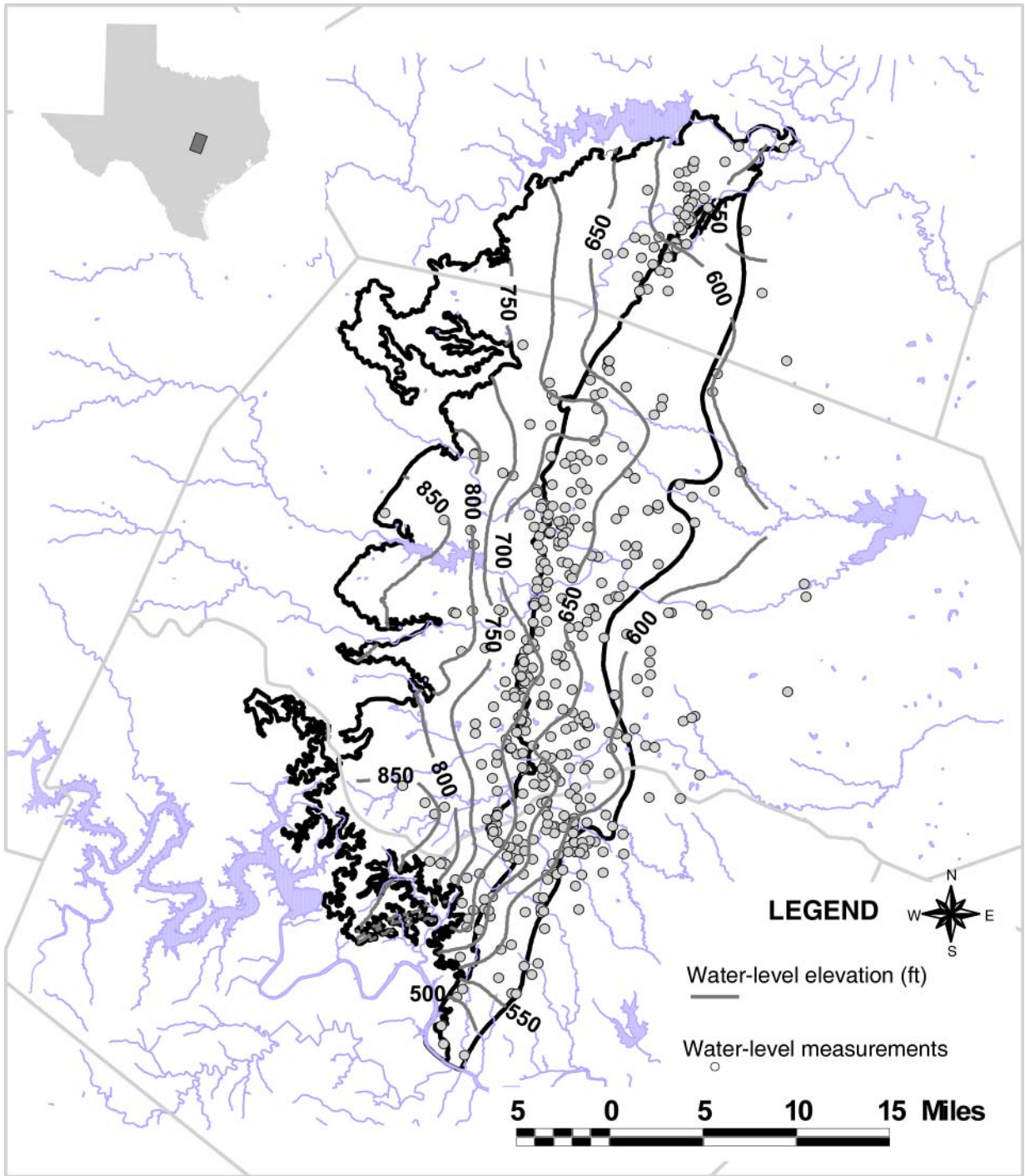
Figure 5-7.   Water-level elevations in the northern segment of the Edwards aquifer.
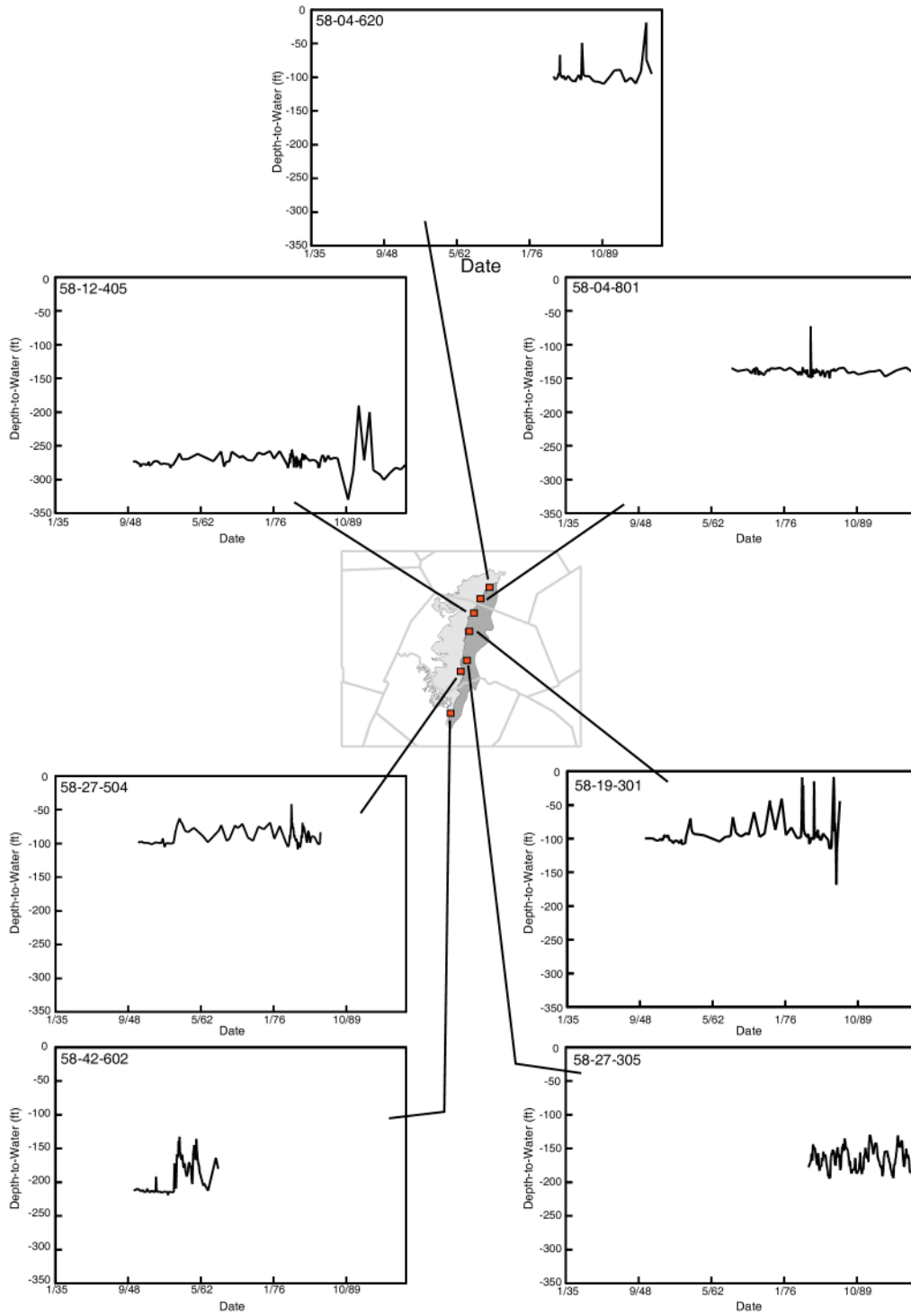
Figure 5-8.   Groundwater hydrographs from selected wells in the study area.

for the influx of saline groundwater from depth. However, large, persistent cones of depression that could potentially produce this influx of saline groundwater have not been identified (Senger and others, 1990).

5.4   *Recharge*

Recharge to the Edwards aquifer takes the form of infiltration of precipitation that falls on the outcrop of the aquifer or infiltration of runoff derived from watershed areas upstream from the aquifer outcrop. The recharge zone in the northern part of the study area consists mainly of gently rolling terrain of the Lampasas Cutplains (fig. 3-5). In the south, the recharge zone is characterized by steeper, more highly dissected terrain of the Jollyville Plateau (Duffin and Musick, 1991). Both areas are characterized by the occurrence of numerous scattered karst features, such as dissolution-enhanced fractures, sinkholes, and caves, which are potential recharge sites. Sinkholes that occur in the Jollyville Plateau can transmit large amounts of water to the aquifer following heavy rainfall events (Kreitler and others, 1987). Recharge also takes the form of infiltration along faults and joints that intersect losing segments of perennial and intermittent streams that cross the study area. These fractures are often enlarged by karstification (Brune and Duffin, 1983). Infiltrating water tends to perch within the Georgetown Formation because of the occurrence of low-permeability shale members. Resultant lateral flow often discharges from small seeps and springs. Rapid recharge occurs when underlying Edwards and Comanche Peak limestones are encountered (Dahl, 1990).

Recharge processes are more complex in the north, where whether stream segments are gaining or losing depends on relative elevations of the water table and streambeds and thus may vary seasonally (Duffin and Musick, 1991). Streamflow studies by the United States Geological Survey (USGS) in 1978 and 1979 indicate that, in the north, streams generally act as points of groundwater discharge rather than recharge (fig. 5-9); (Senger and others, 1990; Duffin and Musick, 1991; Slade and others, 2002). Recharge in the north occurs primarily by intermittent streams and by infiltration of precipitation on the outcrop. Recharge also occurs in losing segments of the major rivers that occur along the western margin of the aquifer (Dahl, 1990; Slade and others, 2002). This recharge results in the formation of groundwater mounds along the upstream margin of the aquifer (fig. 5-7). Potential for recharge by cross-formational flow also exists from the underlying Trinity aquifer (Duffin and Musick, 1991).

Recharge estimates in the Salado Creek basin by Dahl (1990) indicate recharge of 15 percent of precipitation over the aquifer outcrop and 60 percent of storm runoff originating from upstream of the aquifer outcrop. These estimates of precipitation recharge were based on groundwater-level responses and an assumption of 2 percent porosity. The storm-runoff recharge was estimated based on stream discharge measurements above and below losing stream segments. Dahl (1990) indicated that recharge of precipitation in the Salado Creek basin contributes much larger volumes of water to the aquifer (about 29,000 acre-feet in 1985) than storm runoff (about 2,700 acre-feet).

Recharge due to cross-formational flow from the underlying Trinity aquifer is a possibility. However, it is unlikely that such cross-formational flow would contribute significantly to the Edwards aquifer because the two aquifers are separated by low-permeability units of the Glen Rose Formation hundreds of feet thick.
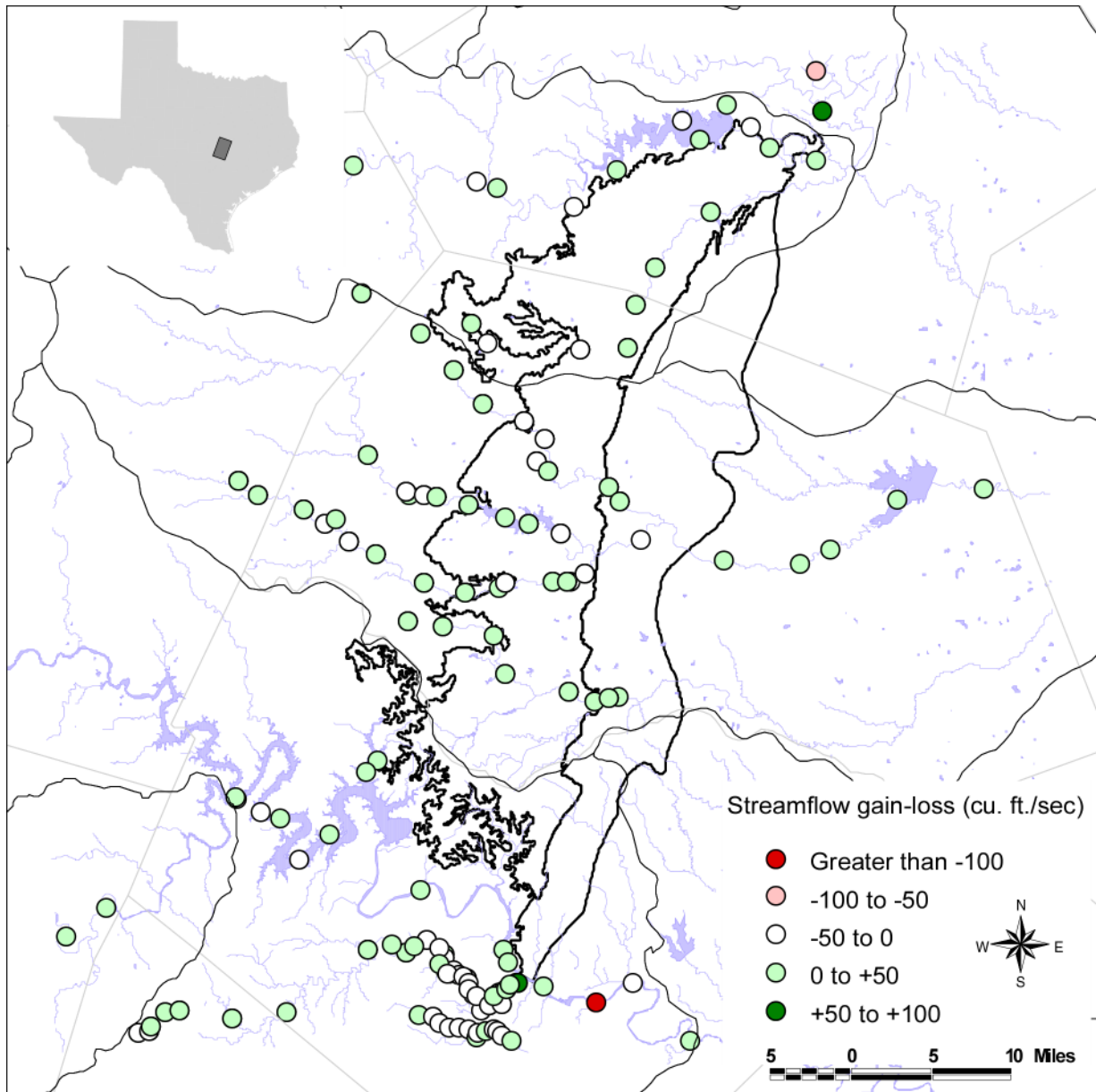
Figure 5-9.   Streamflow gain-loss data from Slade and others (2002).

5.5   *Rivers, Streams, Springs and Lakes*

The northern segment of the Edwards aquifer is bisected by the hydrologic divide between the Colorado and Brazos River basins (fig. 5-10). This hydrologic divide coincides approximately with the boundary between Travis and Williamson counties. Consequently, surface water flows to the north and east toward the Brazos River in Bell and Williamson counties and toward the south to the Colorado River in Travis County. The Lampasas and Colorado rivers that form the northern and southern boundaries of the study area are the largest rivers in the area. Smaller rivers and creeks, such as Brushy Creek, Berry Creek, Salado Creek, and San Gabriel River,
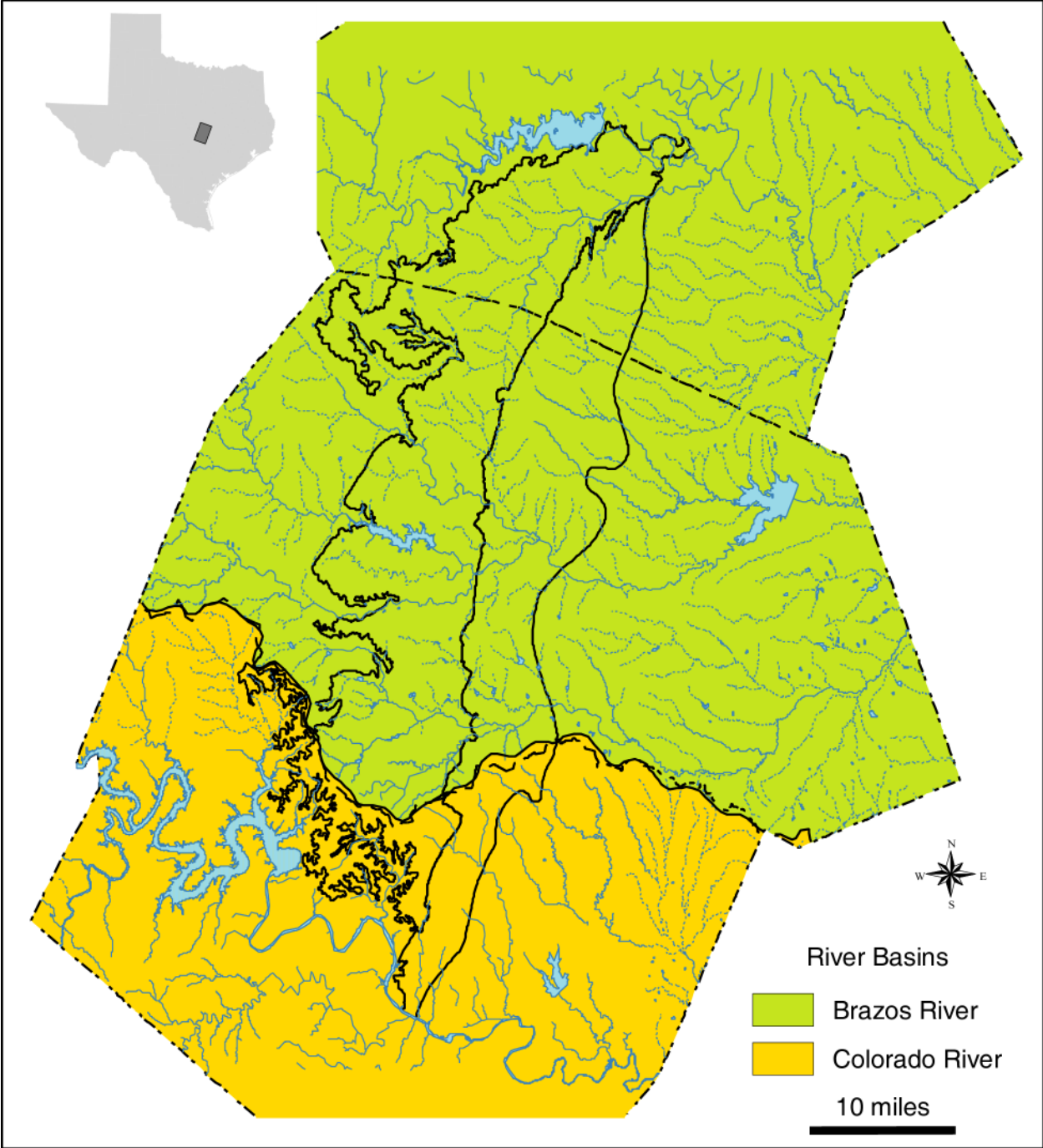
Figure 5-10.   Location of river-basin boundaries in the study area.

cross the outcrop of the aquifer and are likely recipients of groundwater discharge, indicated by their perennial flow. Smaller tributaries of these rivers and creeks often flow intermittently as a result of storm-related runoff. Groundwater and surface-water systems are closely related in recharge and discharge zones, where interchange occurs as a result of recharge and discharge processes, respectively (Baker and others, 1986). Groundwater-surface-water interaction along gaining and losing stream segments of major rivers and creeks varies by location and hydrologic conditions because of significant hydrologic connections between streams and the underlying aquifer (Land and Dorsey, 1988).

In the study area, the relative impact on streamflow of storm-related runoff and groundwater discharge in the form of baseflow varies. Streams in which streamflow is dominated by baseflow are characterized by relatively small flow-rate fluctuations. Salado Creek, which is dominated by spring discharge, especially from Salado Springs, is an example of this type of stream (fig. 5-11). Streams dominated by storm runoff, such as Shoal Creek, are characterized by rapid recession after storms and low baseflow. Streamflow in Berry Creek is more representative of the streams in the study area, and streamflow fluctuations indicate inputs from both baseflow and storm-related runoff. Comparison of streamflow at pairs of stream gages can be used to indicate whether the stream is losing flow owing to recharge or receiving groundwater discharge (fig. 5-12). Decreased downstream flow commonly indicates a losing stream because of recharge to the underlying aquifer, whereas consistent increases in flow are quite often the result of groundwater discharge entering the stream. In the study area, decreased streamflow in downstream parts of Shoal Creek is consistent with recharge to the aquifer, whereas increased downstream flow in Berry Creek and the San Gabriel River can be attributed to groundwater discharge through numerous springs and seeps that occur in the area (fig. 5-12).

Spring and seeps in the western part of the aquifer discharge mostly from fractures or cavities in the Edwards Limestone or along the contact between the Edwards and Comanche Peak Limestones (Kreitler and others, 1987). In the east, major springs are associated with major faults, generally occurring some distance east of these faults.

5.6   *Hydraulic Properties*

As one would expect in a karst system, the hydraulic properties of Edwards aquifer rocks are highly variable. This variability can be attributed to many factors, such as (1) limestone primary porosity due to facies changes within or between individual stratigraphic units, (2) fracture densities, and (3) development of karst features. Hovorka and others (1996) showed that limestones deposited in subtidal environments exhibit lower porosities than carbonate sandstones or dolomite. On the basis of outcrop descriptions, Hovorka and others (1998) showed that fractures and karst features make up 1 to 3 percent of the outcrop area, and karst features develop preferentially adjacent to faults and in dolomitized limestone. Matrix permeability accounts for only about 1 percent of the flow through the aquifer, and the remainder is contributed by fractures and karst features.

Transmissivity estimates for the Edwards and associated limestones in the northern segment of the Edwards aquifer vary widely, lying in the range of 0.5 to 4×10^6 ft^2/day, seven orders of magnitude (fig. 5-13). These transmissivity estimates are calculated from specific-capacity data from the Texas Water Development Board (TWDB) well database using methods outlined in
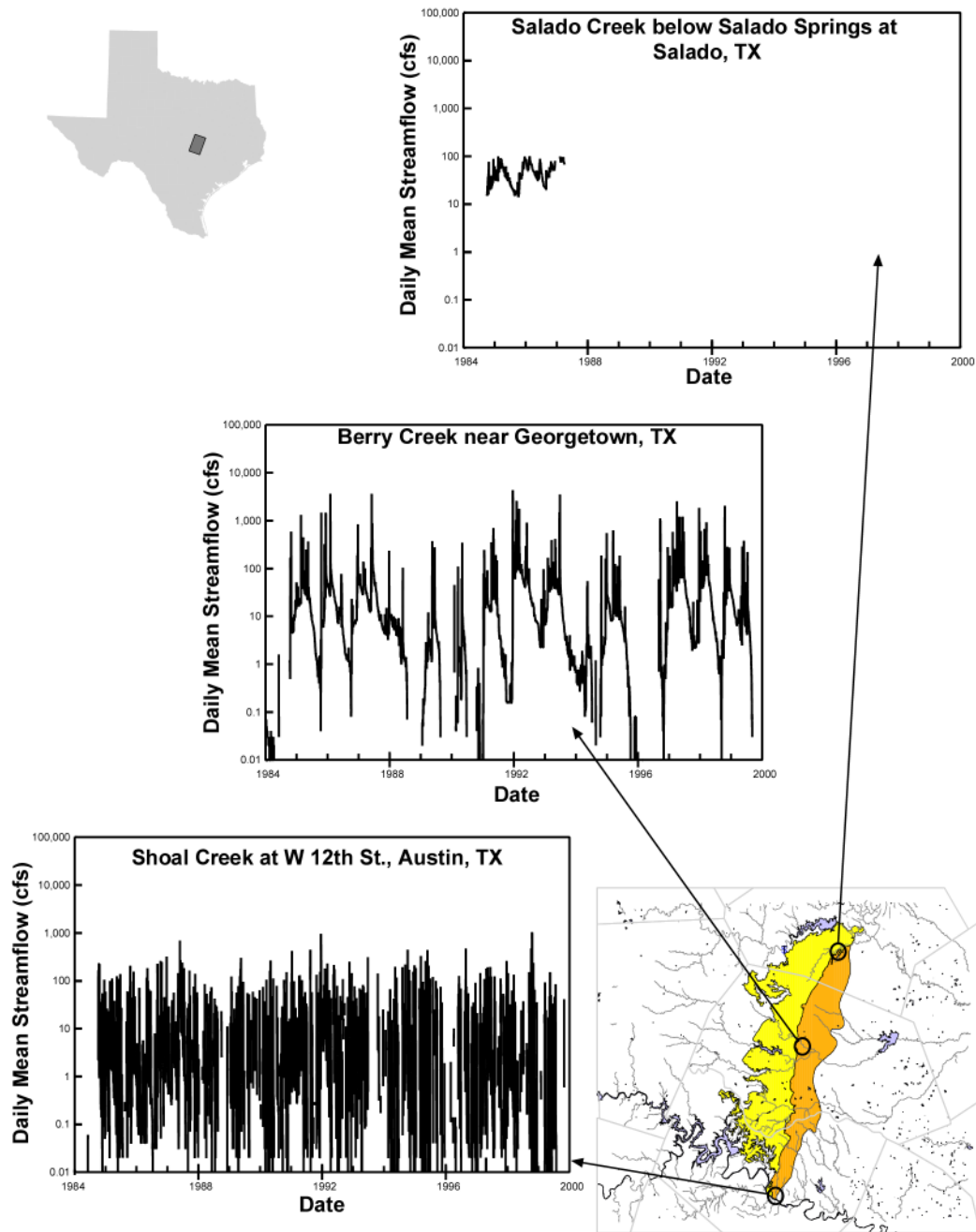
Figure 5-11.   Historical mean daily streamflow at selected USGS gaging stations in the study area.

Mace (2001a). The highest transmissivities can be attributed to cave systems, whereas solution-enhanced fracture porosity and intergranular porosity produce intermediate and low transmissivities, respectively (Hovorka and others, 1998). In the aquifer, transmissivity in the central part of the unconfined aquifer is generally higher than along the eastern or western boundaries. This phenomenon is attributed to fracture densities that are associated with the major faults of the Balcones Fault Zone.
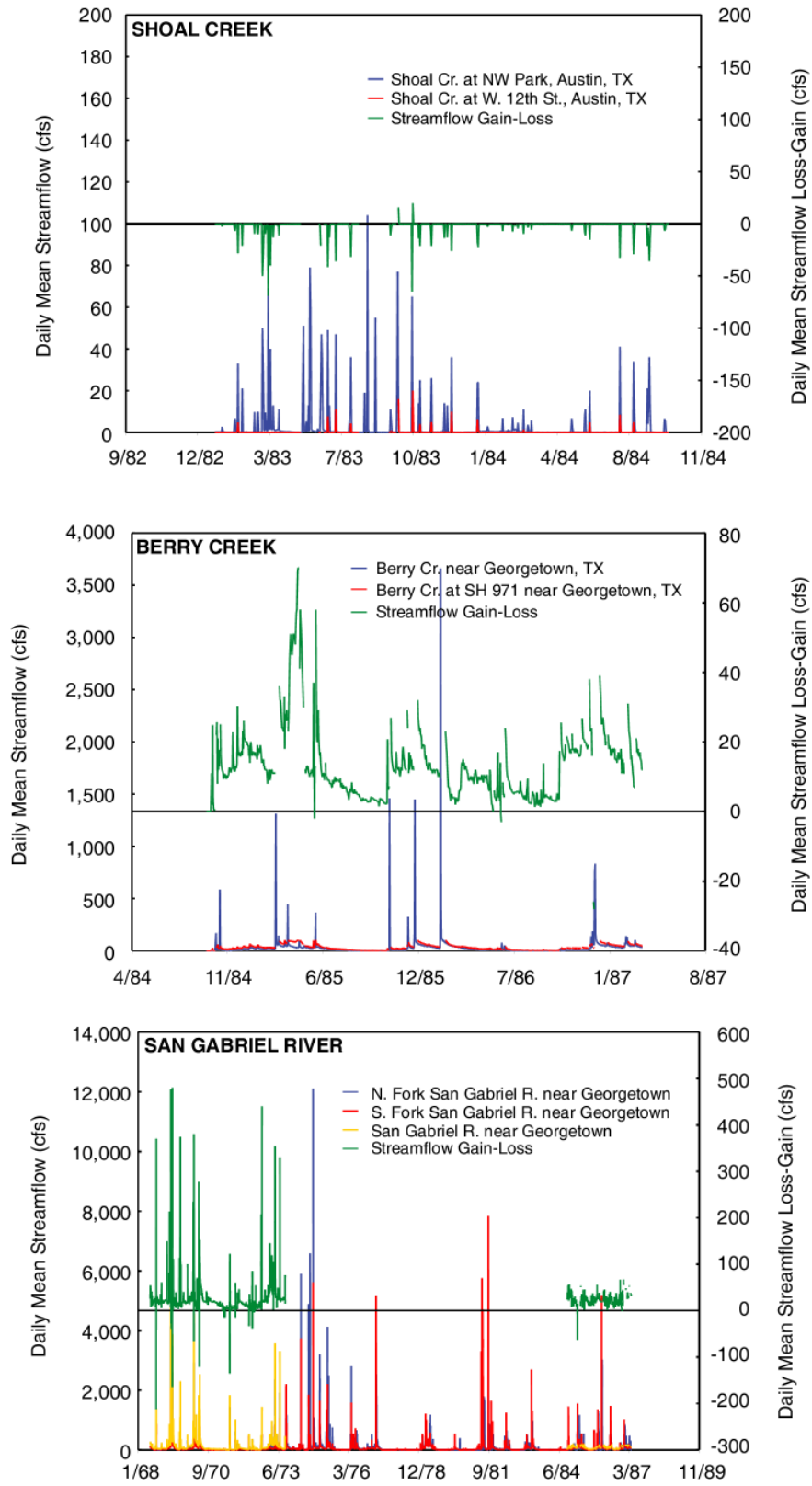
Figure 5-12.   Mean daily streamflow and streamflow gain-loss at upstream-downstream
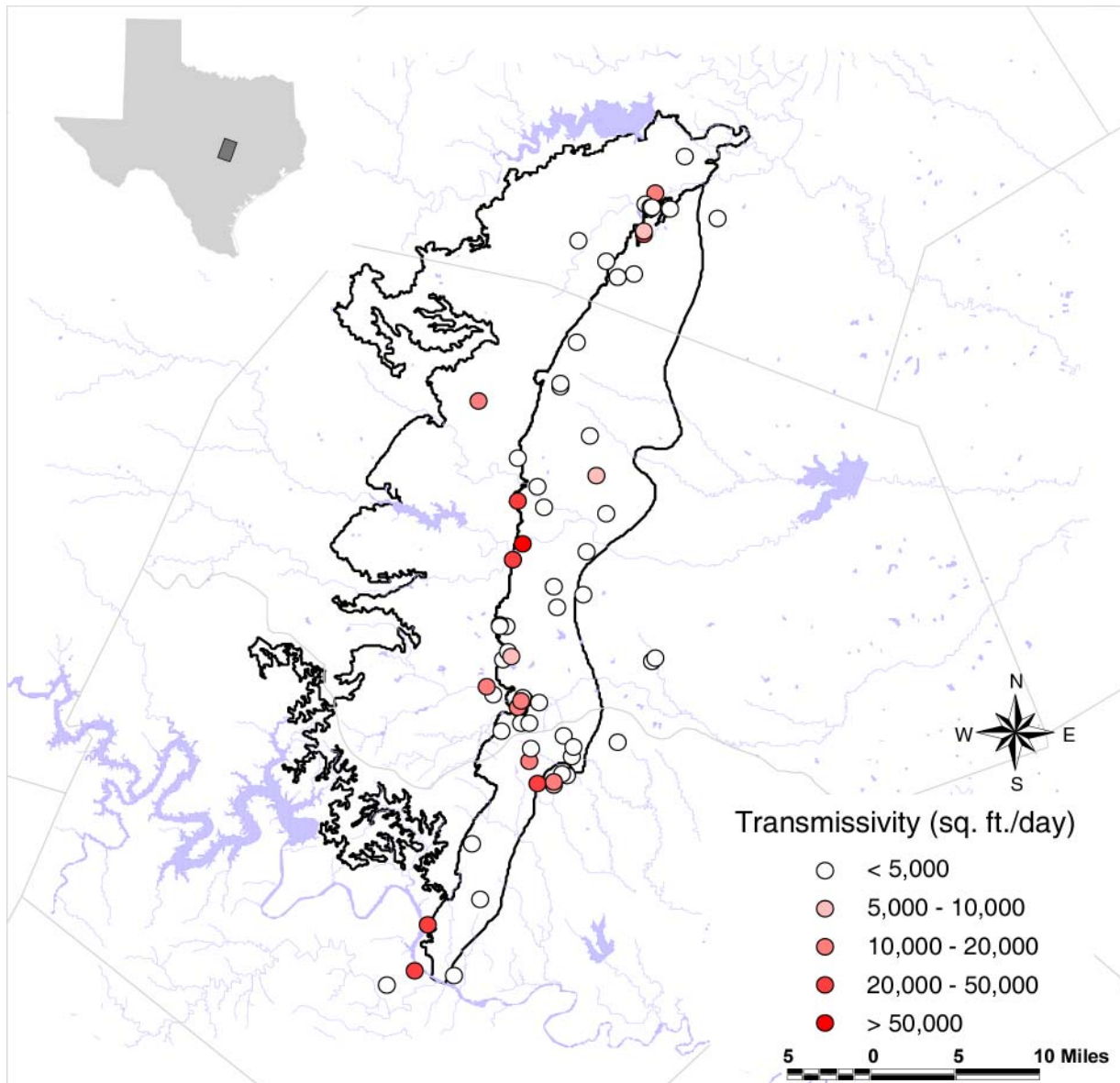
Figure 5-13.   Transmissivity estimates based on specific capacity data.

There is little hydraulic conductivity data that are based on pumping tests for the northern segment of the Edwards aquifer. Transmissivity data from the available specific capacity test data were converted to hydraulic conductivity based on aquifer thickness (fig. 5-14). Resultant hydraulic conductivity values range between 0.01 and more than 30,000 ft/day, and median and geometric mean values are 9 ft/day. These values overlap with hydraulic conductivity data $(2.7 \times 10^{-5}$ to 13 ft/day) for the San Antonio segment of the Edwards aquifer (Hovorka and others, 1996). There is very little hydraulic conductivity data on the unconfined part of the aquifer. Spatial distribution of the data suggests no trends, with the highest hydraulic conductivity occurring within a few hundred feet of very low hydraulic conductivity values. Initially it was decided to distribute hydraulic conductivity in the model in three zones, the Jollyville Plateau

30
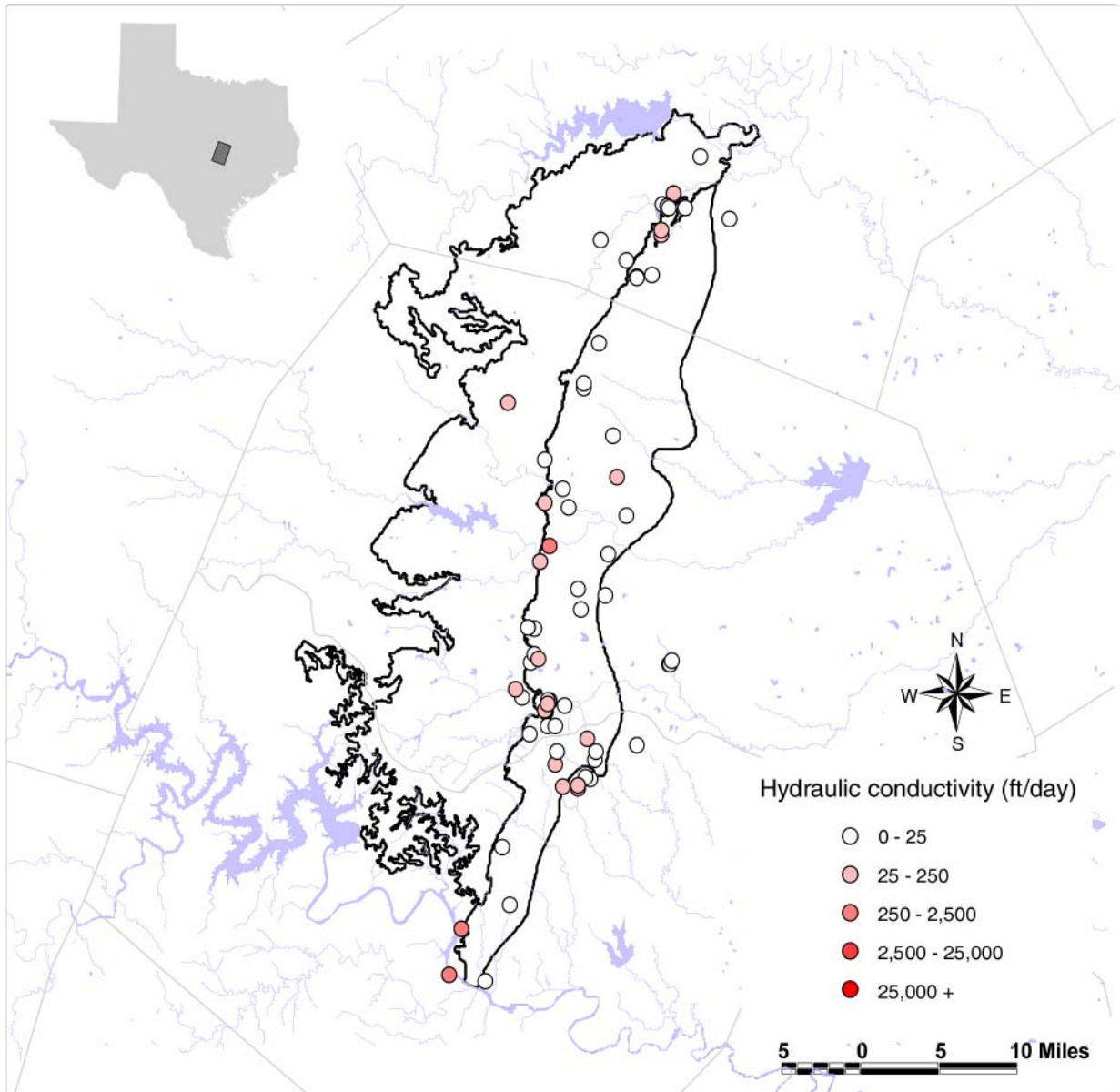
Figure 5-14.   Hydraulic conductivity estimates based on specific capacity data.

outcrop, the remainder of the Edwards aquifer outcrop, and the confined part of the aquifer. The Jollyville Plateau zone coincided with the outcrop of relatively low permeability stratigraphic units, such as the Keys Valley Marl, Comanche Peak Limestone, and Cedar Park Limestone. The remainder of the aquifer outcrop is composed of the Edwards Limestone and Georgetown Formation, which have generally higher permeability than the Jollyville Plateau. The lower hydraulic gradients in the downdip part of the aquifer were initially thought to indicate higher permeability.

No published storativity data exist for the northern segment of the Edwards aquifer. Consequently, specific yield and specific storage values from the groundwater availability model

31

for the adjacent Barton Spring segment of the Edwards aquifer were used to represent storage in the northern segment of the Edwards aquifer (Scanlon and others, 2001).

5.7   *Discharge*

Groundwater discharge from aquifers can take the form of pumping, discharge to springs or seeps, or cross-formational flow to an adjacent aquifer.

The northern segment of the Edwards aquifer is only slightly to moderately developed. Consequently, natural discharge through springs and seeps is thought to be much larger than well pumping (Duffin and Musick, 1991). TWDB pumping estimates indicate total groundwater pumping of 30,000 acre-feet during 1999 (fig. 5-15). Municipal and rural domestic pumping together account for almost 90 percent of the groundwater withdrawn from the aquifer. Unlike in the San Antonio segment, irrigation pumping is insignificant in the northern segment of the Edwards aquifer. Municipalities that use northern Edwards groundwater are located mainly in the northern part of the aquifer segment and include Salado, Georgetown, Pflugerville, and Round Rock. During the 1980s and 1990s, rural domestic pumping fluctuated between 10,000 and 15,000 acre-feet per year (fig. 5-16). During the same period, irrigation pumping estimates rose rapidly from 1 to 3 acre-feet per year in the early 1980s to approximately 18 acre-feet per year in the early 1990s. Municipal pumping also fluctuated, ranging from 6,000 to 13,000 acre-feet per year. In both rural domestic and municipal pumping, pumping generally increased over the time period. Irrigation pumping in the study area apparently ceased in 1994. Manufacturing pumping increased gradually through the 1980s and 1990s, from 1,500 acre-feet per year to 2,500 acre-feet per year. Livestock pumping increased during the early 1980s, from less than 50 acre-feet per year to about 150 acre-feet per year, and has remained generally constant since then. Overall, total pumping from the northern segment of the Edwards aquifer increased rapidly during the early 1980s, from less than 20,000 acre-feet per year to about 25,000 acre-feet per year (fig. 5-15). In subsequent years, pumping from the northern Edwards aquifer has increased gradually.

The spatial distribution of pumping has been determined based on the spatial distribution of respective users: rural domestic, municipal, irrigation, manufacturing, and livestock (fig. 5-17). For example, rangeland used for rearing livestock is located primarily on the western side of the study area. Consequently, one would expect that pumping for livestock would be concentrated on the western, unconfined part of the aquifer. Pumping for rural domestic uses is a function of population density outside city limits. Consequently, the spatial distribution of rural domestic pumping varies with population density. Municipal and manufacturing wells extracting water from the northern segment of the Edwards aquifer are located primarily adjacent to the boundary between the confined and unconfined parts of the aquifer. These wells are located mostly in southern and central Williamson County and are associated with the municipalities that depend on Edwards aquifer groundwater, such as Georgetown, Round Rock, and Pflugerville. Irrigation pumping is relatively minor in the study area. Cultivated farmland and associated irrigation are located primarily in the eastern part of the aquifer. Seasonally, pumping peaks during the dry summer months and declines from fall through spring, when most rainfall occurs (Kreitler and others, 1987).
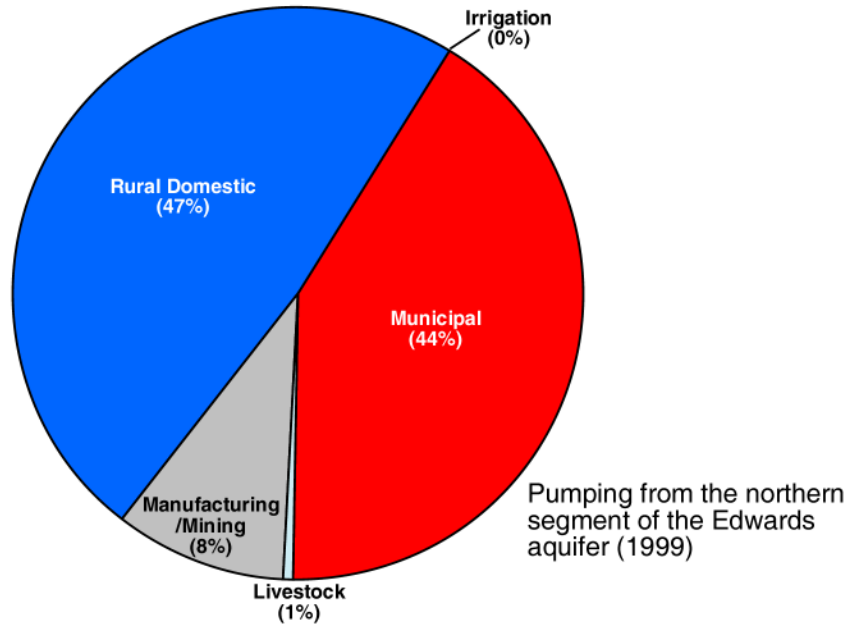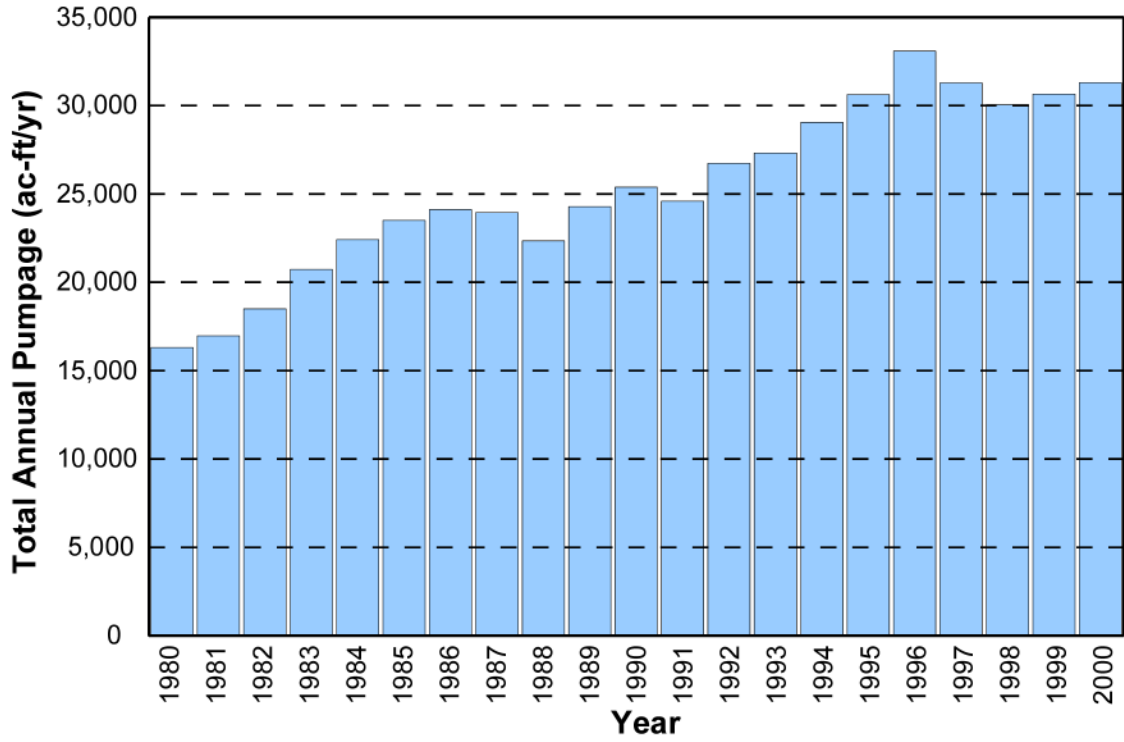
Figure 5-15.   Total annual groundwater withdrawals from Edwards aquifer (1980-2000).
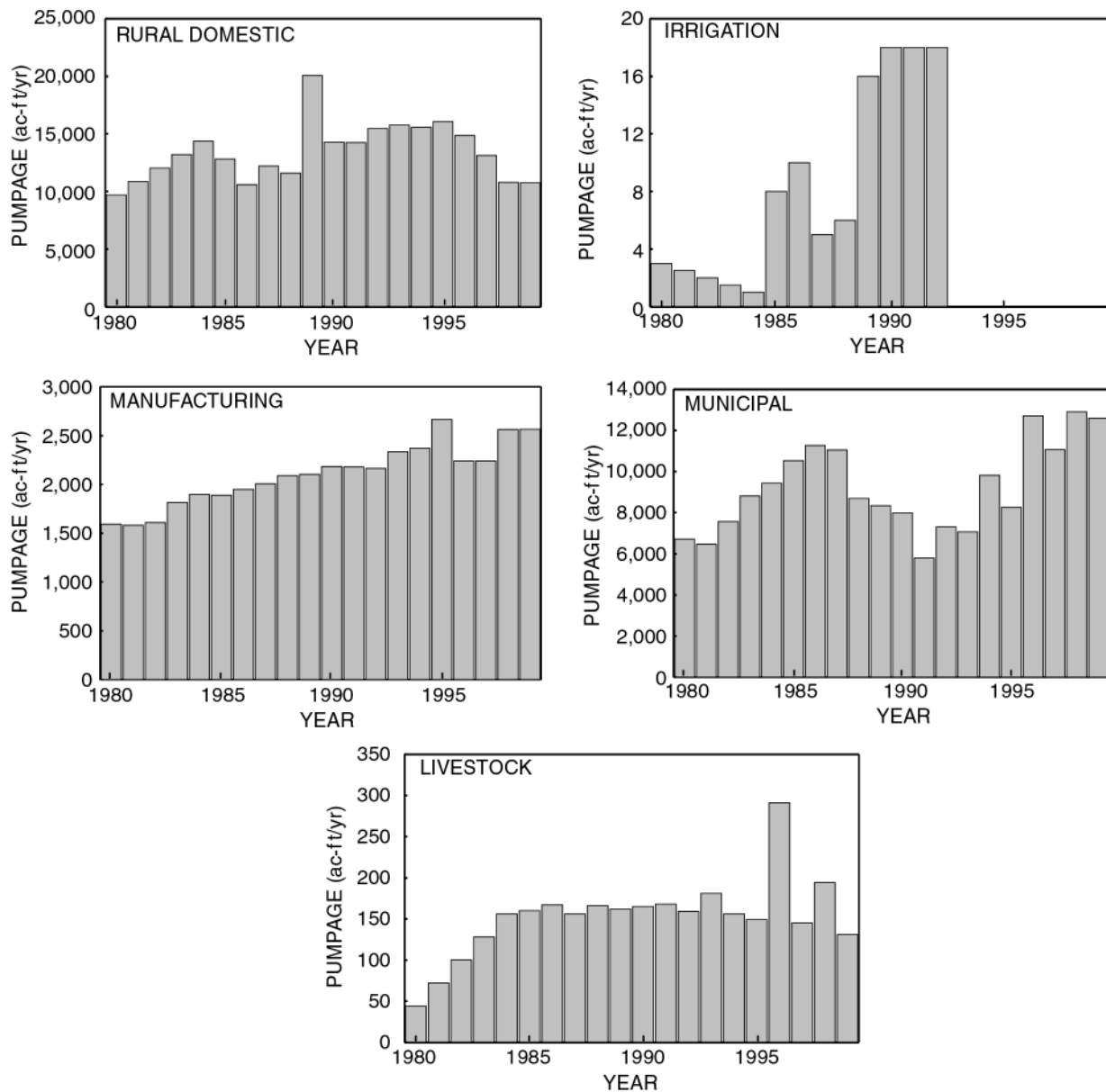
Figure 5-16.   Annual groundwater withdrawals for rural domestic, irrigation, manufacturing, municipal, and livestock uses.

Precipitation over the recharge zone and the upstream contributing zone results in rapid increases in spring discharge. The lag time between precipitation events and spring response varies from almost immediate to more than 1 week (Brune and Duffin, 1983). Faulting frequently results in the juxtaposition of relatively impermeable Del Rio Clay and Buda Limestone and Edwards aquifer rock. This juxtaposition restricts groundwater flow across faults and often results in upward flow along the fault and discharge through springs (Brune and Duffin, 1983; Land and Dorsey, 1988; Senger and others, 1990). Hence the occurrence of several major springs—for example, Mount Bonnell, Salado, San Gabriel, and Berry springs, adjacent to the boundary between unconfined and confined parts of the aquifer (fig. 5-18). Other major springs occurring

34
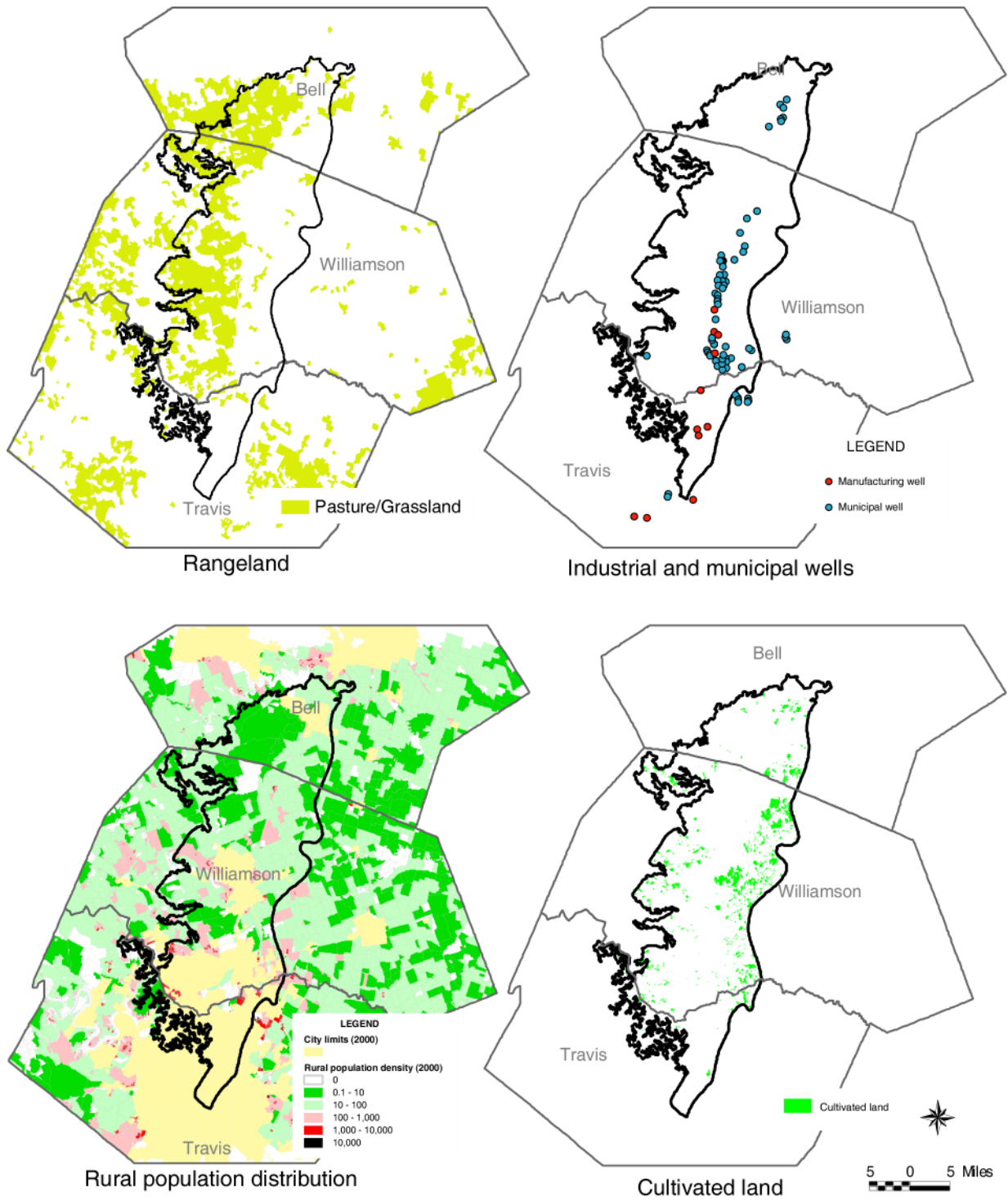
Figure 5-17. Spatial distribution of pumping for rural domestic, irrigation, manufacturing, municipal, and livestock uses.
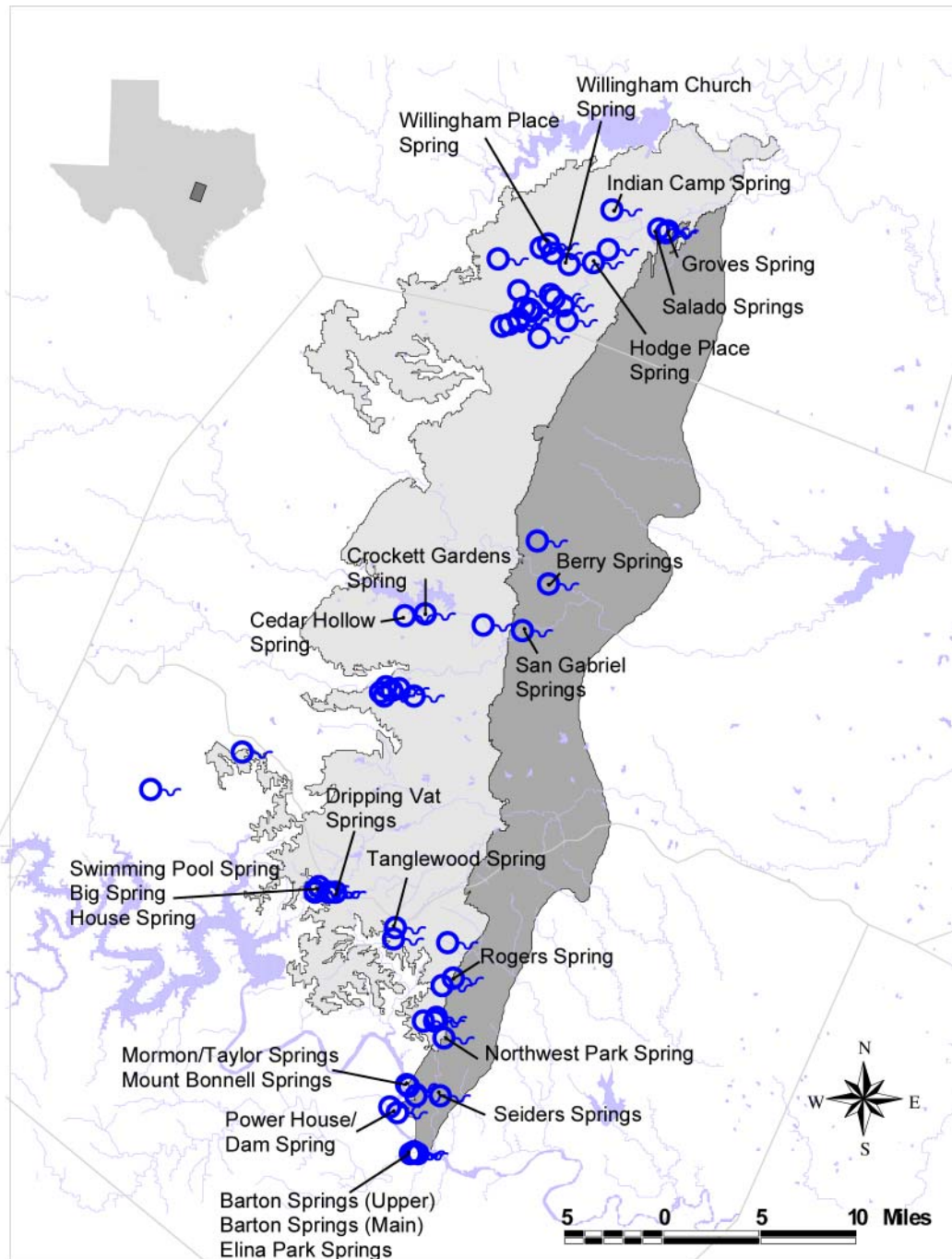
Figure 5-18.   Location of major springs discharging from the Edwards aquifer in the study area.

in the study area include Childers Springs in Bell County; Deep Eddy, Mormon, Power House, and Seiders springs in Travis County; and Berry, Knight, San Gabriel, and Manske springs in Williamson County (Brune, 1975). Along the southern margin of the study area, discharge from

the aquifer often takes the form of numerous small springs or seeps located along the southern margin of the Jollyville Plateau (Senger and others, 1990).

Discharge through springs and seeps is most likely to occur within or adjacent to the unconfined part of the aquifer. Discharge in the confined part of the aquifer takes the form of cross-formational flow from the Edwards aquifer, through the Del Rio Clay, into overlying aquifer units such as the Austin Chalk.

5.8   *Water Quality*

Geochemical compositions of groundwater in the Edwards aquifer are used in defining the downdip margin of the aquifer. This boundary, referred to as the bad-water line, is defined as the easternmost extent of freshwater in the aquifer. Freshwater is defined as water with total dissolved solids (TDS) of less than 1,000 mg/l. Use of the bad-water line as the eastern boundary of the aquifer is justified because high-TDS groundwater is associated with restricted groundwater circulation (Ridgeway and Petrini, 1999), which has been confirmed by the occurrence of relatively low concentrations of tritium compared with those of updip parts of the aquifer.

Groundwater in the northern segment of the Edwards aquifer becomes progressively more mineralized from the outcrop recharge zone in the west to downdip parts of the aquifer in the east (Figure 4-19). Groundwater TDS varies from 200 to 400 mg/l in the recharge zone and increases to more than 3,000 mg/l downdip (Baker and others, 1986). Intense faulting in the south creates barriers to eastward groundwater flow and results in the occurrence of slightly to moderately saline groundwater within 1 to 2 miles of the recharge zone. This distance is much less than that of parts of the aquifer farther north, where faulting is less intense and saline groundwater occurs more than 10 miles from the recharge zone. In addition to variations of TDS across the aquifer, groundwater geochemical compositions also vary downdip from $Ca-HCO_3$- to $Na-SO_4$-type waters and $Na-Cl$-type water (fig 5-19); (Brune and Duffin, 1983). These hydrochemical patterns indicate hydrochemical evolution of groundwater along flow paths. In the south, where faults are more abundant, hydrochemical zones are much narrower than in the north. The large faults that disrupt groundwater flow may also provide pathways for an influx of deep saline groundwater, especially in the south (Senger and others, 1990).

The spatial distribution of groundwater having different geochemical compositions reflects the interaction of two main flow systems in the aquifer. These flow systems involve (1) rapid circulation of fresh groundwater from the recharge zone and (2) a slow influx of saline groundwater from downdip (Senger and others, 1990). The $Ca-HCO_3$-type water that occurs within or adjacent to the recharge zone is characterized by high tritium of 7 to 11 Tritium Units (TU). The slowly circulating groundwater is characterized by low tritium (< 1 TU) and mixed-cation-HCO_3-, $Na-HCO_3$-, and Na-mixed-anion-type groundwater (fig. 5-19). The contrasting low and high tritium in confined and unconfined parts of the aquifer, respectively, indicate that most groundwater circulation in the aquifer occurs in the unconfined part of the aquifer. The boundary between low- and high-tritium groundwater coincides with the bad-water line, indicating relatively little circulation of recently recharged groundwater in the saline parts of the aquifer. The bad-water line also follows the downdip boundary of the $Na-HCO_3$ zone in the north. In the south, where the $Na-HCO_3$ zone disappears, the bad-water line forms an irregular
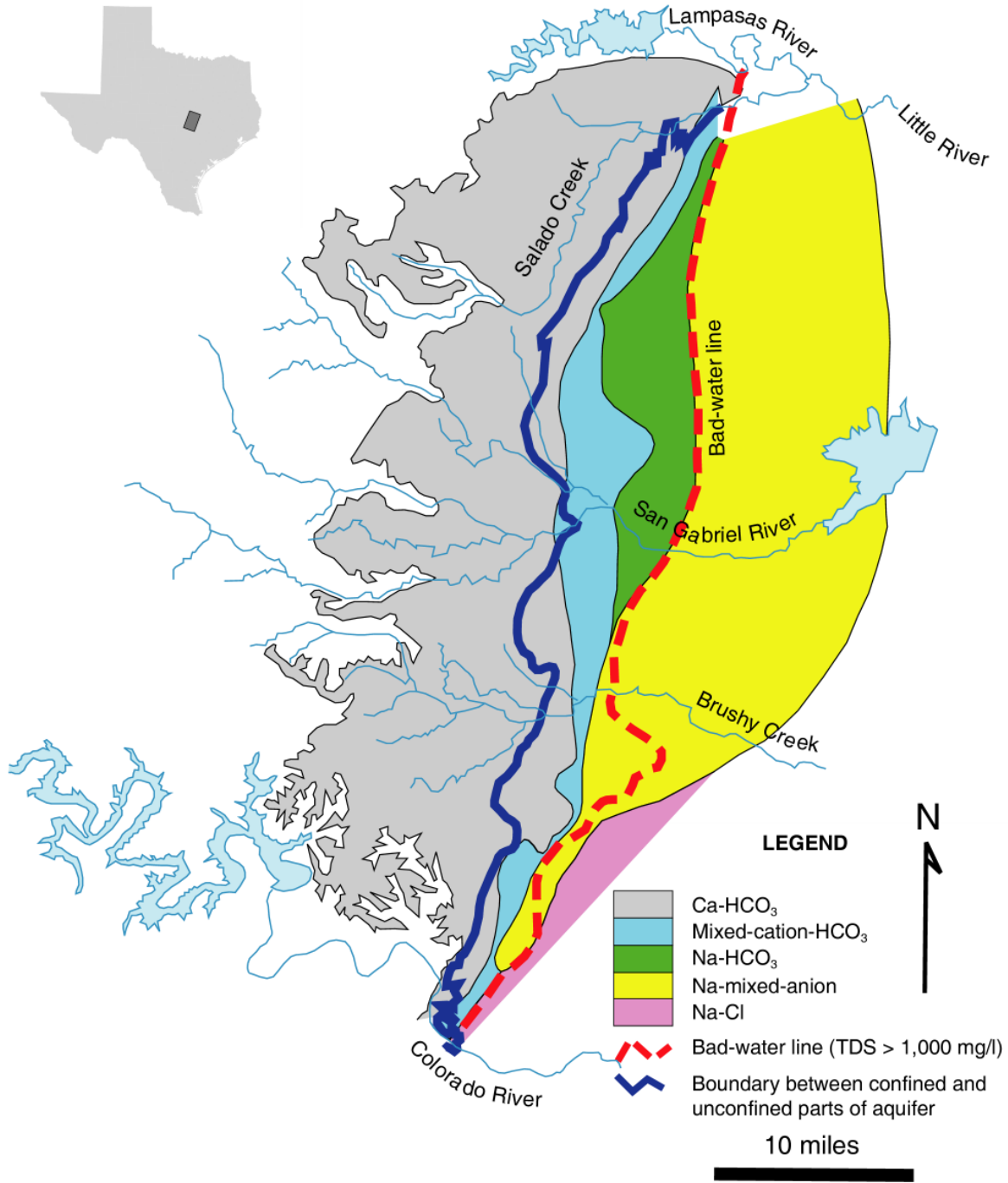
Figure 5-19. Variation of Edwards aquifer groundwater chemical compositions in the study area (modified from Senger and others, 1990).

pattern partly because of localized recharge along faults. At the Colorado River, the bad-water line coincides with the updip boundary of the Na-Cl zone. The north-south variation of groundwater geochemical zones can be explained by the relative influence of fresh and saline groundwater flow systems. In the south, where the influx of freshwater is restricted because of faulting, groundwater geochemical compositions are influenced largely by updip movement of Na-Cl brines from the Gulf Coast Basin. In the north, groundwater geochemical compositions are influenced by downdip hydrochemical evolution of fresh groundwater (Senger and others, 1990). Groundwater compositions do not apparently vary with fluctuating water levels (Baker and others, 1986). However, Flores (1990) suggested less fresh to slightly saline groundwater in the aquifer as compared with that indicated by a 1986 study. This difference suggests a slightly westward shift of the bad-water line over time (Flores, 1990).

6.0   Conceptual Model of Flow in the Aquifer

The conceptual model reflects our best understanding of the hydrology of the aquifer. The model describes predicted groundwater flow paths, as well as the processes, such as recharge and discharge, that constitute the water budget of the aquifer.

Precipitation that falls on the outcrop of the northern segment of the Edwards aquifer is the primary source of recharge water (fig. 6-1). This widespread recharge takes the form of direct infiltration through soil and rock and infiltration from numerous intermittent streams. Additional recharge results from infiltration of water from streams that cross the aquifer outcrop. Groundwater flows generally toward the east, except along the southern margin of the aquifer, where there is southward flow toward the Colorado River. Water quality parameters such as tritium indicate that there is very little groundwater flow beyond the bad-water line. The groundwater potentiometric surface indicates groundwater flow converging on Brushy and Salado Creeks, indicating discharge to these streams. This discharge is confirmed by the fact that both streams are perennially gaining streams. Other major discharge zones occur on the Colorado River along the southern margin of the aquifer, the San Gabriel River, and the Lampasas River along the northern margin of the aquifer. This discharge takes the form of springs and seeps that flow into the perennial rivers and streams that cross or are adjacent to the aquifer.

The northern segment of the Edwards aquifer is used primarily as a source of water for municipalities located mostly in the central and northern parts of the study area, such as the cities of Round Rock, Georgetown, Salado, and Pflugerville. Consequently, groundwater use is greater in Williamson and Bell counties than in Travis County. Despite annual increases in groundwater pumping averaging 5 percent per year over the past decade, total pumping in the northern segment of the Edwards aquifer is relatively small compared with that of the much larger San Antonio segment. Estimated pumping for 1999 was approximately 30,000 acre-feet in the northern segment of the Edwards aquifer, compared with pumping in excess of 400,000 acre-feet per year in the San Antonio segment. In addition to discharge to streams and pumping, groundwater discharge from the northern segment of the Edwards aquifer also occurs by cross-formational flow. Cross-formational flow occurs in the confined part of the aquifer, where groundwater discharges by upward flow from the Edwards aquifer to overlying units, such as the Austin Chalk.
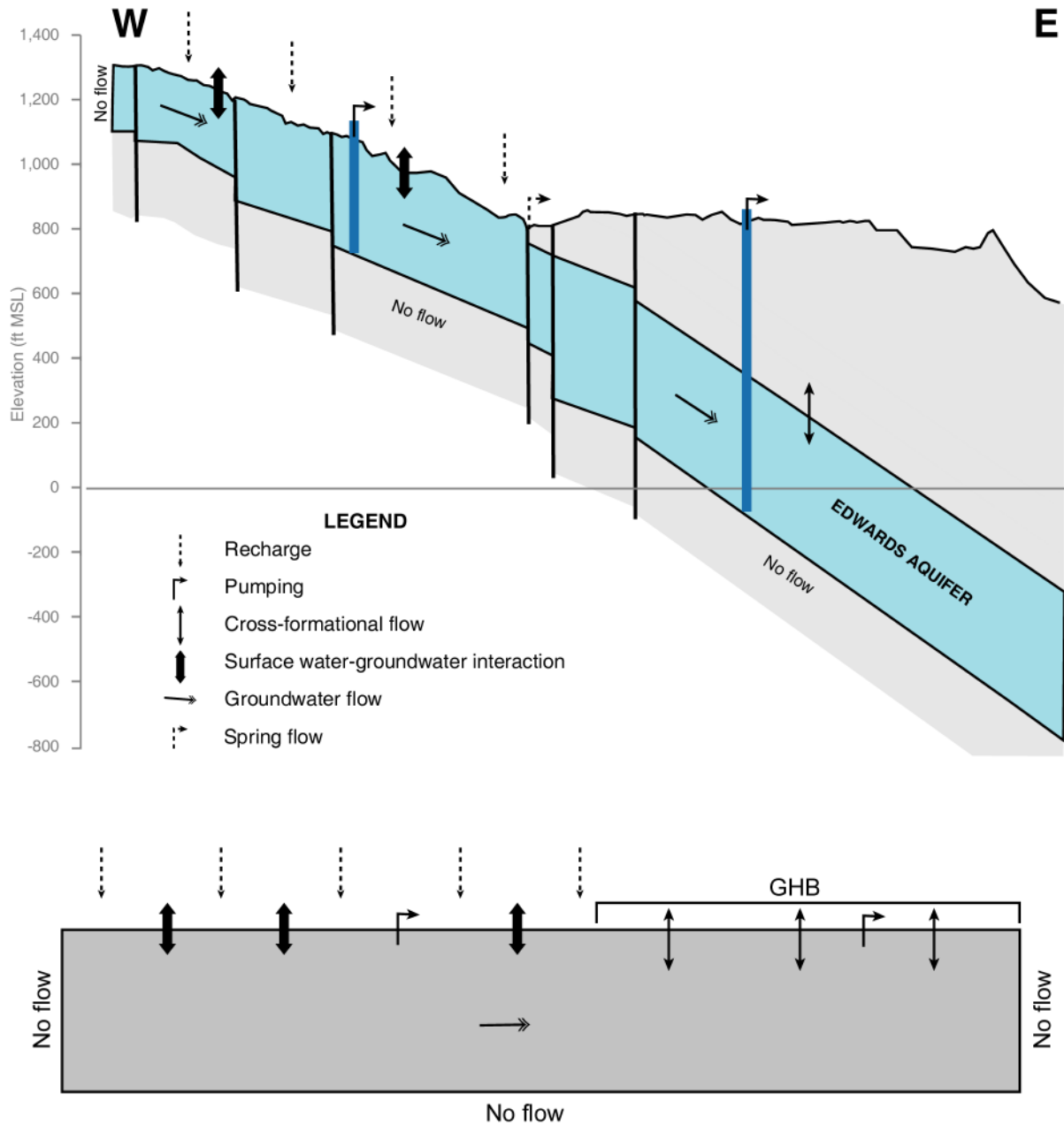
Figure 6-1.   Conceptual model of groundwater flow in the study area.

7.0 Model Design

Model design includes (1) choice of code and processor, (2) discretization of the aquifer into layers and cells, and (3) assignment of model parameters. The model design must agree as much as possible with the conceptual model of groundwater flow in the aquifer.

7.1   Code and Processor

Groundwater flow through the northern segment of the Edwards aquifer was simulated using MODFLOW-96, a widely used modular finite-difference groundwater flow code written by USGS (Harbaugh and McDonald, 1996). This code was selected because of (1) its capabilities of simulating regional-scale groundwater processes in the Edwards aquifer, (2) its documentation and wide use (McDonald and Harbaugh, 1988; Anderson and Woessner, 1992), (3) the availability of a number of third-party pre- and post-processors for facilitating easy use of the modeling software, and (4) its easily available public domain software. Processing MODFLOW for Windows (PMWIN) version 5.3 aided in our loading data into the model and viewing model outputs (Chiang and Kinzelbach, 2001). Other pre- and post-processors should be able to read source files for MODFLOW-96. This model was developed and run on a Dell Optiplex GX150 with a 930 MHz Pentium III processor and 256 MB RAM running Microsoft Windows 2000 (v. 5).

7.2   Layers and Grid

The lateral extent of the model differs slightly from those of the previously defined aquifer boundaries. The eastern boundary of the model coincides with the easternmost occurrence of groundwater with TDS of less than 3,000 mg/l (fig. 7-1). These data differ from the TWDB definition of the northern segment of the Edwards aquifer, where the eastern boundary is the bad-water line, as defined by a TDS of 1,000 mg/l. As a precaution, the downdip boundary of the model was moved eastward to test whether groundwater flowed beyond the previously defined aquifer boundary. This model has one layer that is composed of the undifferentiated Edwards and associated limestones. The model grid has 160 columns and 250 rows, for a total of 40,000 cells. Of these cells, 15,076 are active. The model grid is oriented 20° east of north. The cells have uniform dimensions of 1,320 feet by 1,320 feet. This cell size was selected to reflect the density of input data while providing adequate output resolution. The uniform cell size facilitates the use of spreadsheets and grid-based contouring software for easy data manipulation.

7.3   Model Parameters

The model layer was assigned as a confined/unconfined layer type, allowing MODFLOW to calculate transmissivity and storativity from simulated saturated thickness and assigned hydraulic conductivity and specific storage values. The length and time units used in this model were feet and days, respectively. ArcView® was used to distribute model parameters spatially, such as aquifer base and top elevations, hydraulic conductivity, specific yield, and specific storage.

The top and base of the aquifer were based on structural data compiled by the Bureau of Economic Geology (fig. 5-4 and 5-5); (Collins and others, 2002). The top of the aquifer was defined as land surface in the unconfined part of the aquifer and the top of the Georgetown Formation in the confined part of the aquifer. The base of the aquifer was defined as the base of the Comanche Peak Limestone.Hydraulic conductivity was initially assigned to different zones in the model. These zones represented the Jollyville Plateau, aquifer outcrop, and downdip parts
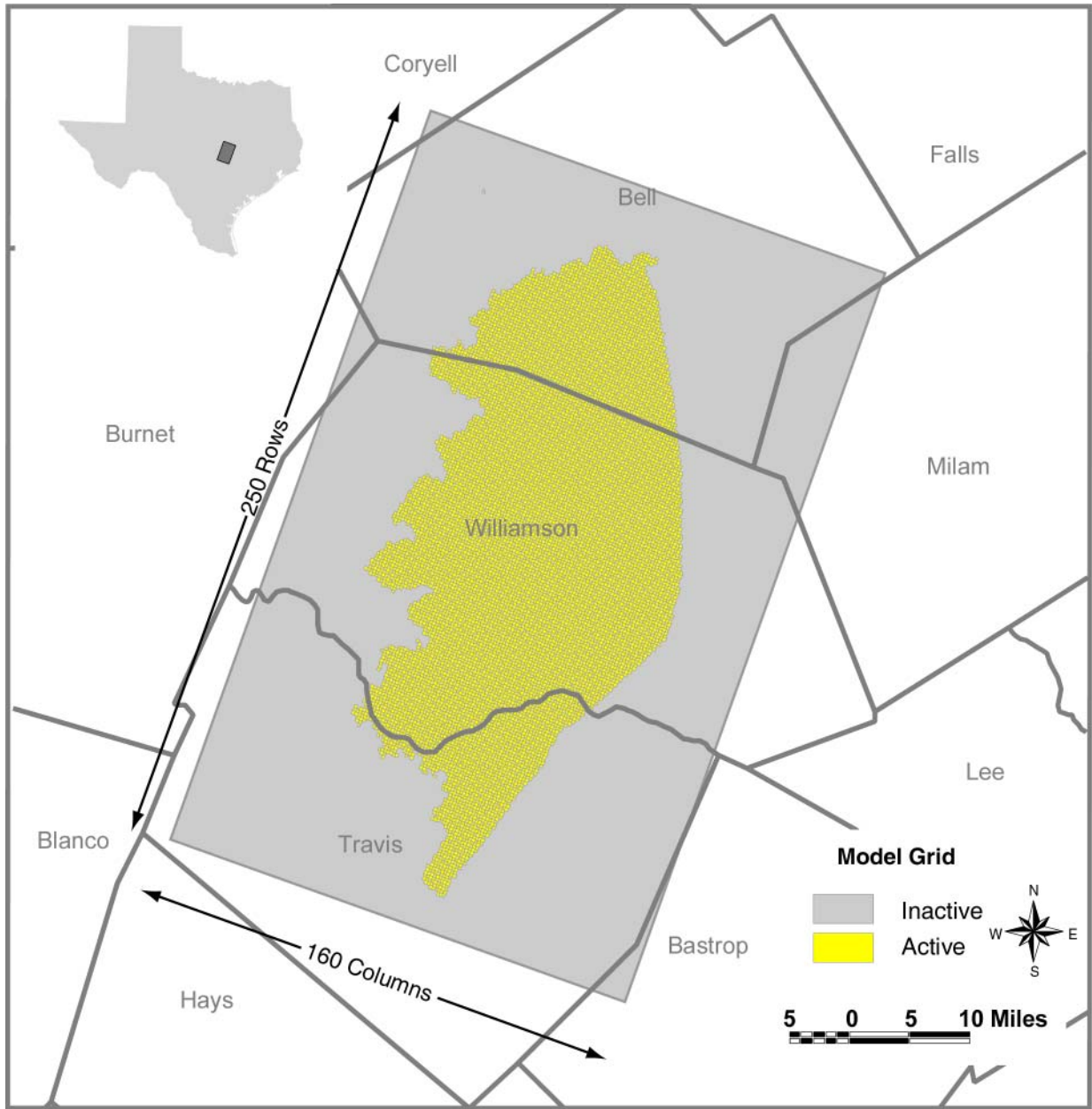
Figure 7-1.   Model grid.

of the aquifer and were initially assigned hydraulic conductivity values to zones based on the geology.

Specific yield and specific storage were assigned uniformly throughout the model grid using values similar to those used in the groundwater availability model for the Barton Springs segment of the Edwards aquifer (Scanlon and others, 2001). The values for specific yield and specific storage used in this model were 0.005 and 5×10^{-6} per foot, respectively.

The Slice Successive Over-Relaxation (SSOR) package was used to solve the groundwater flow equation. The convergence criterion for iterations was set at 0.01 foot.

7.4   Model Boundaries

Model boundaries were assigned for (1) recharge, (2) pumping, (3) streams and springs, and (4) initial conditions. ArcView® was used to distribute model boundaries spatially, such as initial water-level elevations, drains, general-head boundaries (GHB), recharge, and pumping.

Initial water-level elevations were interpolated from average water levels for respective wells in the TWDB Well Database (fig. 4-7). These water-level elevations represent water-level measurements made during the month of January during the years 1990 through 1999. Average water levels were used because (1) the aquifer responds rapidly to precipitation, resulting in water-level fluctuations of up to 100 feet and (2) there is no apparent long-term regional-scale water-level decline in the northern segment of the Edward aquifer.

The Drain package in MODFLOW was used to simulate groundwater discharge to seeps, springs, and perennial streams (fig. 7-2). Discharge from the aquifer takes place only when simulated water levels in the drain cells exceed set elevations that represent streambed or spring orifice elevations. Discharge through drains is also a function of hydraulic conductance. In this model, initial drain hydraulic conductance was set at 1,000,000 ft^2/day— a value set high so that resistance to flow from the aquifer into the streams could be minimized. This action is justifiable because in the study area streambeds sediments are often composed of highly permeable gravel or fractured limestone. Drains were used to simulate discharge to perennial streams because in this segment of the Edwards aquifer, few losing segments are in the perennial streams (fig. 3-1).

The GHB Package was used to simulate cross-formational groundwater flow between the Edwards aquifer and overlying units. The GHB cells are located primarily in the downdip margin of the model and along major topographic lows formed by the major river valleys that cross the aquifer (fig. 7-3). These topographic lows have the greatest potential for groundwater discharge by cross-formational flow. Discharge through the GHB is head-dependent, as determined by the elevation of simulated hydraulic heads relative to GHB heads. The GHB heads were set to represent hydraulic heads in an overlying unit. In this model, GHB heads were set to an elevation 90 feet below land surface to simulate hydraulic heads in overlying stratigraphic units, such as the Eagle Ford Group and Buda Limestone. If simulated hydraulic heads exceeded GHB heads, groundwater flowed upward out of the aquifer. Otherwise, cross-formational flow entered the aquifer. In addition to relative heads, cross-formational flow discharge was also influenced by hydraulic conductance initially being set at 3,500 ft^2/day. The initial GHB conductance value was based on assumption of a very low confining-unit hydraulic conductivity factored over the area of each cell.

Recharge to the northern segment of the Edwards aquifer was spatially distributed based on assumptions that (1) recharge takes the form of widespread infiltration from numerous intermittent streams and through soils that overlie the aquifer outcrop and (2) recharge is a fraction of annual precipitation. Recharge in the model was set initially at 0.000343 ft/day, or 5 percent of average annual precipitation.
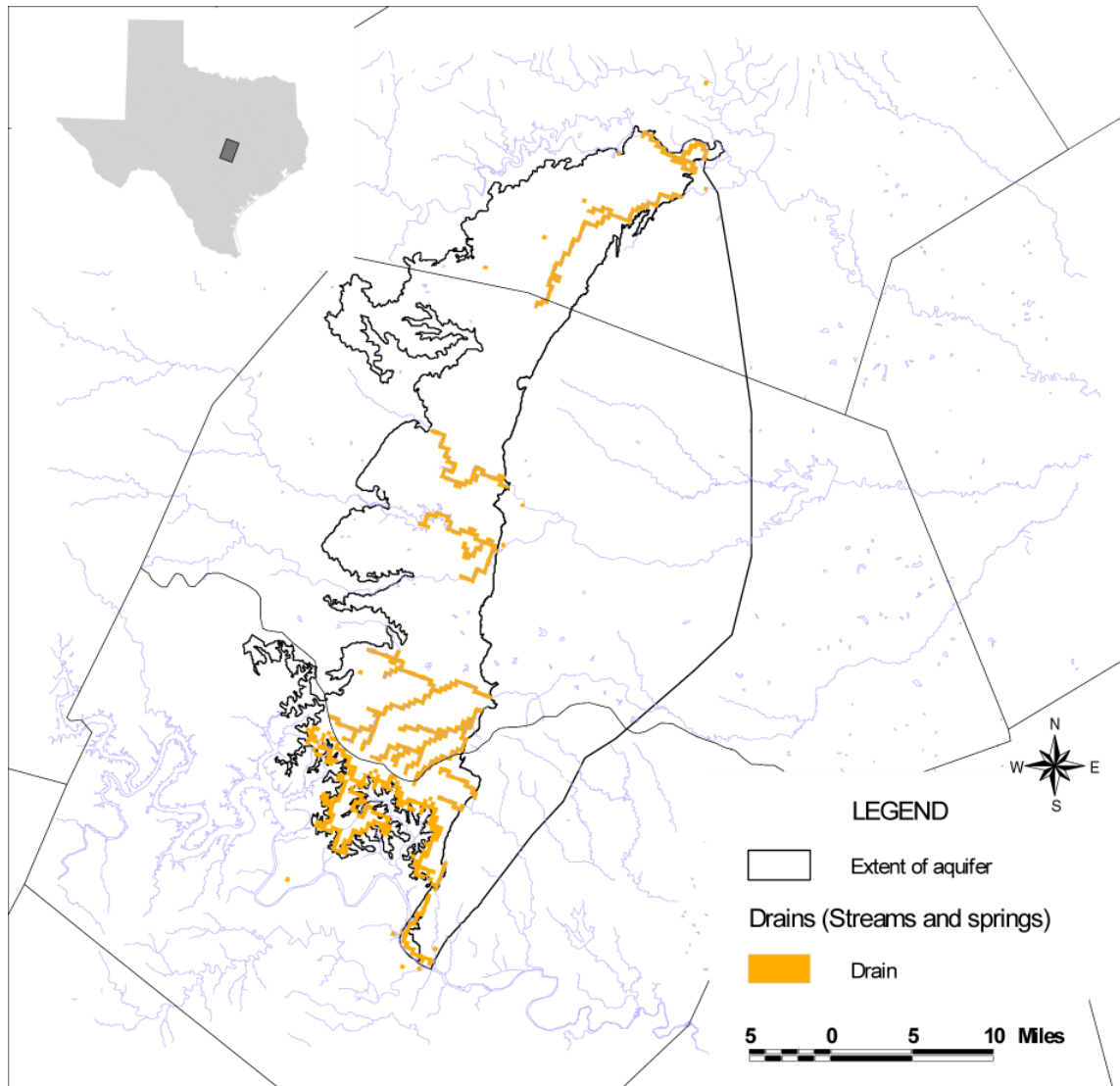
Figure 7-2.   Distribution of drain cells in the model grid.

This model simulates the regional effects of pumping for rural domestic, municipal, irrigation, industrial, and livestock uses (table 7-1 and 7-2). Municipal and manufacturing pumping was distributed based on known well locations and pumping data from the TWDB Water Use Survey (fig.5-16 and 7-4). The other uses (domestic, irrigation, and livestock) were distributed throughout the model grid, reflecting the spatial distribution of associated land use. Rural domestic pumping was distributed based on the spatial distribution of population outside major urban areas that lie within the model grid. Pumping was distributed based on population data for the respective counties from 1990 and 2000 censuses such that pumping is proportional to the population within each active model cell. Irrigation pumping was distributed based on 1:250,000-scale Land Use and Land Cover data from USGS. Irrigation was assumed to occur on all land classified as orchards, row crops, or small grains. Livestock pumping was also distributed based on 1:250,000-scale Land Use and Land Cover data from USGS. Livestock pumping was assumed on all rangeland.
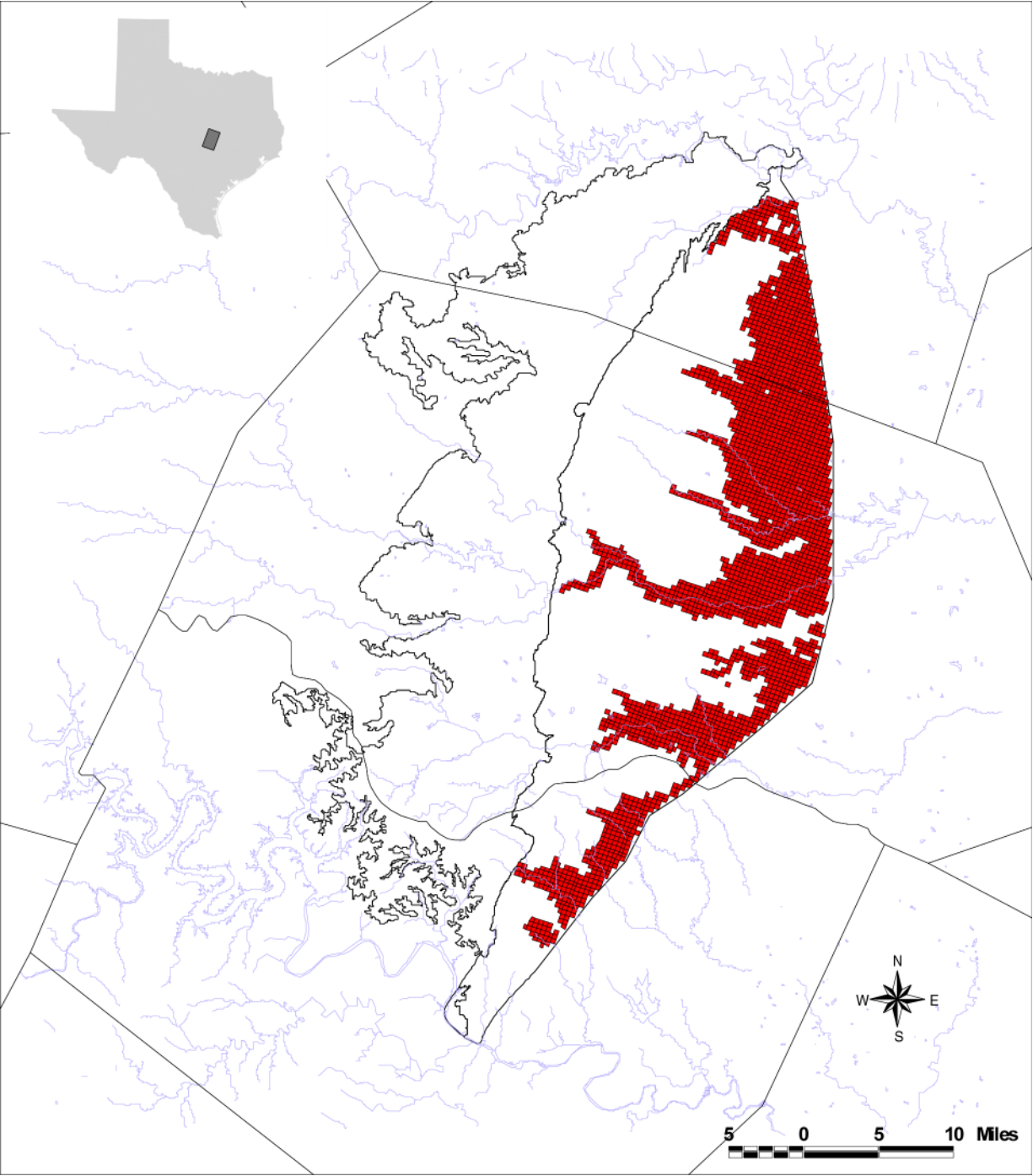
Figure 7-3. General-head boundary cells in the model.

Table 7-1.   Rate of total groundwater withdrawal from the northern segment of the Edwards aquifer. Values expressed in acre-feet per year (data for 1980 through 2000 from TWDB water use surveys, 2001 through 2050 from regional water planning groups).

County Year	Bell	Travis	Williamson
1980	1,200	3,900	11,200
1981	1,100	4,500	11,400
1982	1,100	4,700	12,700
1983	1,100	5,200	14,400
1984	1,200	6,100	15,100
1985	1,100	6,200	16,200
1986	1,100	5,600	17,400
1987	1,100	5,700	17,200
1988	1,100	6,400	14,900
1989	1,700	7,000	15,500
1990	1,800	7,600	15,900
1991	1,800	8,000	14,800
1992	2,000	8,100	16,700
1993	2,100	8,800	16,400
1994	2,100	9,100	17,800
1995	2,100	9,700	18,800
1996	2,300	10,100	20,700
1997	2,100	9,000	20,100
1998	2,300	9,500	18,300
1999	2,400	9,700	18,600
2000	2,400	9,600	19,300
2010	470	2,600	2,900
2020	530	3,000	2,800
2030	590	4,400	2,900
2040	640	4,500	3,200
2050	690	4,700	3,100

Table 7-2. Rate of rural domestic, irrigation, livestock, manufacturing, and municipal groundwater withdrawal from the northern segment of the Edwards aquifer. Values expressed in acre-feet per year (data for 1980 through 2000 from TWDB water use surveys, 2001 through 2050 from regional water planning groups).

County	Rural Domestic			Irrigation			Manufacturing/Mining			Municipal			Livestock		
Year	Bell	Travis	Williamson	Bell	Travis	Williamson	Bell	Travis	Williamson	Bell	Travis	Williamson	Bell	Travis	Williamson
1980	1,000	3,400	3,600	3	0	0	0	240	1,300	140	260	6,300	20	10	20
1981	910	3,900	3,900	2	0	0	0	200	1,400	160	280	6,100	10	40	20
1982	920	4,100	4,200	1	0	0	0	150	1,500	180	360	7,000	10	70	20
1983	910	4,600	4,500	1	0	1	0	150	1,700	200	400	8,200	10	100	20
1984	920	5,200	4,900	0	0	1	0	230	1,700	260	570	8,500	10	130	20
1985	800	5,100	5,000	6	0	2	0	220	1,700	250	740	9,500	10	130	20
1986	800	4,400	6,600	7	0	2	0	280	1,700	250	860	10,100	10	140	20
1987	810	4,400	5,600	3	0	2	0	320	1,700	260	860	9,900	10	130	20
1988	810	4,800	5,900	5	0	1	0	400	1,700	300	1,100	7,300	10	140	20
1989	1,300	5,500	6,900	0	0	16	0	400	1,700	460	1,000	6,800	10	140	20
1990	1,400	6,000	7,500	0	0	18	0	480	1,700	450	970	6,700	10	140	20
1991	1,300	6,500	7,500	0	0	18	0	430	1,800	480	900	5,500	10	140	20
1992	1,400	6,400	7,400	0	0	18	0	460	1,700	580	1,100	7,500	10	140	10
1993	1,500	6,800	8,000	0	0	0	0	500	1,800	610	1,400	6,600	10	160	10
1994	1,400	6,900	8,500	0	0	0	0	580	1,800	640	1,600	7,500	10	130	20
1995	1,400	7,200	8,600	0	0	0	0	660	2,000	700	1,800	8,100	10	130	10
1996	1,500	7,200	9,300	0	0	0	0	480	1,700	820	2,200	9,700	10	260	20
1997	1,300	6,300	6,800	0	0	0	0	470	1,700	780	2,100	11,600	10	120	10
1998	1,400	6,300	6,800	0	0	0	0	570	2,000	890	2,400	9,500	10	140	10
1999	1,400	6,300	6,800	0	0	0	0	580	2,000	990	2,600	9,800	10	140	10
2000	1,400	6,300	6,800	0	0	0	0	580	2,000	990	2,600	10,500	10	140	10
2010	20	770	850	0	280	0	0	1,100	310	350	300	1,800	110	150	0
2020	20	1,100	1,000	0	250	0	0	1,100	260	410	370	1,500	110	150	0
2030	20	2,400	940	0	230	0	0	1,100	260	470	440	1,700	110	150	0
2040	20	2,500	1,000	0	210	0	0	1,200	260	520	490	2,000	110	150	0
2050	20	2,600	920	0	200	0	0	1,200	260	560	540	2,000	110	150	0
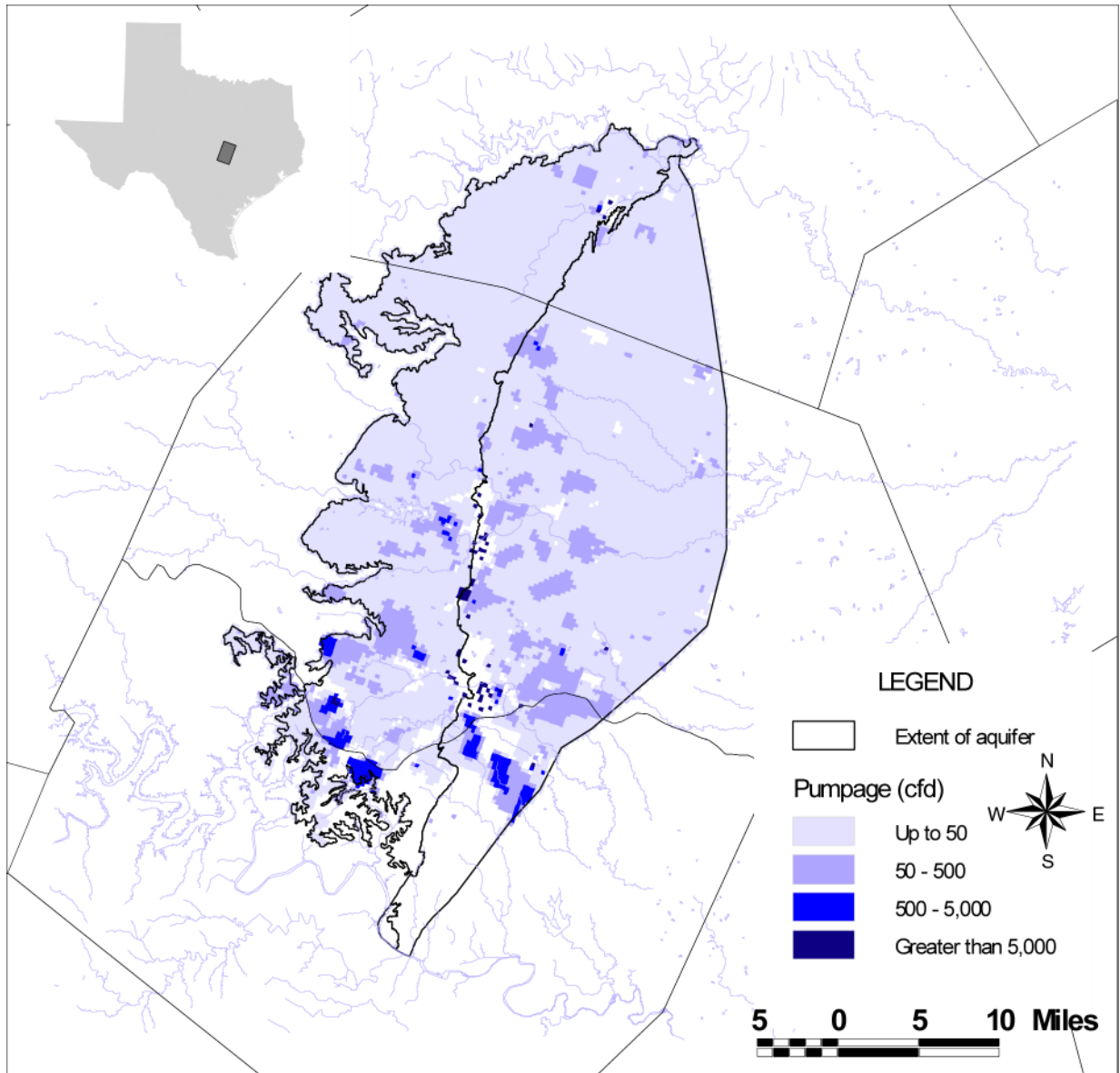
Figure 7-4.   Distribution of total pumping in the model for 1980.

8.0   Modeling Approach

The process of modeling the northern segment of the Edwards aquifer included (1) steady-state model calibration, (2) historical transient model calibration, and (3) predictions of water-level variations over a 50-year planning period based on the transient model and pumping predictions developed by the Brazos G and Lower Colorado Regional Water Planning Groups. The steady-state model was developed first to facilitate easier calibration because some parameters, such as aquifer storage and water-level variations over time, do not need to be taken into consideration.

In the steady-state model, calibration requires consideration only of spatial variations in the aquifer.

The steady-state model was calibrated to reproduce water levels for early 1980. The steady-state model was used to investigate (1) recharge rates, (2) hydraulic properties, (3) boundary conditions, and (4) flow budget. Model calibration in the steady-state model involved matching simulated water levels and streamflow with available measurement data. Steady-state calibration was quantified using the root mean square error (RMSE) between measured and simulated water levels,

$$RMSE = \left[\frac{1}{n} \sum_{i=1}^{n} \left(h_m - h_s \right)_i^2 \right]^{0.5},$$

where n is the number of calibration points and h_m and h_s are measured and simulated water-level elevations, respectively, at point i. The calibration process for the steady-state model is designed to minimize the RMSE of the model with a target RMSE less than 10 percent of the range of measured water-level values.

Once steady-state calibration was achieved, the resultant model was the basis for the historical transient model. In the historical transient model, calibration involved matching water-level and streamflow fluctuations with available measurements. After the historical transient model was calibrated, it was used to predict how water levels may change over the next 50 years in response to predicted pumping and drought.

9.0   Steady-State Model

After input data were assembled and the model framework was constructed, the steady-state model was calibrated to fit measured parameters. Upon successful calibration, sensitivity of the model to selected input parameters was assessed.

9.1   Steady-State Calibration

Recharge, hydraulic conductivity, and GHB conductance were adjusted to calibrate the steady-state model. Minor adjustments were also made to aquifer base elevations to reduce very large elevation changes between adjacent cells that otherwise resulted in unrealistic dry cells during model simulations.

Recharge was varied during the calibration process, resulting in a final uniform recharge rate of 0.0012 ft/day, or 20 percent of average annual precipitation in the model area. Effects of recharge were greatest in the recharge zone. Hydraulic conductivity of the model was adjusted by varying values in zones that make up the confined part of the aquifer, as well as different parts of the unconfined part of the aquifer. The model was relatively insensitive to hydraulic conductivity. Therefore, a uniform hydraulic conductivity of 25 ft/day was assigned to active cells in the calibrated model. This value is close to the median hydraulic conductivity (9 ft/day) but differs from initial zoned values that varied from 5 to 2,000 ft/day. The use of zones could not be justified because of (1) the insensitivity of the model, (2) the RMSE not changing whether

hydraulic conductivity was uniform or distributed in zones, and (3) the zones not being supported by available hydraulic conductivity data that were restricted mostly to the confined part of the aquifer. The GHB conductance in the calibrated model was reduced from the initial value of 3,500 ft^2/day to 20 ft^2/day. The effects of varying GHB conductance are greatest in the downdip parts of the aquifer. Recharge and GHB conductance have the combined effect of influencing the hydraulic gradient across the model.

Simulated water levels from the calibrated steady-state model are fairly close to measured water levels (fig. 9-1). The RMSE of the calibrated model is 32 feet, which is approximately 9 percent of the 343-foot range of measured water levels (fig. 9-2). This fact indicates that the average difference between measured and simulated water levels in the model is ±32 feet —acceptable because the result lies within the 10-percent target for model calibration.

In addition to the comparison of measured and simulated water levels, a comparison of measured streamflow and simulated drain discharge was used to indicate how well the model reproduces groundwater discharge to major streams and springs in the study area (fig. 9-3). There is general agreement between measured stream discharge of Shoal Creek, Lampasas River, Salado Creek, San Gabriel River, and Berry Creek, indicating that the steady-state model does a good job of reproducing baseflow to springs and streams.

The water budget of the steady-state model indicates that total groundwater flow through the model is approximately 80,000 acre-feet per year (table 9-1). Of this flow, 55 percent discharges to streams, 30 percent discharges through cross-formational flow, and 15 percent is pumped mostly for municipal and rural domestic uses. The water budget indicates that most natural discharge (~65 percent) and almost all recharge takes place in the unconfined part of the aquifer. This fact indicates that most groundwater circulation in the northern segment of the Edwards aquifer takes place in the unconfined part of the aquifer.

9.2   Steady-State Sensitivity Analysis

After calibration of the steady-state model was completed, the input parameters were analyzed to assess the sensitivity of model results to respective input parameters, that is, hydraulic conductivity, GHB conductance, pumping, and recharge. Sensitivity analysis is a method of quantifying uncertainty of the calibrated model related to uncertainty in the estimates of respective aquifer parameters, stresses, and boundary conditions (Anderson and Woessner, 1992). Determining the sensitivity of the model to specific parameters offers insights into the uniqueness of the calibrated model. Sensitivity analysis identifies which parameters have the greatest influence on water levels and groundwater discharge to springs and streams. A model is sensitive to a specified input parameter if relatively small changes in that parameter result in relatively large changes in simulated water levels. In other words, calibration is possible only over a narrow range of values and, consequently, model uncertainties are relatively low. A model is insensitive if relatively large changes of a specific input parameter produce relatively small water-level changes. Insensitivity results in higher uncertainties because the model will calibrate over a large range of input parameter values.
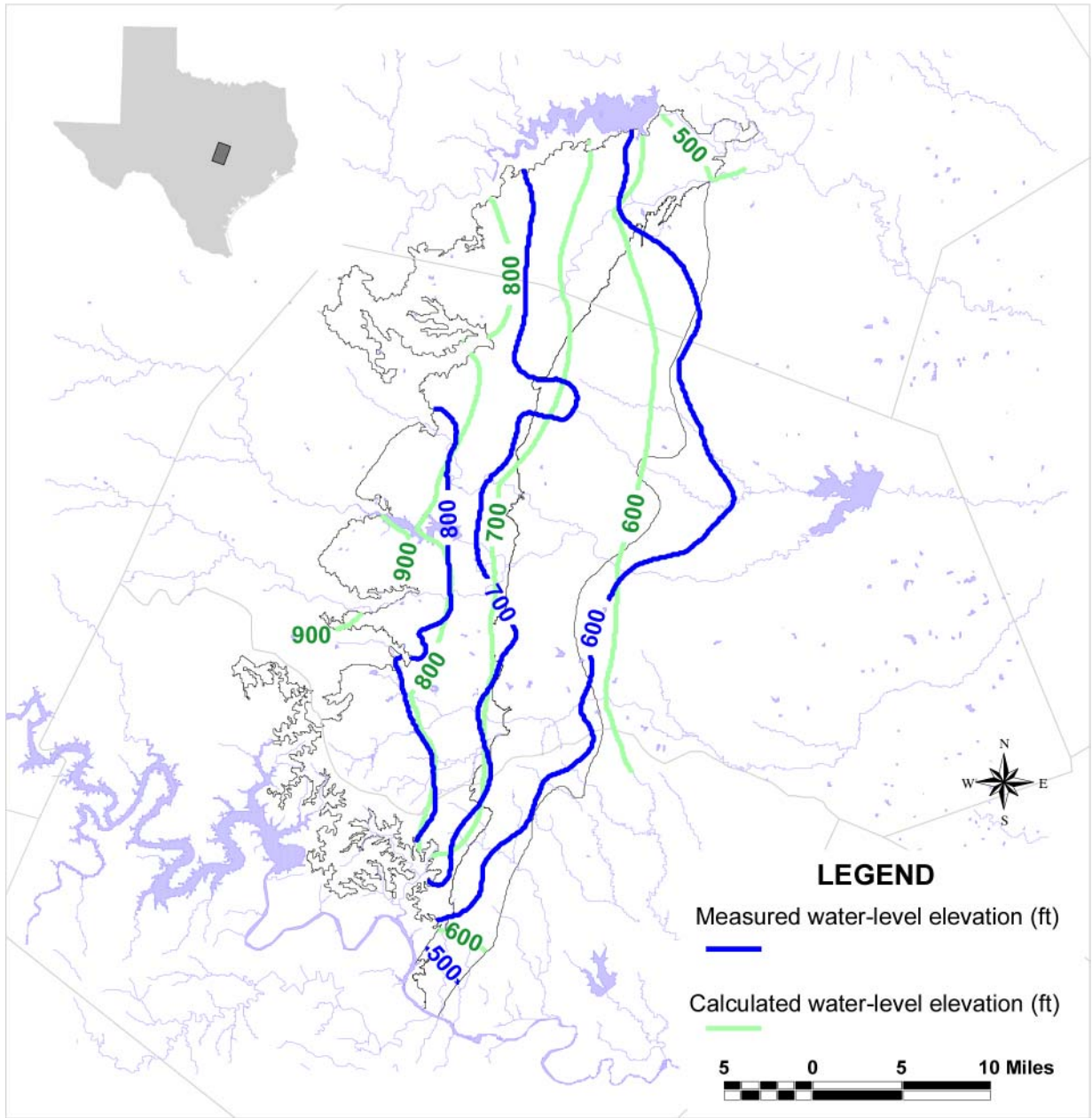
Figure 9-1.   Distribution of measured and calculated water levels from the steady-state model.
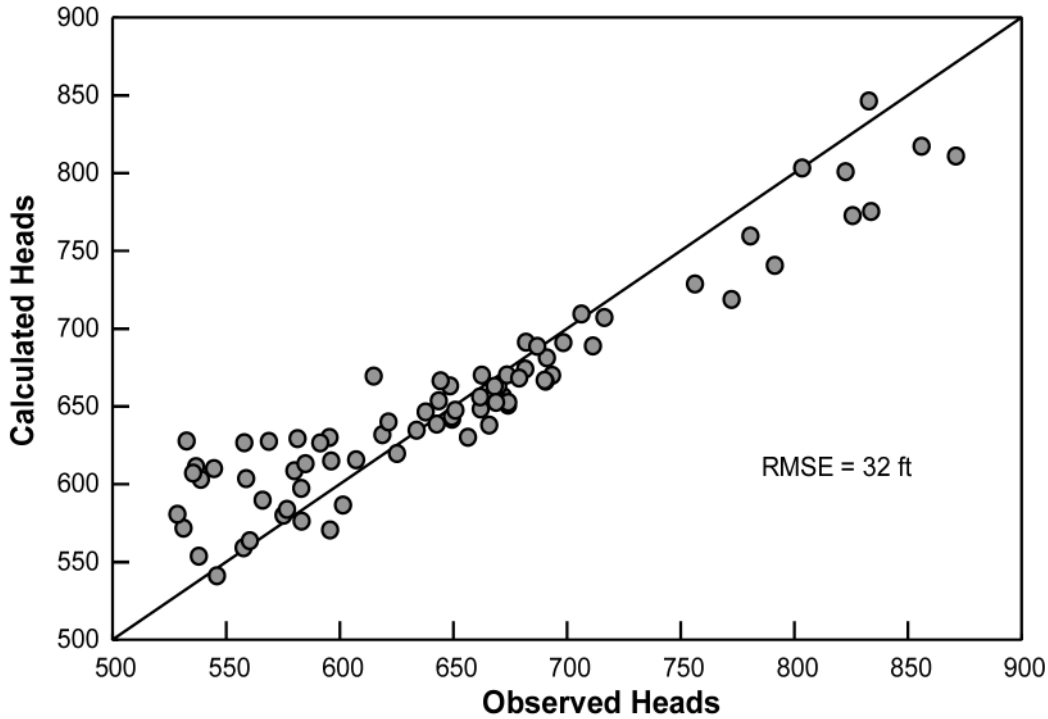
Figure 9-2.   Measured and calculated water levels from the steady-state model.

Sensitivity is analyzed by systematically varying a parameter value and noting changes in water levels at the well locations used to calibrate the model. The water-level changes are quantified by calculating the Mean Difference as follows:

$$MD = \frac{1}{n}\sum_{i=1}^{n}\left(h_{sen} - h_{cal}\right)$$

where: n is the number of points, h_{sen} is the simulated water level for the sensitivity analysis, and h_{cal} is the calibrated water level. The Mean Difference is positive if water levels are higher than calibrated values and negative if they are lower than calibrated values.

Water levels in the model of the northern segment of the Edwards aquifer are most sensitive to recharge, and, to a lesser extent, to GHB conductance and pumping (fig. 9-4). The insensitivity of the model to hydraulic conductivity can be explained partly by the drain cells that simulate groundwater discharge to springs and streams in the unconfined part of the aquifer. Drain cells reduce the variation of water levels in the unconfined part of the aquifer. Discharge from the drains varies, counteracting the effects of hydraulic conductivity changes on water levels. Effects of recharge are greatest in the unconfined part of the aquifer because recharge is restricted to areas where aquifer rock is exposed at land surface. Effects of GHB conductance are greatest in the downdip parts of the aquifer, where GHB cells are located. General-Head Boundary conductance and recharge regulate the regional gradient of the aquifer. Varying recharge and GHB conductance raises and lowers water levels in up-gradient and down-gradient parts of the aquifer, respectively.

52
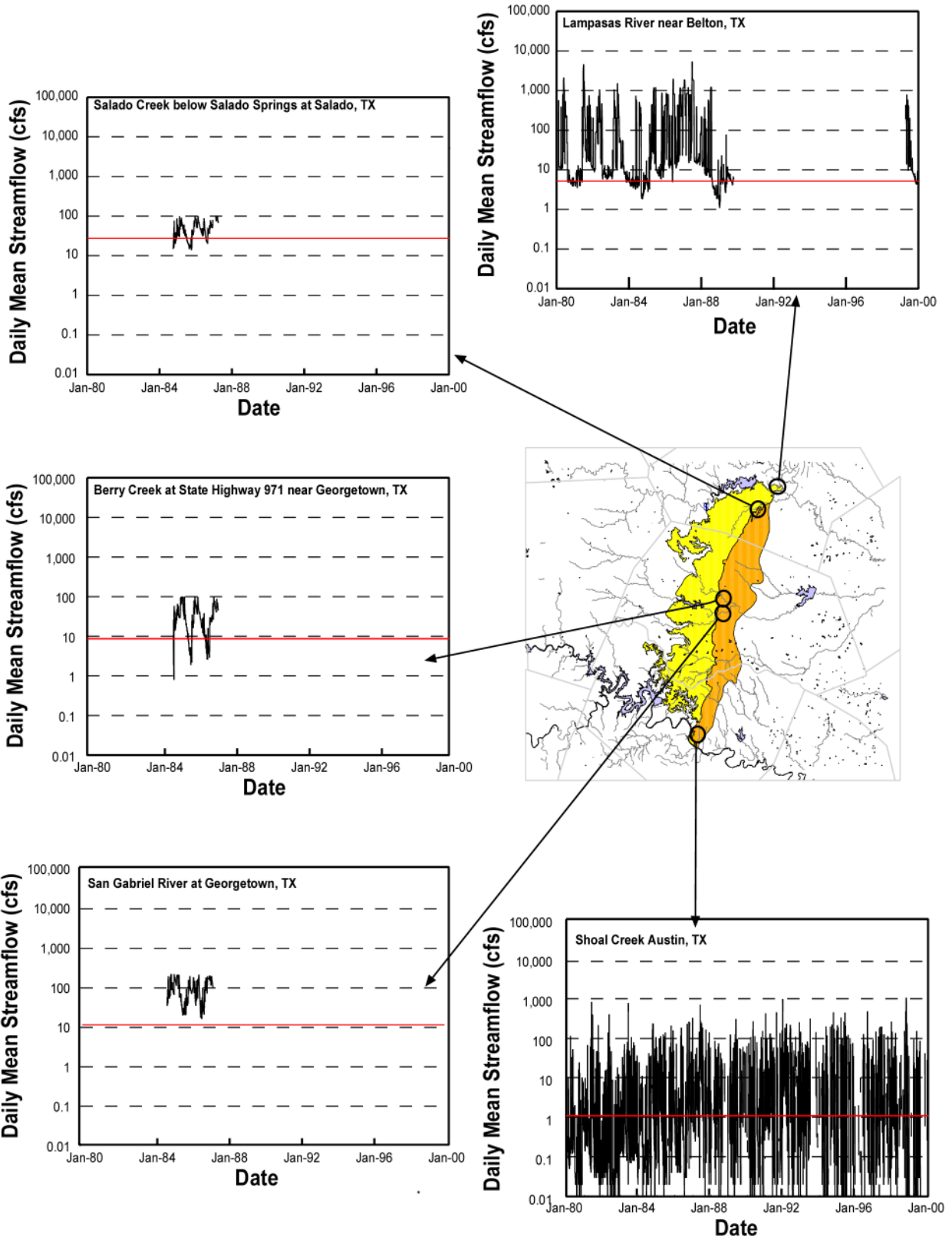
Figure 9-3.   Measured (black) and calculated (red) streamflow from the steady-state model.

Table 9-1.   Water budget for the calibrated steady-state model for 1980. Values expressed in acre-feet per year.

	In	Out	Net
Wells	-	13,000	-13,000
Drains	-	44,000	-44,000
Recharge	79,000	-	79,000
GHB	160	24,000	-24,000
% Difference			0.4%

County	Bell	Travis	Williamson
Recharge	23,000	53,000	4,000
Rivers	-24,000	-19,000	-1,400
GHB	-3,800	-18,000	-1,700
Wells	-400	-12,000	-600
Lateral Inflow	5,000	1,800	1,500
Lateral Outflow	-130	-6,600	-1,600
Total In	28,000	54,000	5,600
Total Out	-28,000	-55,000	-5,400
% Difference	-0.6%	-0.7%	3.3%

Figure 9-4.   Sensitivity of numerically predicted water levels for 1980.

54

10.0 Transient Model

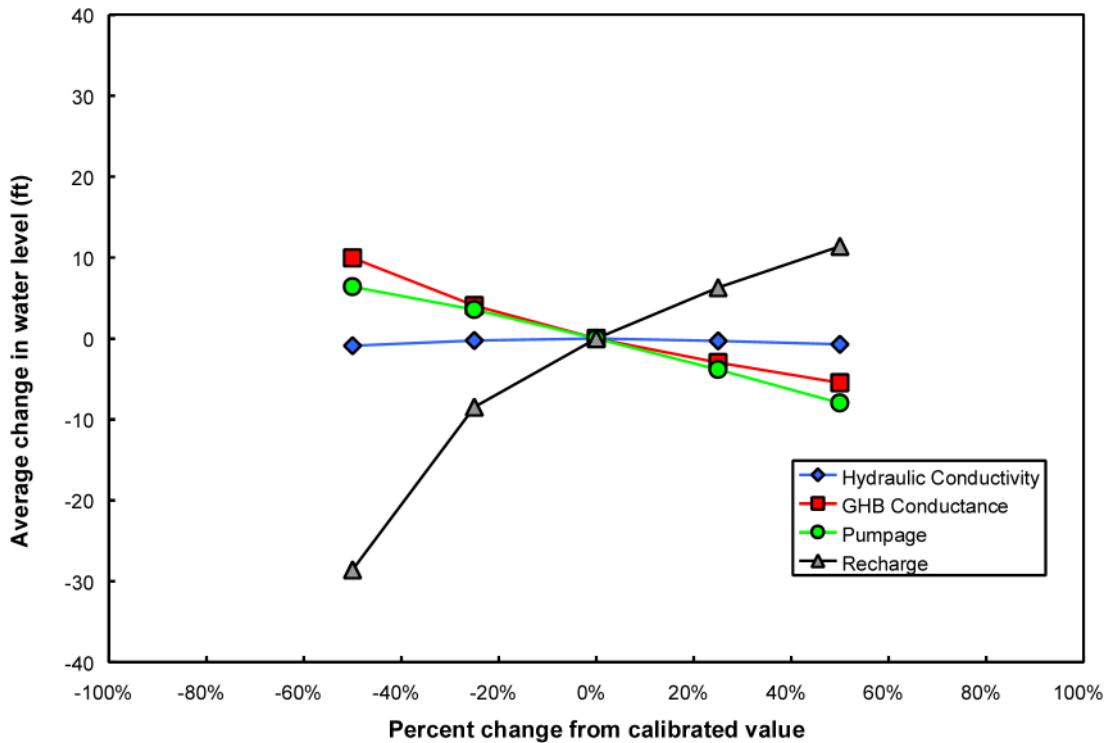After calibration of the steady-state model to conditions in 1980, the model was then calibrated to simulate transient conditions during the period 1980 through 2000.

10.1 Transient Calibration

Water-level fluctuations during the period 1980 through 2000 were simulated using monthly stress periods. Calibration was achieved by adjusting storage parameter values, specific storage, and specific yield until the model responses approximated water-level fluctuations observed in wells in the model area. Specific yield is applicable to the unconfined part of the aquifer and is defined as the volume of water that an unconfined aquifer releases from storage per unit surface area of aquifer per unit decline in the water level. Specific storage is applicable to the confined part of the aquifer and is defined as a measure of the volume of water per unit volume of aquifer rock that enters or leaves storage per unit change in water level. Specific storage and specific yield are important factors in transient calibration because they influence water-level responses to changes in recharge and discharge. Low specific storage or specific yield values result in water-level fluctuations that are larger and more rapid than those of higher specific storage or specific yield values. This difference occurs because less water is required to produce a given water-level change.

Best results were obtained using a specific storage of 5×10^{-6} per foot and a specific yield of 0.0005. In a small area in the western part of the model, characterized by very small water-level fluctuations over the transient period, a much higher specific yield of 0.05 was used (fig. 10-1). The specific storage value is the same as the value used in the groundwater availability model for the Barton Springs segment of the Edwards aquifer (Scanlon and others, 2001), which is not surprising because of the proximity of the two segments of the Edwards aquifer. The calibrated specific yield values (0.0005 to 0.05) in this model, although generally lower, overlap with the range of previous specific yield estimates in the region of 0.005 to 0.06 (Brune and Duffin, 1983; Slade and others, 1985; Scanlon and others, 2001). Overall, this model does a good job matching observed seasonal and interannual water-level and streamflow fluctuations (fig. 10-2 and 10-3). Differences between simulated and observed water-level fluctuations can be attributed to the influence of local-scale conditions that are not represented in this regional-scale model.

Over the calibration period, water-level fluctuations are generally greater in the unconfined part of the aquifer than in the confined part of the aquifer. This difference can be attributed to water-level responses to seasonal and interannual variation of recharge, coupled with the fact that most discharge from the aquifer also takes place in the unconfined part of the aquifer.

Comparison of model results and observations by Ridgeway and Petrini (1999) indicated general similarities. Despite rapid water-level fluctuations, the general trend over time indicates gradual water-level declines in the southern part of the model area, especially in the Pflugerville-Georgetown area (fig. 10-2). No long-term water-level declines occur in the less-populated, northern part of the model area.
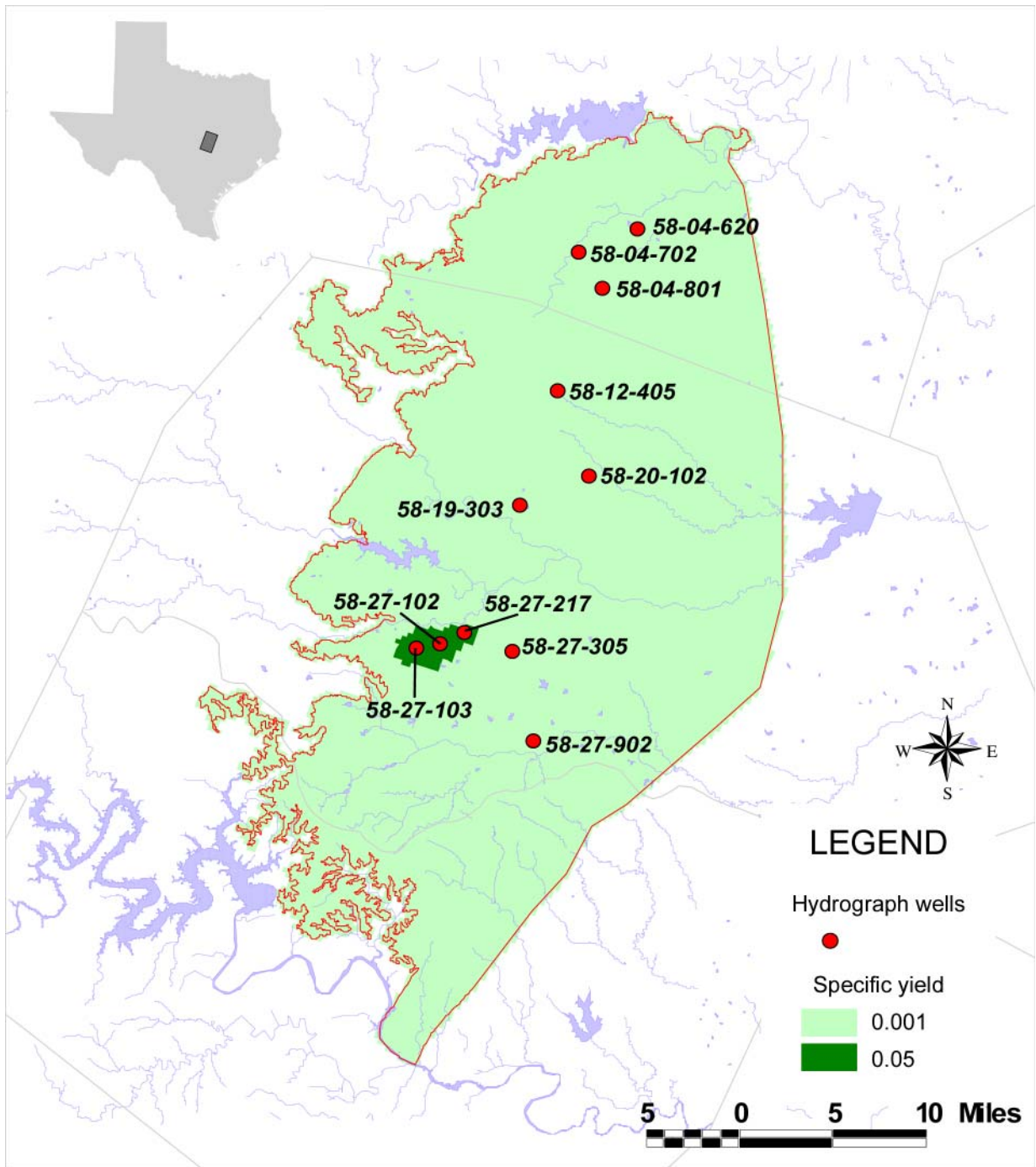
Figure 10-1.   Distribution of specific yield in the model.
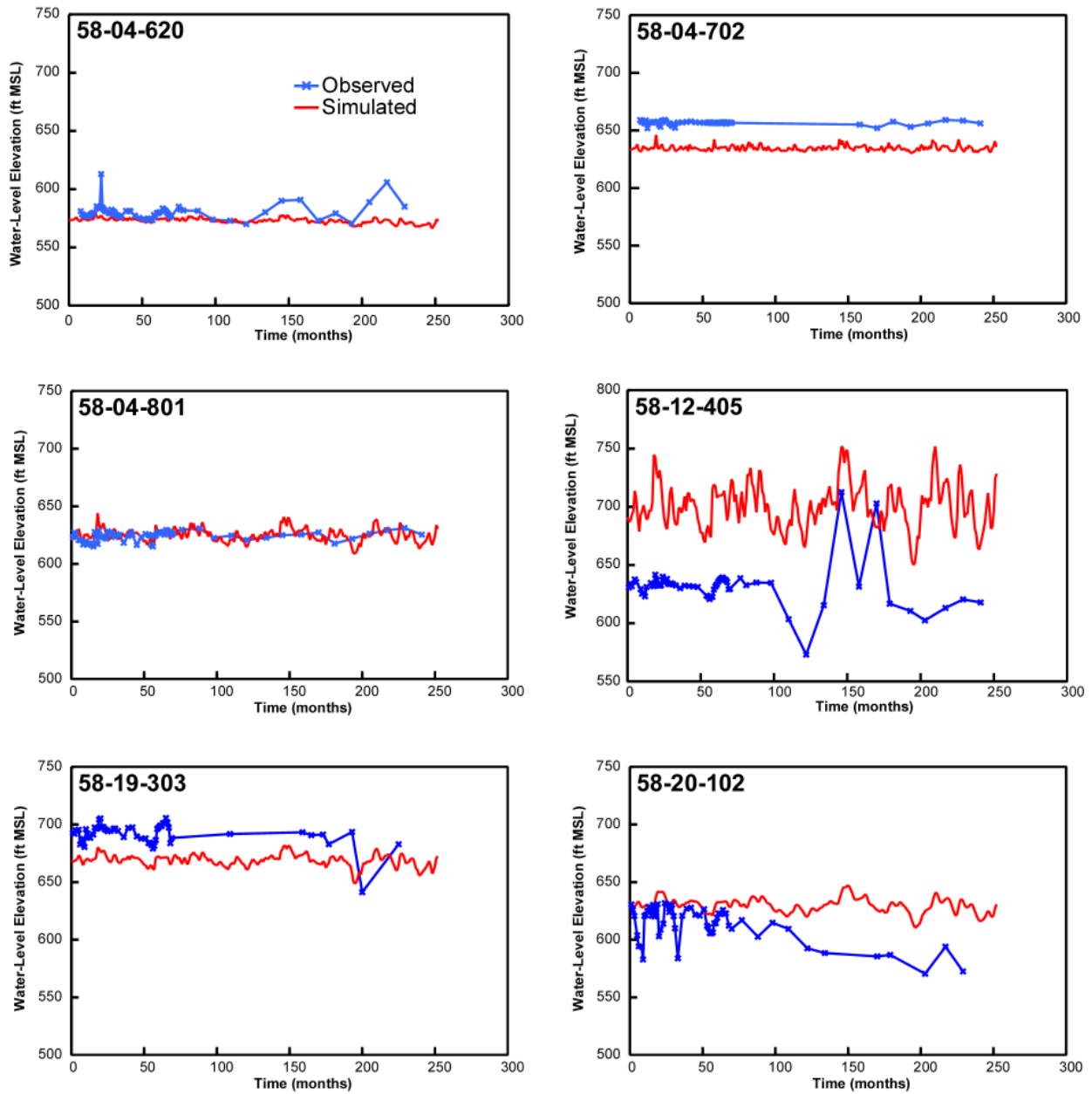
Figure 10-2.   Measured and calculated water-level fluctuations for the period 1980 through 2000.
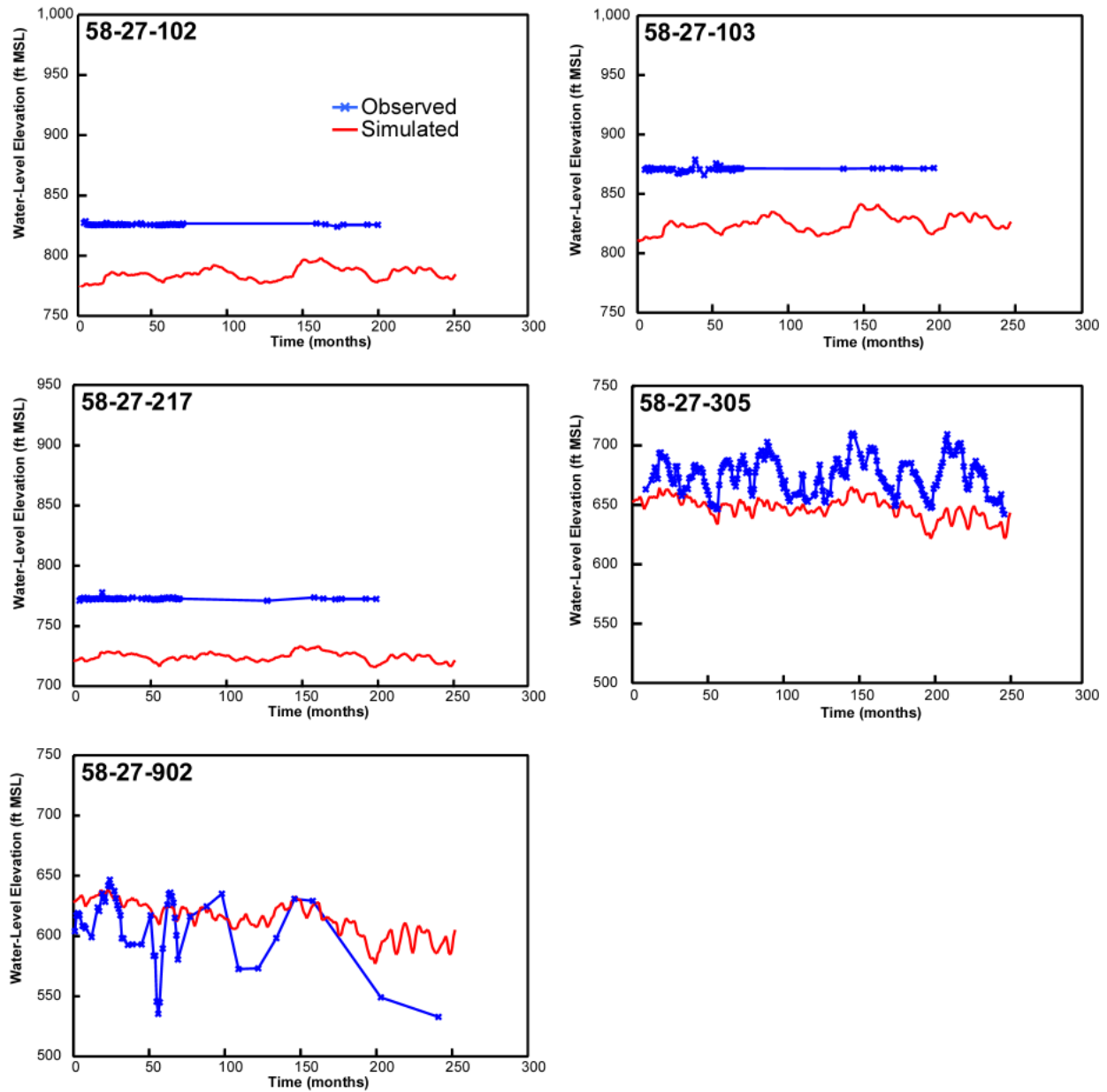
Figure 10-2.   (cont.).

10.2   Transient Sensitivity Analysis

Upon completion of transient model calibration, the storage parameters were assessed to determine the sensitivity of the model to specific yield and specific storage. Sensitivity was analyzed by systematically varying specific yield and specific storage to determine associated changes in aquifer response over the transient model run.

Sensitivity analysis indicates that the overall model is more sensitive to variation of specific yield than specific storage. Variation of specific storage values ranging from 5×10^{-7} to 5×10^{-5}
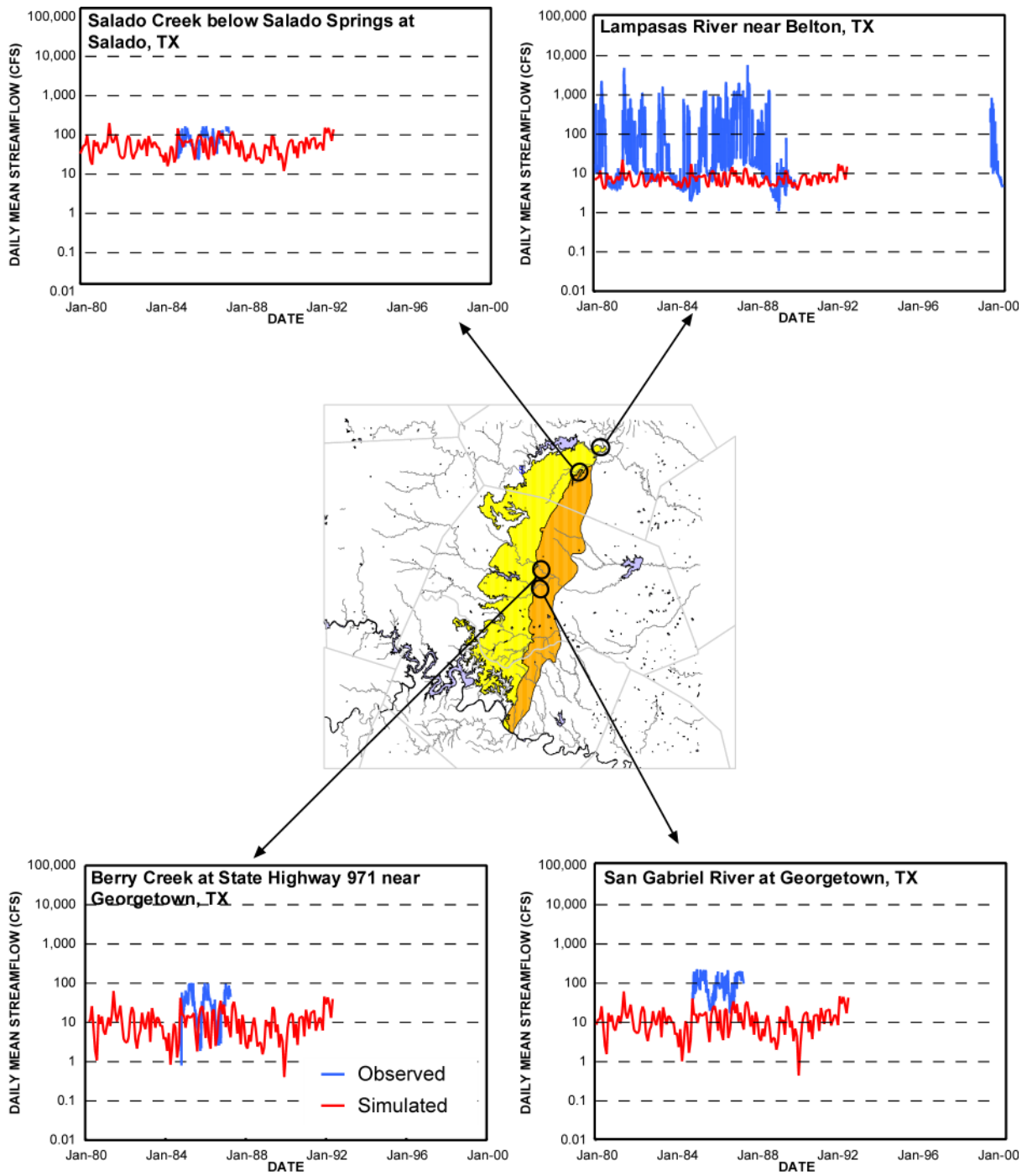
Figure 10-3.   Measured and calculated streamflow fluctuations for the period 1980 through 2000.

per foot resulted in significant changes in simulated water-level responses only at calibration sites within the confined part of the aquifer (fig. 10-4). Variation of specific yield from 0.0005 to 0.05 produced significant variation of simulated water levels at calibration sites throughout the model area (fig. 10-5).
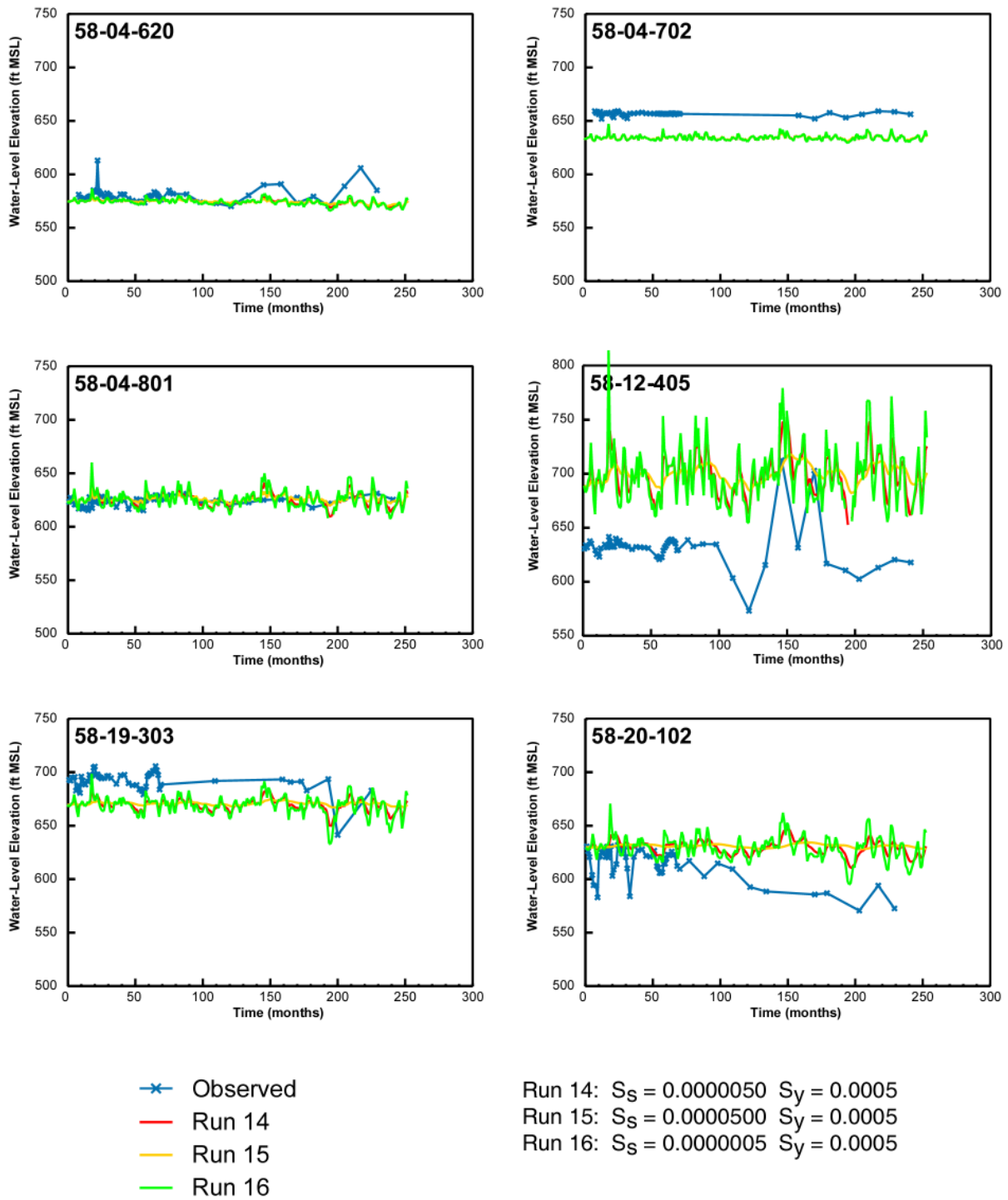
Figure 10-4.   Sensitivity of model to specific storage.
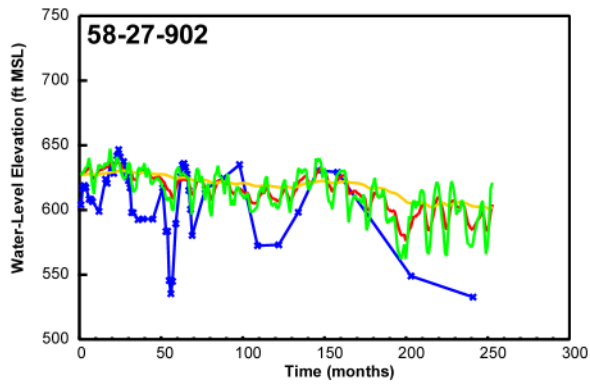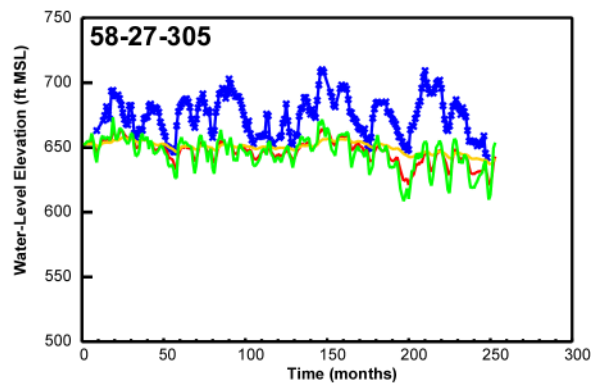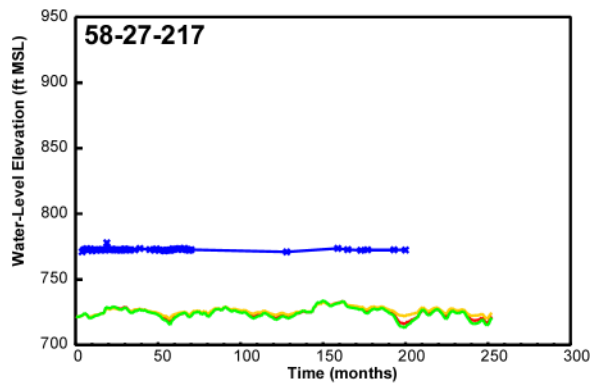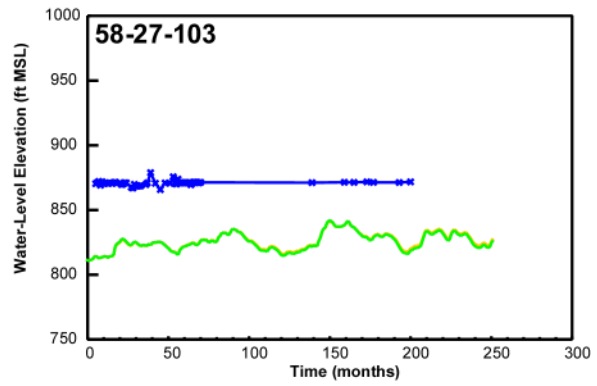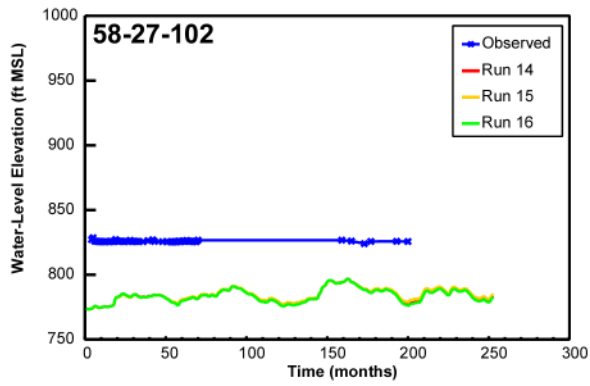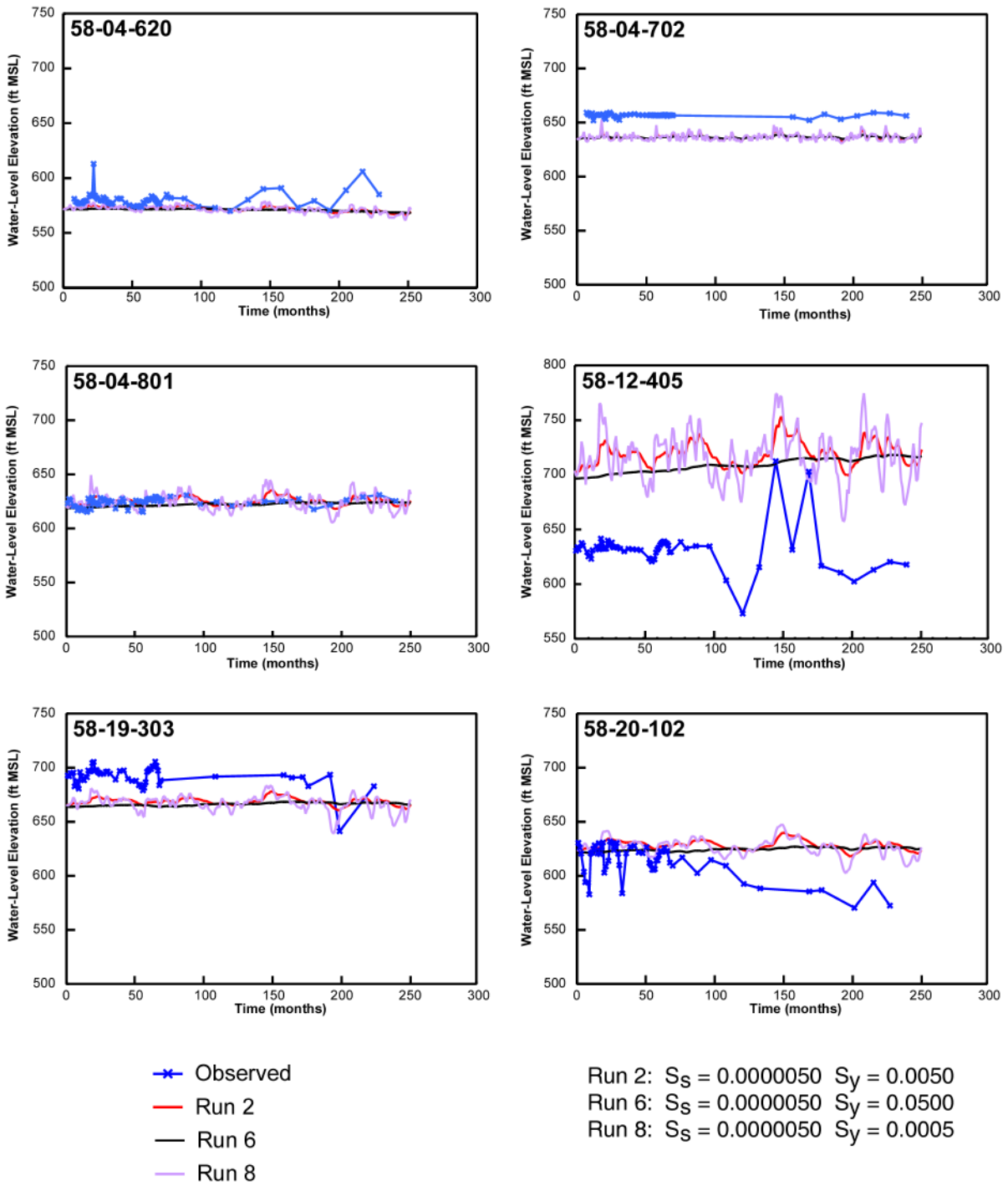
Figure 10-4.　　(cont.).

Figure 10-5.   Sensitivity of model to specific yield.
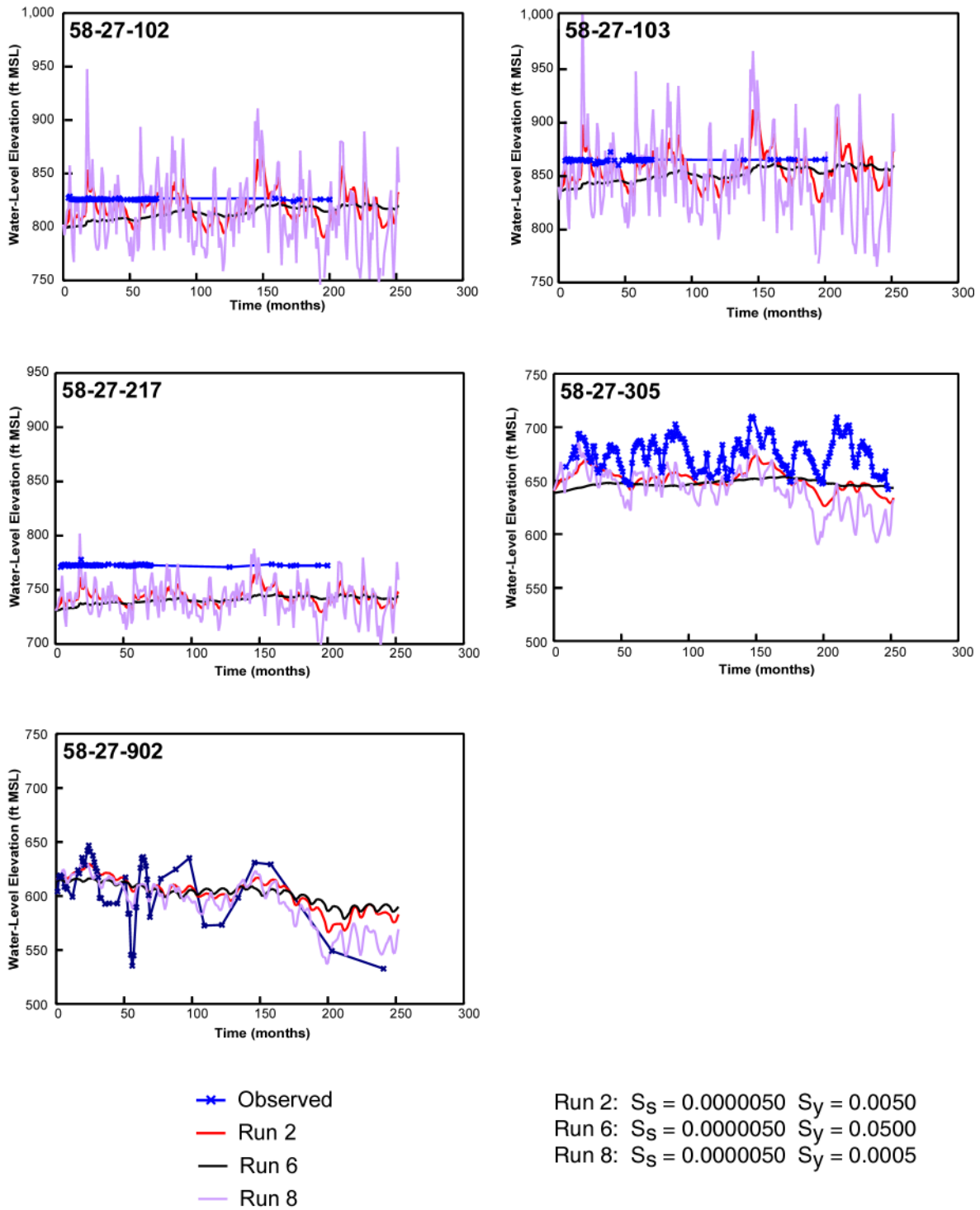
Figure 10-5.   (cont.).

11.0 Predictions

As part of regional water planning, the regions assessed water demand and current supplies. If water demand exceeded current supplies, then there was a need for water. The regions then developed and recommended water management strategies to meet any water needs. In general, recommended water management strategies exceeded the needs for water. In these cases, the volume of water from current supplies plus recommended water management strategies exceeded projected demands. We decided that pumping assigned in the model needed to reflect projected demands more and not the full capacity of all recommended water management strategies. Therefore, in cases where demand exceeded current supplies and recommended water management strategies, we proportionally lowered the water needed from the different recommended water management strategies. We used a proportional approach because regions did not prioritize the different water management strategies and because a proportional approach does not favor one strategy over another.

To assess future availability of groundwater in the northern segment of the Edwards aquifer, the calibrated model was used to predict future water levels under average recharge and drought-of-record conditions. These simulations used projected groundwater pumping that took into account projected demand and water management strategies set by the regional planning groups in the study area. Water planning under drought conditions is a requirement of Senate Bill 1 water planning. The purpose of this water resources planning is to ensure that the state's future water needs are met, even during times of severe drought.

A drought can be defined as a period of deficient rainfall sufficient in length and severity to cause at least partial crop failure or to impair the ability to meet a normal water demand (Wilson and Moore, 1998). A drought of record is the most severe drought during the period of record in terms of duration and severity. For this model, the drought of record was determined by evaluating precipitation records for four stations in the model area. These stations are located at the Austin airport, Jarrell, Taylor, and Temple (fig. 3-8). The period of record for three of these stations began in the late 1920s and early 1930s, whereas records for the fourth station, Temple, extend back to 1900. Evaluation of these precipitation data indicates that the drought of record occurred during the period of 1954 through 1956. This drought coincides with the drought of record that affected most of Texas during the 1950s. At three of the four stations, 1954 is the driest year on record, although the drought of record in the study area was probably not as severe as in other parts of Texas. In the study area, the drought lasted only 3 years, and the precipitation during the second year of the drought (1955) approached, and in some cases exceeded, average annual precipitation.

In predictive model runs, the drought of record was simulated by recharge equivalent to 20 percent of the average of precipitation at the four stations during the years 1954, 1955, and 1956. These recharge rates are 0.0006, 0.0013, and 0.0008 ft/day, respectively. For non-drought years, average recharge (0.0012 ft/day) was used. To simulate future water levels in the aquifer over the period 2001 through 2050, six scenarios were run: (1) the 2010 Run, average recharge through 2007 and drought of record for the remaining 3 years; (2) the 2020 Run, average recharge through 2017 and drought of record for the remaining 3 years; (3) the 2030 Run, average recharge through 2027 and drought of record for the remaining 3 years; (4) the 2040 Run,

Table 11-1.   Water budgets for the steady-state, transient, and predictive model runs expressed in acre-feet per year.

Year	Storage	Wells	Drains	Recharge	GHB
1980	-	-13,000	-44,000	79,000	-23,000
1990	-5,000	-18,000	-51,000	96,000	-21,000
2000	-9,500	-24,000	-68,000	120,000	-18,000
2010	3,300	-5,100	-29,000	53,000	-24,000
2020	3,400	-5,200	-29,000	53,000	-24,000
2030	3,400	-6,000	-28,000	53,000	-23,000
2040	3,400	-6,500	-28,000	53,000	-23,000
2050	3,400	-6,600	-28,000	53,000	-23,000
2050*	0	-6,600	-49,000	79,000	-25,000
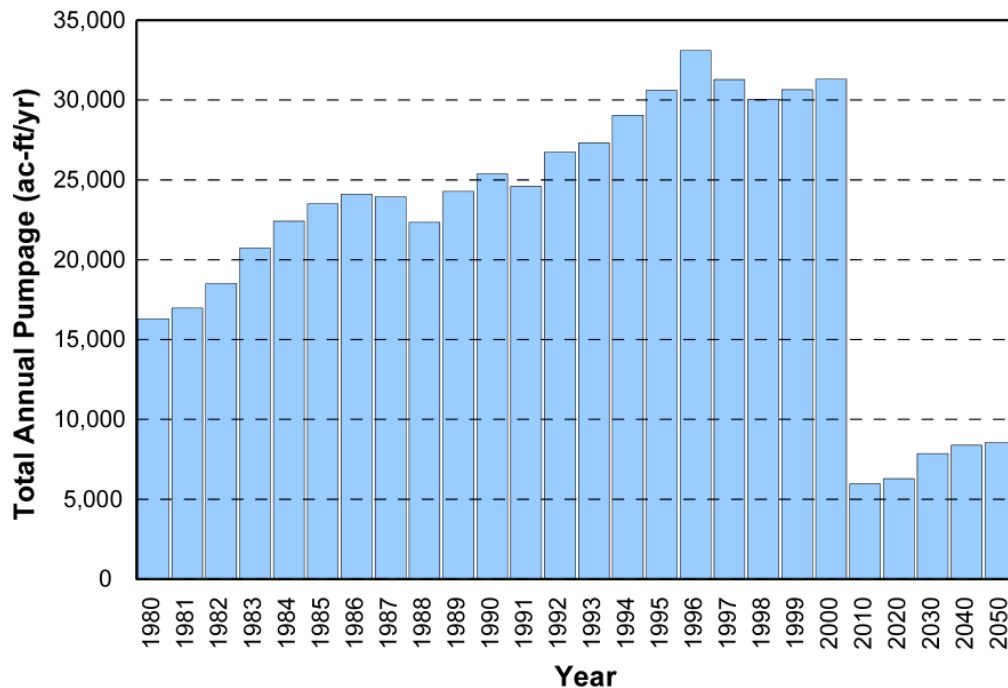
Figure 11-1.   Historical and projected total pumping in the study area.

average recharge through 2037 and drought of record for the remaining 3 years; (5) the 2050 Drought Run, average recharge through 2047 and drought of record for the remaining 3 years; and (6) the 2050 Average Run, average recharge through 2050 (table 11-1). Predicted pumping data used in this model were obtained from the respective regional water planning groups. These data indicate projected pumping from the northern segment of the Edwards aquifer at much lower rates than at present (fig. 11-1). This difference is the result of conversion from the use of Edwards aquifer groundwater to surface water from reservoirs such as the Stillhouse Hollow Lake.
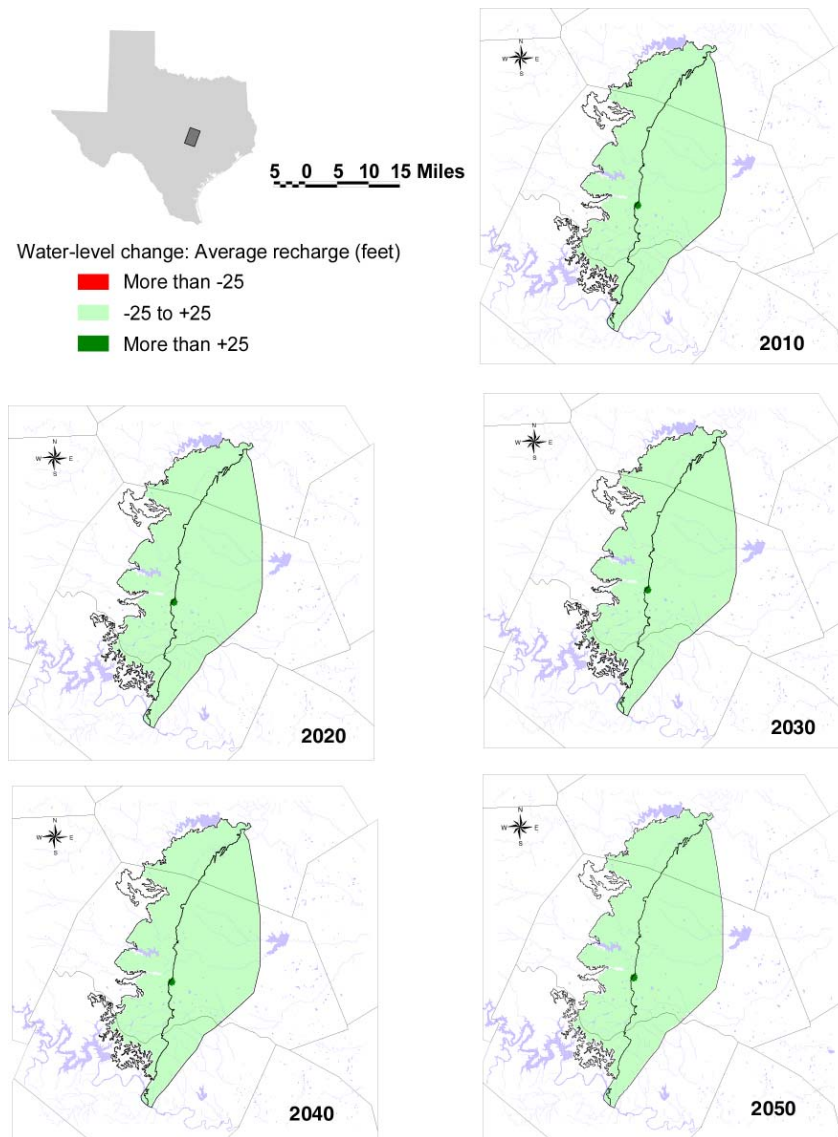
Figure 11-2.   Simulated water-level changes 2010 through 2050, with average recharge.

Projected water-level changes for each decade were calculated by subtracting predicted water levels at the end of each decade from 1980 water levels, the beginning of transient calibration. Water levels from 1980 were selected as the baseline for determining predicted water-level change because they were characterized by average recharge. Consequently, differences in water levels between 1980 and future decades can not be attributed to differences in recharge rates except during drought years.

Under conditions of average recharge, predictive modeling indicates that future water levels in the northern segment of the Edwards aquifer will change less than 25 feet, compared with 1980 water levels (fig. 11-2). Under drought-of-record conditions, water-level declines occur primarily along the western margin of the aquifer (fig. 11-3).
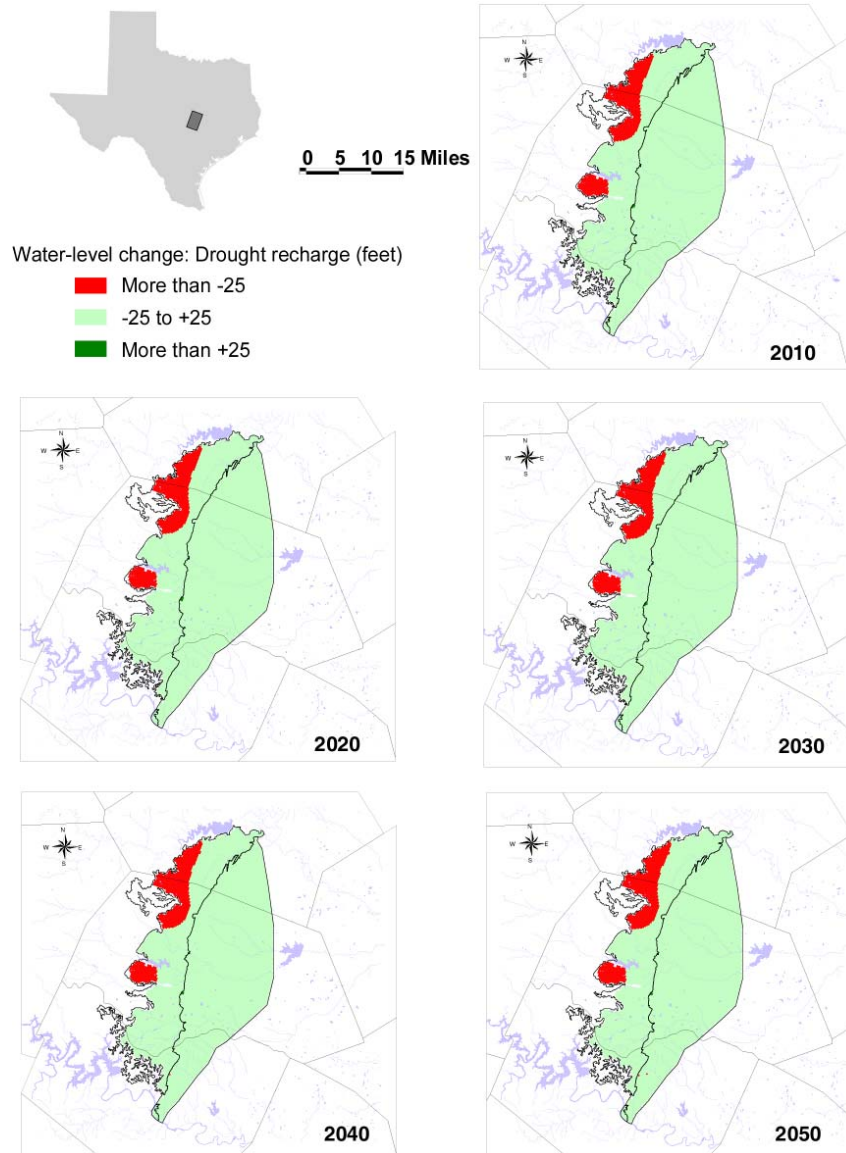
Figure 11-3.   Simulated water-level changes 2010 through 2050, with drought-of-record recharge.

12.0 Limitations of the Model

All numerical groundwater flow models have limitations. These limitations are usually associated with (1) the extent of current understanding of the workings of the aquifer, (2) availability and accuracy of input data, and (3) assumptions and simplifications used in developing the conceptual and numerical models. The limitations determine the spatial and temporal variation of uncertainties in the model because calibration uncertainty decreases with increased availability of input data. Additionally, many of the assumptions, degree of simplification, and spatial resolution of groundwater flow models are influenced by availability of input data.

12.1 Input Data

Several input parameter data sets for the model are based on limited information. These include recharge, water-level and streamflow data, hydraulic conductivity, specific storage, and specific yield.

No information on the spatial or seasonal distribution of recharge to the northern segment of the Edwards aquifer has been published. Calibrated recharge rates of 20 percent of annual precipitation were obtained by trial-and-error. Application of this recharge rate to the transient model assumes that (1) a linear relationship exists between precipitation and recharge and (2) no threshold must be exceeded before recharge occurs. This assumption suggests the possibility of overestimating recharge during dry periods, when all precipitation may be taken up by evapotranspiration or absorbed by dry soils. A uniform spatial distribution of recharge to the aquifer was assumed for the model. This assumption follows the literature that suggests that recharge to the northern segment of the Edwards aquifer takes the form of generally diffuse recharge through soils, fractures, and intermittent streams in the aquifer outcrop (Duffin and Musick, 1991). The relatively good correlation between observed and simulated water levels and stream discharge suggests that, despite recharge uncertainties, the model water budget approximates the aquifer water budget.

Information on the spatial distribution of water levels in the northern segment of the Edwards aquifer is limited, especially along the updip and downdip margins of the aquifer. There is also model uncertainty associated with the number of wells with annual or more frequent water-level measurements. This uncertainty is especially apparent during the 1990s, when water-level measurements were made less frequently in the aquifer.

Uncertainty results from the paucity of streamflow data for the perennial streams that cross the aquifer outcrop. Available streamflow data for Berry Creek, Salado Creek, and the San Gabriel River are only for a few years during the mid- to late1980s. Streamflow data for the 1990s are absent for the Lampasas River. Uncertainty in stream discharge in the southern part of the model exists because (1) no streamflow data are available for Brushy Creek and (2) calibrating the model to stream discharge is difficult in perennial streams, such as Shoal and Walnut creeks, because they have low baseflow components.

Available transmissivity and hydraulic conductivity data for the northern segment of the Edwards aquifer is derived primarily from specific-capacity data obtained from wells located mostly in the central and southern parts of the model area. Most of these wells are located adjacent to the boundary between the confined and unconfined parts of the aquifer. No data exist from the unconfined part of the aquifer. These limited data are apparently random, suggesting local influences. Consequently, we decided to use a uniform hydraulic conductivity, based initially on the geometric mean of the available data, in this regional-scale model.

12.2 Assumptions

Several assumptions were made in the construction of this model. The most important assumptions were that (1) no groundwater flows between the northern segment of the Edwards

aquifer and the underlying Trinity aquifer; (2) recharge is restricted to the aquifer outcrop; (3) the Drain package of MODFLOW can be used to simulate discharge to streams flowing over the aquifer outcrop; (4) the GHB package of MODFLOW can be used to simulate cross-formational flow between the Edwards aquifer and overlying units, such as the Austin Chalk; and (5) negligible groundwater flow beyond the 3,000 mg/l isocon.

The northern segment of the Edwards aquifer is underlain by the Walnut Formation, which is reported to yield little or no water in the study area (Duffin and Musick, 1991). Consequently, it is unlikely that the Walnut Formation transmits significant amounts of groundwater between the Edwards and Trinity aquifers.

The Drain package of MODFLOW was used to simulate groundwater discharge to perennial streams in the study area. The Drain package allows water to move from the aquifer to rivers or streams, but not the reverse. Use of this package implies the assumption that the perennial streams are always gaining. This assumption is supported by streamflow gain-loss studies by Slade and others (2002). Additionally, steady-state and transient calibration results indicate overall agreement between measured and simulated discharge to perennial streams.

The GHB package was used to simulate cross-formational flow between the Edwards aquifer and overlying units. The spatial distribution of GHB cells in the model is based on the assumption that cross-formational flow takes place in downdip parts of the aquifer and along some valleys (Figure 6-3). It is also assumed that the hydraulic head on the boundary is equivalent to 90 feet below land surface and does not vary over time.

12.3   Scale of Application

The limitations described earlier and the nature of regional groundwater flow models affect the scale of application of the model. This model is most accurate in assessing regional-scale groundwater issues, such as predicting aquifer-wide water-level changes over the next 50 years that may result from different proposed water management strategies. Accuracy and applicability of the model decreases when moving from addressing regional- to local-scale issues because of limitations of the information used in model construction and the model cell size that determines spatial resolution of the model. Consequently, this model is not likely to accurately predict water-level declines associated with a single well because (1) these water-level declines depend on site-specific hydrologic properties not included in detail in regional-scale models and (2) the cell size used in the model is too large to resolve changes in water levels that occur over relatively short distances. Addressing local-scale issues requires a more detailed model, with local estimates of hydrologic properties, or an analytical model. This model is more useful in determining the impacts of groups of wells distributed over a few square miles. The model predicts changes in ambient water levels rather than actual water-level changes at a specific location, such as an individual well.

13.0 Future Improvements

The TWDB plans periodically to update, and thus improve, groundwater availability models. This model can be improved by incorporating greater complexity or hydrologic information that

was not available initially. Model uncertainty can be reduced with additional information on aquifer hydraulic properties, streamflow, water-level elevations, and recharge.

Additional streamflow data are required in order for us to better determine the seasonal and spatial distribution of stream discharge gain and loss. This ability will facilitate the use of the streamflow package of MODFLOW as a potentially superior alternative to the Drain package and to provide additional data for model calibration.

Additional hydraulic head measurements and aquifer-test data are required for the northern segment of the Edwards aquifer, especially the unconfined part of aquifer. This information can be used to improve calibration of the model by increasing the number and spatial distribution of sites for comparing measured and simulated water levels. Water-level data are needed for the stratigraphic units overlying the Edwards aquifer in order for the GHB to be better constrained. Aquifer tests will facilitate determination of whether improving the model by spatially distributing hydraulic conductivity, specific storage, and specific yield can be justified.

This model can also be improved by an investigation of the spatial and temporal distribution of recharge. Determination of the hydrologic conditions required for the occurrence of recharge to the northern segment of the Edwards aquifer will facilitate better constraints on the seasonal distribution of recharge to the aquifer.

14.0 Conclusions

A numerical groundwater flow model was constructed to simulate groundwater flow through the northern segment of the Edwards aquifer. It is to be used as a tool to evaluate groundwater resource management strategies by predicting water-level changes in response to pumping and drought. Model construction was based on available hydrologic and geologic data for the northern Edwards aquifer. The model is composed of one layer with 40,000 cells, 12,877 of which are active. The modeling approach included construction and calibration of steady-state (1980) and historical transient (1980 through 2000) models and using the resultant calibrated transient model to predict aquifer responses through 2050 under average recharge and drought-of-record conditions. The predictive model runs used projected pumping developed by the Brazos G and Lower Colorado Regional Water Planning Groups.

The calibrated model does a good job of matching water-level distribution and fluctuations in the aquifer and stream discharge. The RMSE for the steady-state model is 32 feet, about 9 percent of the hydraulic-head drop across the study area. Calibration of the steady-state and transient models resulted in (1) an average recharge rate of 20 percent of mean annual precipitation, (2) hydraulic conductivity of 25 ft/day, (3) specific yields of 0.05 to 0.0005, and (4) specific storage of 5×10^{-6} per foot. The model is most sensitive to changes in specific yield, recharge, and GHB conductance. This model indicates that approximately 50 to 70 percent of groundwater flow occurs within the unconfined part of the aquifer, resulting in discharge to perennial streams. Pumping, mostly for municipal, rural domestic, and industrial uses, accounts for less than 20 percent of groundwater discharge from the aquifer; the remaining 10 to 30 percent is discharge by cross-formational flow in the confined parts of the aquifer. The much larger water-level fluctuations in the unconfined compared with the confined part of the aquifer can be attributed to

a more active groundwater flow system, with almost all of the recharge and most of the groundwater discharge occurring from the unconfined part of the aquifer. Calibration of the transient model indicates that the model is able to reproduce historical water-level fluctuations that indicate gradual water-level declines in the Georgetown-Pflugerville area.

Predictive model runs indicate that under average recharge conditions, water levels will rise slightly relative to 1980 water levels throughout most of the study area over the 50-year planning period as a result of reduced pumping starting in 2001. Under drought-of-record conditions, water levels in the northern segment of the Edwards aquifer will decline, especially along the updip margin of the aquifer. In the predictive scenarios run, higher water levels occur in the central part of the study area. These higher water levels are the result of projected municipal and industrial pumping rates in the Round Rock-Georgetown area that are much lower than historical pumping rates. Pumping rates are expected to rise over the 2001 through 2050 period but will still be much lower than pre-2000 pumping rates. These lower pumping rates will result from conversion from the use of Edwards aquifer groundwater to surface water to meet water demands. Effects of these rising pumping rates are most apparent in the southern part of the study area.

15.0 Acknowledgements

16.0 References

Anderson, M. P., and Woessner, W. W., 1992, Applied groundwater modeling: Simulation of flow and advective transport: Academic Press, Inc., San Diego, 381 p.

Baker, E. T., Slade, R. M., Jr., Dorsey, M. E., Ruiz, L. M., and Duffin, G. L., 1986, Geohydrology of the Edwards aquifer in the Austin area, Texas: Texas Water Development Board, Report 293, 177 p.

Barrett, M. E., 1996, A parsimonious model for simulation of flow and transport in a karst aquifer: The University of Texas at Austin, Ph.D. dissertation, 180 p.

Brune, G., 1975, Major and historical springs of Texas: Texas Water Development Board, Report 189, 95 p.

Brune, G., and Duffin, G. L., 1983, Occurrence, availability, and quality of groundwater in Travis County, Texas: Texas Department of Water Resources, Report 276, 219 p.

Bureau of Economic Geology, 1981, Austin sheet: Geology Atlas of Texas, 1:250,000, 1 sheet.

Campana, M. E., 1975, Finite-state models of transport phenomena in hydrologic systems: University of Arizona, Ph.D. dissertation.

Chiang, W., and Kinzelbach, W., 2001, 3D-groundwater modeling with PMWIN: Springer-Verlag, New York, 2nd ed., 346 p.

Collins, E. W., 1987, Characterization of fractures in limestones, northern segment of the Edwards aquifer and Balcones Fault Zone, central Texas: Gulf Coast Association of Geological Societies Transactions, v. 37, 43-54 p.

Collins, E. W., Woodruff, C. M., Jr., and Tremblay, T. A., 2002, Geologic framework of the northern Edwards aquifer, central Texas: Gulf Coast Association of Geological Societies Transactions, v. 52, 135-137 p.

Dahl, S. L., 1990, Hydrogeology and stream interactions of the Edwards aquifer in the Salado Creek basin, Bell and Williamson Counties, central Texas: Baylor University, Master's thesis, 154 p.

Duffin, G., and Musick, S. P., 1991, Evaluation of water resources in Bell, Burnet, Travis, Williamson and parts of adjacent counties, Texas: Texas Water Development Board, Report 326, 105 p.

Flores, R., 1990, Test well drilling investigation to delineate the downdip limits of usable-quality ground water in the Edwards aquifer, Texas: Texas Water Development Board, Report 325, 70 p.

Harbaugh, A. W., and McDonald, M. G., 1996, User's documentation for MODFLOW-96, an update to the U.S. Geological Survey modular finite-difference ground-water flow model: U.S. Geological Survey Open-File Report 96-485, 56 p.

Hovorka, S. D., Dutton, A. R., Ruppel, S. C., and Yeh, J. S., 1996, Edwards aquifer ground-water resources: geologic controls on porosity development in platform carbonates, South Texas: The University of Texas at Austin, Bureau of Economic Geology Report of Investigations No. 238, 75 p.

Hovorka, S. D., Mace, R. E., and Collins, E. W., 1998, Permeability structure of the Edwards aquifer, South Texas—implications for aquifer management: The University of Texas at Austin, Bureau of Economic Geology Report of Investigations No. 250, 55 p.

Klemt, W. B., Knowles, T. R., Elder, G. and Sieh, T., 1979, Ground-water resources and model applications for the Edwards (Balcones Fault Zone) aquifer in the San Antonio region, Texas: Texas Department of Water Resources, Report 239, 88 p.

Klemt, W. B., Perkins, R. D., and Alvarez, H. J., 1975, Groundwater resources of part of central Texas with emphasis on the Antlers and Travis Peak Formations: Texas Water Development Board Report 195, v. 1 & 2.

Knowles, T., and Klemt, W. B., 1978, Calibration of the Edwards aquifer model: verification of mathematical and physical models in hydraulic engineering: Proceedings of the Hydraulics Division Specialty Conference, no. 26, 94-100 p.

Kreitler, C. W., Senger, R. K., and Collins, E. W., 1987, Geology and hydrology of the northern segment of the Edwards aquifer with emphasis on the recharge zone in Georgetown, Texas, area: The University of Texas at Austin, Bureau of Economic Geology, report prepared for the Texas Water Development Board, 115 p.

Kuniansky, E. L., 1993, Multilayer finite-element model of the Edwards and Trinity aquifers, Central Texas, in Dutton, A. R. (ed.), Toxic substances and the hydrologic sciences: American Institute of Hydrology, p. 234-249.

Kuniansky, E. L., and Holligan, K. Q., 1994, Simulations of flow in the Edwards-Trinity aquifer system and contiguous hydraulically connected units, west-central Texas: U.S. Geological Survey Water-Resources Investigations Report 93-4039, 40 p.

Land, L. F., and Dorsey, M. E., 1988, Reassessment of the Georgetown Limestone as a hydrogeologic unit of the Edwards Aquifer, Georgetown area, Texas: - U.S. Geological Survey, Water-Resources Investigations, WRI 88-4190, 49 p.

Mace, R. E., 2001a, Estimating transmissivity using specific-capacity data: The University of Texas at Austin, Bureau of Economic Geology, Geological Circular No. 01-2, 44 p.

Mace, R. E., 2001b, Regional groundwater flow modeling in Texas: Texas Water Development Board, Unpublished paper, 27 p.

Maclay, R. W., and Land, L. F., 1988, Simulation of flow in the Edwards aquifer, San Antonio Region, Texas, and refinements of storage and flow concepts: U.S. Geological Survey Report Water-Supply Paper 2336, 48 p.

Mahin, D. A., 1978, Analysis of groundwater flow in the Edwards limestone aquifer, San Antonio area, Texas: University of Nevada, Reno, M.S. thesis.

Mahin, D. A., and Campana, M. E., 1983, Discrete-state compartment model of a limestone ground-water reservoir—the Edwards aquifer near San Antonio, Texas: University of Nevada, Desert Research Institute Water Resources Center Publication 41077, 41 p.

McDonald, M. G., and Harbaugh, A. W., 1988, A modular three-dimensional finite-difference ground-water flow model: U.S. Geological Survey, Techniques of Water-Resources Investigations of the United States Geological Survey, Book 6: Model Techniques, Chapter A1.

Proctor, C. V., Jr., Brown, T. E., McGowen, J. H., and Waechter, N. B., 1974, Austin sheet: The University of Texas at Austin, Bureau of Economic Geology, Geologic Atlas of Texas, scale 1:250,000.

Ridgeway, C., and Petrini, H., 1999, Changes in groundwater conditions in the Edwards and Trinity aquifers, 1987-1997, for portions of Bastrop, Bell, Burnet, Lee, Milam, Travis, and Williamson Counties, Texas: Texas Water Development Board, Report 350, 38 p.

Rose, P. R., 1972, Edwards Group, surface and subsurface, Central Texas: The University of Texas at Austin, Bureau of Economic Geology Report of Investigations No. 74, 198 p.

Scanlon, B. R., Mace, R. E., Dutton, A. R., and Reedy, R., 2001, A groundwater flow model of the Barton Springs segment of the Edwards aquifer: The University of Texas at Austin, Bureau of Economic Geology, contract report prepared for the Lower Colorado River Authority, 91 p.

Senger, R. K., and Kreitler, C. W., 1984, Hydrogeology of the Edwards aquifer, Austin area, Central Texas: The University of Texas at Austin, Bureau of Economic Geology Report of Investigations No. 141, 35 p.

Senger, R. K., Collins, E. W., and Kreitler, C. W., 1990, Hydrogeology of the northern segment of the Edwards aquifer, Austin region: The University of Texas at Austin, Bureau of Economic Geology, Report of Investigations No. 192, 58 p.

Slade, R. M., 1987, Transmissivities of the northern Edwards Aquifer, in Yelderman, J. C. (ed.), Hydrogeology of the Edwards aquifer: Northern Balcones and Washita Prairie segments: Austin Geological Society, Guidebook 11, 9-10 p.

Slade, R. M., Jr., Bentley, J. T., and Michaud, D., 2002, Results of streamflow gain-loss studies in Texas, with emphasis on gains from and losses to major and minor aquifer: U.S. Geological Survey Open-File Report 02-068, 49 p.

Slade, R. M., Jr., Ruiz, L., and Slagle, D., 1985, Simulation of the flow system of Barton Springs and associated Edwards Aquifer in the Austin area, Texas: U.S. Geological Survey Water-Resources Investigations Report 85-4299.

Trippet, A. R., and Garner, L. E., 1976, Guide to points of geologic interest in Austin: The University of Texas at Austin, Bureau of Economic Geology, Guidebook No. 16, 38 p.

Tucker, D. R., 1962, Subsurface Lower Cretaceous stratigraphy, central Texas: The University of Texas at Austin, Ph.D. dissertation, 137 p.

Uliana, M. M., and Sharp, J. M., Jr., 1996, Springflow augmentation possibilities at Comal and San Marcos springs, Edwards Aquifer: AAPG Bulletin, v. 80, no. 9, 1516 p.

Wilson, W. E., and Moore, J. E. (eds.), 1998, Glossary of hydrology: American Geological Institute, Alexandria, VA, 248 p.

Woodruff, C. M., Jr., Snyder, F., De La Garza, L., and Slade, R. M., Jr., (eds.), 1985, Edwards Aquifer, northern segment, Travis, Williamson, and Bell Counties, Texas: Austin Geological Society, Guidebook 8, 104 p.

Yelderman, J. C., Jr., Slade, R. M., Jr., Sharp, J. M., Jr., and Woodruff, C. M., Jr., 1987, Hydrogeology of the Edwards Aquifer, northern Balcones and Washita Prairie segments: Austin Geological Society, Guidebook 11, 91 p.